UNIVERSITY OF NAIROBI

SCHOOL OF ENGINEERING

DEPARTMENT OF MECHANICAL AND MANUFACTURING ENGINEERING

DETERMINATION OF THE OPTIMUM HYBRID RENEWABLE ENERGY SYSTEM FOR POWERING THE SCHOOL OF ENGINEERING, UNIVERSITY OF NAIROBI

BY

FABIAN CHIDUBEM EZE

SUPERVISORS

PROF. JULIUS MAIMA OGOLA

DR. REUBEN MWANZA KIVINDU

MAY 2019

Declaration

I declare that this work has not been submitted and approved for the award of a degree by this or any other University. To the best of my Knowledge and belief, the project report contains no materials published or written by another person except where due reference is made in the report itself.

Signature _____

Fabian Chidubem Eze

F56/7789/2017

Date _____

Approval by supervisors

I confirm that the study was carried out under my supervision and has been submitted for examination with my approval as University supervisor.

Signature _____ Signature_____

Prof. Julius Maima Ogola Dr. Reuben Mwanza Kivindu

Date _____ Date _____

Dedication

I dedicate this work to all those who put their efforts in meeting the world's growing need for energy while mitigating the effects of climate change.

Acknowledgment

My first gratitude goes to the almighty God for the strength, wisdom and knowledge he gave me to accomplish this work. Special thanks to the Association of Commonwealth Universities for making the fund available

I wish to acknowledge immensely my supervisors for their moral and academic support throughout the period of this achievement. I also acknowledge Prof J.A. Nyang'aya and the technical team of the Eenovators Limited for their helps towards my data collection.

To my family and well-wishers, I say thank you.

Abstract

Off-the-grid and on-the-grid hybrid renewable energy systems have become effective solutions to providing reliable, affordable and environmentally protected electricity for the rural communities where extension of the conventional grid is not feasible and institutions where the cost of electricity is relatively high.

The goal of this research project was to determine the optimum hybrid renewable energy system that can supply reliable and affordable power to the School of Engineering, University of Nairobi. The load profile of the site was determined using Power and Energy Logger (PEL) and data analysis was done using DataView software. The total power demand and consumption of the establishment were found to be 84.59kW and 1172kWh/day respectively while scaled average of 144.62kW and 1200kWh/day were simulated and optimized. In addition, the wind speed scaled average measured at 50m height, the mean global horizontal solar scaled average radiation and the temperature scaled average were found for this site as 4.76m/s and 5.93kWh/m^2/day and 19.9^{0}C respectively. Grid/wind turbine/photovoltaic/diesel generator/battery bank/converter was simulated and optimized in HOMER Pro Microgrid Analysis Tool with the total net present cost calculated for 25 years in order to find the lowest cost of energy for the optimal system.

The optimum hybrid system has been found to be Grid/Photovoltaic/Diesel generator system. This system gives COE of Ksh 7.89, NPC of ksh 69,512,100.00, Initial capital cost of ksh 30,264,100.00, renewable fraction of 71.6%, simple payback period of 6.15years, discounted payback period of 7.76years, present worth of Ksh 12,819,300.00, annual worth of ksh 965,700.00, excess electricity generation of 2.48% etc. The system proves to have reduced the power being purchased from the grid from 100% to 23% approximately (90kW to 20kW). 9 sensitivity cases were used for sensitivity analysis and the result gave the same configuration except in cases where the sizes and prices of some components were changed.

The study had put into perspective the Feed-in-Tariff policy in Kenya which would allow excess electricity generated by the system to be sold back to the national grid through the PPA policy.

Keywords: Wind Speed, HOMER Energy, Solar Radiation, Grid/PV//diesel generator, NPC, COE, Renewable Fraction.

Table of Content

List of Figures

List of tables

List of Abbreviations

UNSDGs	United Nations Sustainable Development Goals
SDGs	Sustainable Development Goals
OECD	Organization for Economic Cooperation and Development
ERC	Energy Regulatory Commission
UNDESA	United Nations Department of Economic and Social Affairs
IEA	International Energy Agency
CF	Capacity Factor
LF	Load Following
CC	Cycle Charging
PW	Present Worth
AW	Annual Worth
FiT	Feed in Tariff
UNDP	United Nations Development Programme
IRENA	International Renewable Energy Agency
USAID	the United States Agency for International Development
CIA	Central Intelligence Agency
HOMER	Hybrid Optimization of Multiple Energy Resources
NASA	National Aeronautics and Space Administration
NGO	Non-Governmental Organisation
LED	Light Emitting Diode
GIS	Geographical Information System
PV	Photovoltaic
kWh/kW	Kilowatt hour/Kilowatt
TWh	Terawatt hour
GWh	Gigawatt hour

MW	Megawatt
DNI	Direct Normal Irradiation
GHI	Ground Horizontal Irradiation
GDP	Growth Domestic Product
PPP	Purchasing Power Parity
PPA	Power Purchasing Agreement
PV	Photovoltaic
CO_2	Carbon dioxide
KV/KVA	Kilovolts/Kilovolts Amperes
DC/AC	Direct Current/Alternating Current
DOD	Depth of Discharge
LCOE	Levelized Cost of Energy
COE	Cost of Energy
MPPT	Maximum Power Point Tracker
LPSP	Loss of Power Supply Probability
NPC	Net Present Cost
NPV	Net Present Value
β/α/λ	beta/alpha/lambda
km/mm	Kilometre/Millimetre
m/s	meters per second
$ (USD)	United States dollars
€	Euro

CHAPTER ONE

INTRODUCTION

1.1 Background and motivation

Reliable energy supply is fundamental to the sustenance of the economic development of any nation. Access to adequate energy services can contribute immensely to poverty eradication, improved public health, food security; enhance education and income generation [1]. Irrespective of the source, electricity is the basis for development. It is one of the reliable and cleanest energy transfer option [2]. Increased availability of electricity and access to it contribute greatly to improvement of health, education, telecommunication and economic growth. In the present situation of the high fluctuation in electricity prices and due to the projected increase in the world's population and the economic and industrial growth of developing countries, the global power demand is anticipated to rise substantially in the foreseeable future. Also there are worries over fossil fuel exhaustion and increased alertness of the emission of greenhouse gases. Reducing greenhouse gas releases from the use of energy obtained from fossil fuels is necessary in order to tackle climate change and achieve global sustainability. Meeting this world's growing need for energy while mitigating the climate change effects is one of the greatest demanding challenges of our time.

According to [3], Access to energy is the "golden thread" that intertwines together environmental sustainability, economic and human development. Over the years, energy has been known to be crucial for the existence of man.

Slowly, the world is developing different types of energy systems but the challenges remain in three key areas – affordability, reliability and sustainability. The IEA had projected that the increase in the activities in developing countries and the estimated 1.7 billion persons added to the world in mostly urban areas in this developing countries, the energy demand will increase across the globe by 2040 by a value greater than a quarter [3]. Minus the continuous improvement in this sector in the areas of energy efficiency and energy conservation, this increase would double as large. As of 2000, 40% of the world energy demand was attributed to North America and Europe and 20% to developing countries in Asia. The report showed that this energy demand proportion would be reversed by 2040 with Asia and Africa demanding the most.

Electricity access rate has increased substantially over the last few decades. This access rate increased mostly in China and India and this increase is as a result of the swift increase in economic growth of many developing countries, urbanisation increase and several on-going energy programmes for energy accessibility. However, majority of the global population is yet to gain access to electricity. The IEA World Energy Outlook in 2017 estimated that 1.1 billion people (about 14% of world's population) do not have access to electricity while many others are subjected under unreliable electrical energy supply. Table 1.1 shows the regional summary of electricity access. Approximately 84% of the population without access to electricity dwell in rural areas while about 95% of this population are from different countries in Sub-Sahara Africa and Asia. There are progressive moves being made to extend electrical grid to urban and rural locations but the completion is still far-fetched. Since 2000, electricity access in urban and rural areas location across this regions remains in the ratio 2:1.

SOURCE: IEA, Energy Access Outlook 2017

Electricity Access, Regional Summary

	Rate of access						Population without access (million)
	National				Urban	Rural	
	2000	2005	2010	2016	2016	2016	2016
WORLD	73%	76%	82%	86%	96%	73%	1060
Developing Countries	64%	69%	76%	82%	94%	70%	1060
Africa	34%	39%	43%	52%	77%	32%	588
North Africa	90%	96%	99%	100%	100%	99%	<1
Sub-Saharan Africa	23%	27%	32%	43%	71%	23%	588
Developing Asia	67%	74%	83%	89%	97%	81%	439
China	99%	99%	99%	100%	100%	100%	-
India	43%	58%	66%	82%	97%	74%	239
Indonesia	53%	56%	67%	91%	99%	82%	23
Other Southeast Asia	67%	76%	83%	89%	97%	82%	42
Other Developing Asia	32%	39%	53%	73%	87%	65%	135
Central and South America	87%	91%	94%	97%	98%	86%	17
Middle East	91%	80%	91%	93%	98%	79%	17

Table 1. 1 Regional Summary of World Electricity Access [3]

From table 1.1, it can be seen that the population yet to be supplied with electricity in sub-Sahara Africa is the greatest across the world with a value of about 588 million with rate of access of 71% and 23% for urban and rural location respectively in 2016.

The global electricity has been generated from various sources. About 60% of the global electricity is generated through the process of burning fossil fuels and large amount also from coal, natural gas and oil [4]. There problems associated from power generation from these sources including, their ability to deplete in the future and the release of harmful gases which pollute the environment and contribute immensely to climate change.

The gases released by burning of fossil fuels are harmful to plant and animal and due to the increasing concern over this problem; Scientists and Researchers have been working

vehemently towards adequate harnessing of renewable energy sources to alleviate the problem of climate change and meet the increasing demand for energy. Energy that when used can be replenished naturally is known as Renewable energy. They include energy from the sun, geothermal energy, wind energy, tides, waves etc. These sources can provide energy in different important areas including electricity generation, thermal energy utilization, transportation etc.

They are also abundant in nature, free of cost and non-pollutant. The most widely used of them all are the Wind and Solar energy which are otherwise referred to as "Variable Renewable Energy Sources (VRES)" as a result of their great potential naturally.

In the process of Utilization of Renewable energy resources we have to face some challenges like reliability, cost, efficiency and Stability [8]. The main challenges facing renewable energy resources are their inconsistency and fluctuations in nature and their dependency upon weather and atmospheric conditions. In order to provide continuous and reliable power supply we integrate two or more resources and provide power banking system.

Off-the-grid electricity generation system is system designed to provide support for people in remote infrastructure to function without an electric grid and also to be used as cost-effective substitute to grid extension. In this context, off-grid power systems refer to stand-alone electrical power systems configured to provide electricity to a smaller community, institution or an organisation with electricity. A hybrid system on the other hand uses one or the combination of renewable energy sources as principal energy sources and a traditional fossil fuel-based or biofuel-based generator as a backup source [4]. This type of system provides reliability, cost effectiveness, efficiency and Stability of electric power supply.

1.2 Problem Statement

Generally, electricity supply faces great challenges. First, the power generation is less than the power demand and secondly, the terrain of some places especially in the rural areas makes it difficult extending the national grid to the places even if the power generation is enough to meet the demand. Supplying power to these remote places through the extension of transmission lines from the national grid is laborious, time intensive and consequently capital intensive [8]. Also minimising losses due to transmission and distribution can be expensive and involving.

In Kenya, the Urban and Industrial centres are powered by electrical energy. Lack or limited supply of this energy will cause a drastic decline in economic activities and hence the growth and development of the country. Due to the fluctuation of price of electricity in Kenya and its high cost, many institutions and organisations tend to run on a very high operating and maintenance costs. This has impacted negatively on our lecturers and students by retarding learning and research directly and indirectly. Research in renewables and hybrid energy systems are limited in this country. At the moment, generation capacity of 19MW, which translates to about 0.81% of the total electricity generation capacity, is from off-grid [9, 10]. Although some quality research papers have been done on renewable energy in the country, the researchers focused on the valuation of resources potential, policies and regulations etc. The current population of Kenya is approximately 51 million with about 9 million households as of August 16, 2018, according to the United Nations estimates [5]. Out of these 9 million households, only 6.2 million on the approximate is connected to electricity [6]. Over 60% of power generation in Kenya is through hydro-electric power [7.] This depends tremendously on rain water for electric generation. Due to the constant fluctuations of weather, climate change has become a great challenge to countries like Kenya implying that other sources of

power should be investigated for powering rural communities and various research institutions

1.3 Research Questions

What are the feasibilities (technical, economic and environmental) of renewable energy based hybrid systems for electrification in Institutions and Industries in Nairobi? How can the high cost of energy be reduced in Institutional Buildings in Kenya?

1.4 Research Hypothesis

The electric power generation in Kenya meant to power the population of approximately 51 million, including homes, industries and institutions is insufficient despite the existence and high potential of renewable energy. Renewable energy based hybrid systems can improve energy access in School of Engineering, University of Nairobi.

1.5 Research Goal and Objectives

The key goal of this Research is to determine the optimum off-grid and on-grid techno-economic design of a hybrid Renewable Energy system that can supply stable, affordable and reliable electricity to the School of Engineering, University of Nairobi. To comparatively asses the feasibilities of hybrid renewable energy systems (PV/Wind/Diesel generator) for reliable energy supply to this establishment. The following objectives will be achieved in order to accomplish this goal:

- Determination of the load profile of the site and the renewable energy resources potential.
- Find the appropriate renewable energy resources that would be used for modelling the suggested hybrid system and its component selection and costs.
- Modelling and simulation of the hybrid system in HOMER Pro software package.
- Optimization, sensitivity analysis and performance evaluation of the hybrid system in HOMER to determine the optimal hybrid system

1.6 Significance of the Study

- This study will improve significantly the technical and economic performance of electric power supply in the Institution.
- It will enhance the socio-economic benefits by improving stability and reliability of power supply.
- Provide alternative and sustainable solution to electrification in Kenya.
- It will serve as a policy tool for making useful energy policy and planning for the country.
- Contribute to sensitization on renewable energy awareness campaigns in Kenya and in the role of renewable in guaranteeing the country energy safety.
- Contribute to the improvement of the share of renewable energy in power generation in Kenya as well as serve as a tool to investors and attracts government attention for significant investment in the renewable energy sector.
- It will also add on the current knowledge on renewable energy and the alleviation of climate change in the country and the world at large.
- The method used in this research can be applied for designing optimum hybrid systems for any given area with renewable energy potential.

1.7 Limitations of Research

This study will focus mainly on determining the optimum capacities of hybrid renewable energy system components which can supply electricity to the selected establishment in Kenya and the techno-economic analysis of the system. The designed system has the following limitations

- The hybrid system is specifically for the selected location and will not be the optimal configuration for a different location where renewable energy potential is not the same as the selected location even if they have the same load profile.
- Due to the unavailability of other renewable energy resource data in the selected location, only solar and wind energy resources were considered.
- The study does not consider the issues related to the micro-grid stability and control
- The study does not address the complete design of the micro-grid powered by this hybrid system.

1.8 Key Assumption

For accomplishment of the goal and objectives of this research, the following assumptions were made

- Inflation rate for all costs has been considered the same throughout the lifetime of the project.
- Data from NASA meteorology database are sufficiently accurate for estimating PV and wind systems.
- The estimated deferred load is sufficiently accurate.
- The mean annual dissimilarities of solar irradiation and wind speeds occurring throughout the project lifespan remains the same

CHAPTER TWO

LITERATURE REVIEW

2.1 The Electrical Energy Situation in Kenya

The current total installed capacity of electrical energy in Kenya is 2,336.4MW with an effective installed capacity of 2,270MW [10]. The peak power demand amplified from 1,586MW in 2016 to 1,656MW in 2017 [6]. This demand is reported to have been increased to 1,802MW as at June 2018 [11]. Electricity generation is mostly obtained from hydro and burning of fossil fuel (thermal processes) with about 36% and 35% of the installed capacity respectively followed by geothermal with about 27%. At the moment there is no installed capacity from solar energy. Table 2.1 show the energy sources and statistics in Kenya while table 2.2 shows the generation and consumption trend between 2011 and 2016. The number of customers connected has increased from 4,890,373 in 2016 to 6,182,282 in 2017 [6].

Table 2. 1: Energy sources and statistics in Kenya [10]

S/NO.	Category	Capacity Installed (MW)	Percentage (%)
1	Hydro	820.7	35.12
2	Geothermal	627	26.84
3	Co-generation(biomass)	28	1.12
4	Wind	25.2	1.09
5	Thermal (fossil)	816.2	34.94
6	Off-grid	19	0.81
	Total	2336.4	100

Table 2. 2: Energy generation and consumption trend from 2011 to 2016 [10].

S/NO	INDICATOR	2010/11	2011/12	2012/13	2013/14	2014/15	2015/16
1	Installed Capacity (MW)	1,627	1,690	1,800	2,195	2,333	2,341
2	Effective Generation Capacity (MW)	1,539	1,611	1,723	2,095	2,263	2,270
3	Peak Demand in MW	1,194	1,236	1,354	1,464	1,512	1,586
4	Total Electricity Purchased (GWh)	7,303	7,670	8,087	8,840	9,280	
5	Total Electricity Sales(GWh)	6,123	6,341	6,581	7,244	7,655	7,912
6	System Losses as a % of Energy Purchased	16.2	17.3	18.6	18.1	17.5	19.4
7	Number of Customers Connected to Electricity	1,753,348	2,038,625	2,330,962	2,767,983	3,611,904	4,890,373

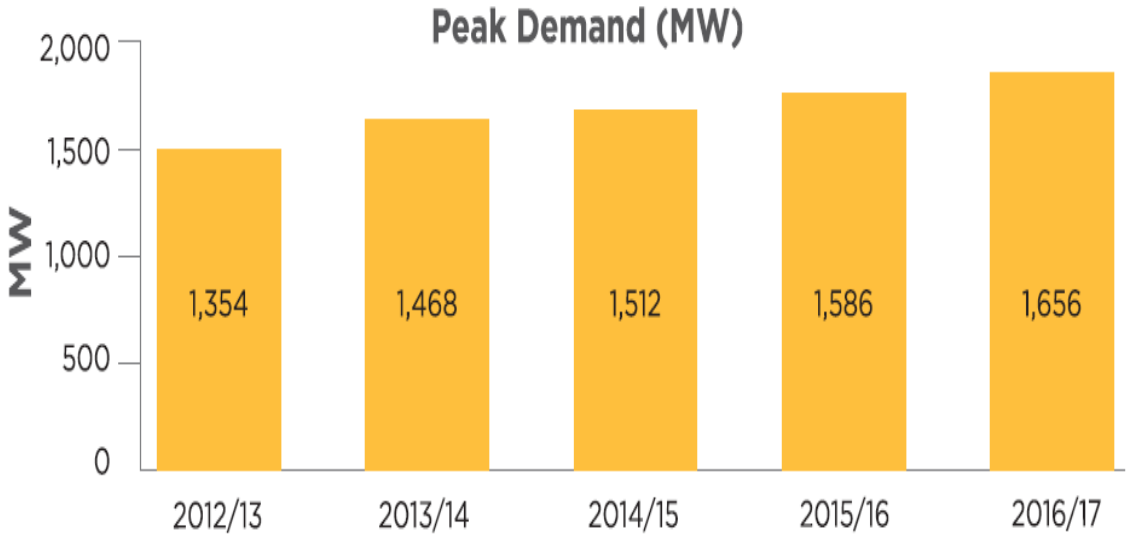

Figure 2. 1: Peak demand from 2013 to 2017 [6]

Recently, oil has been discovered in part of the country but at present, its exploration is yet to commence subjecting the country to importation of extensive amount of natural gas and fossil fuels for its power generation. Exploration of this discovered oil reserve in this country can change the rate of oil importation which is needed to meet about 35% of electricity demand as can see from table 2.1. As of the end of July 2018, electricity access rate in Kenya stands

at about 73%, making the country the highest in Sub-Sahara Africa in terms of electricity access. However, about 3.2 million households are yet to be connected [12]. It is projected that the electricity generation capacity and the power demand in Kenya will escalate to 19,200MW and 15,000MW respectively by 2030 [11].

2.2 Renewable Energy Potential in Kenya

As a developing country, Kenya has a fast growing economy and a growing energy demand. Research funded by the ministry of energy presented that Kenya has fantastic prospective in renewable energy power generation but has only tapped a little potion especially in the area of solar and wind. The government has engaged in seeking development on pwer generation from renewable energy in rural areas through the setup of Rural Electrification Authority (REA) owing to the abundant renewable energy sources. The government has also prioritized the expansion of geothermal energy and wind energy power generation plants together with solar grid-tied mini-grids for supplying power to rural areas [12]. However, the energy development plans for the country has remained slow in adopting most renewable energy into the generation mix.

2.2.1 Solar

Solar energy depends on nuclear fusion of the power originating from the innermost part of the Sun. Energy from the sun can be harnessed and transformed into other forms of energy in many ways. It can be utilised ranging from heating of water for domestic uses (solar water heating) up to electricity generation by converting the energy using photovoltaic cells. Kenya is blessed with a tremendous potential for solar energy including abundant space for it installations. The rate of solar isolation in Kenya is high as a result of mean peak sunshine hours ranging from 5 – 7. The average daily solar isolation in Kenya ranges from 4 – 6 kWh/m^2. Studies had shown that about 10 – 14% of the energy from sunlight in Kenya can be

converted to electricity depending on the PV cell efficiency [12]. Solar energy has been tapped has been tapped and utilised, however small in the form of solar standalone systems in Kenya. Approximately 220 schools at present have been supplied with solar standalone systems accounting for a total capacity of less than 1MW (approximately 574kW) [13]. Currently, tender has been passed for a more institutions of about 117 in number to be supplied power through standalone solar systems. 10 million Euros was also provided to the country by Spain to supply solar power to selected 380 institutions. These on-going projects are as a result of the high solar potential in Kenya. Figure 2.2 shows the solar Irradiation in Kenya.

2.2.2 Wind

Kenya is also blessed with fierce wind for power generation. According to [12], potential output is 22,476 TWh/year (greater than 20%), 4,446 TWh/year (greater than 30%) or 1,739 TWh/year (greater than 40%), depending on the turbine Capacity Factor (CF). Due to its landscape, some areas in Kenya possess outstanding wind speed. The wind speed in Kenya ranges from 5 – 9m/s depending on the location. Literature showed that the wind speed is the greatest at the northwest and some parts in the rift valley with mean wind speed standing at above 9m/s at a height of 50m. At 50m elevation, the wind speed is lowest in the coast ranging from 5 – 7m/s although these values are still promising. Figure 2.3 shows the speed of wind map of Kenya according to [14].

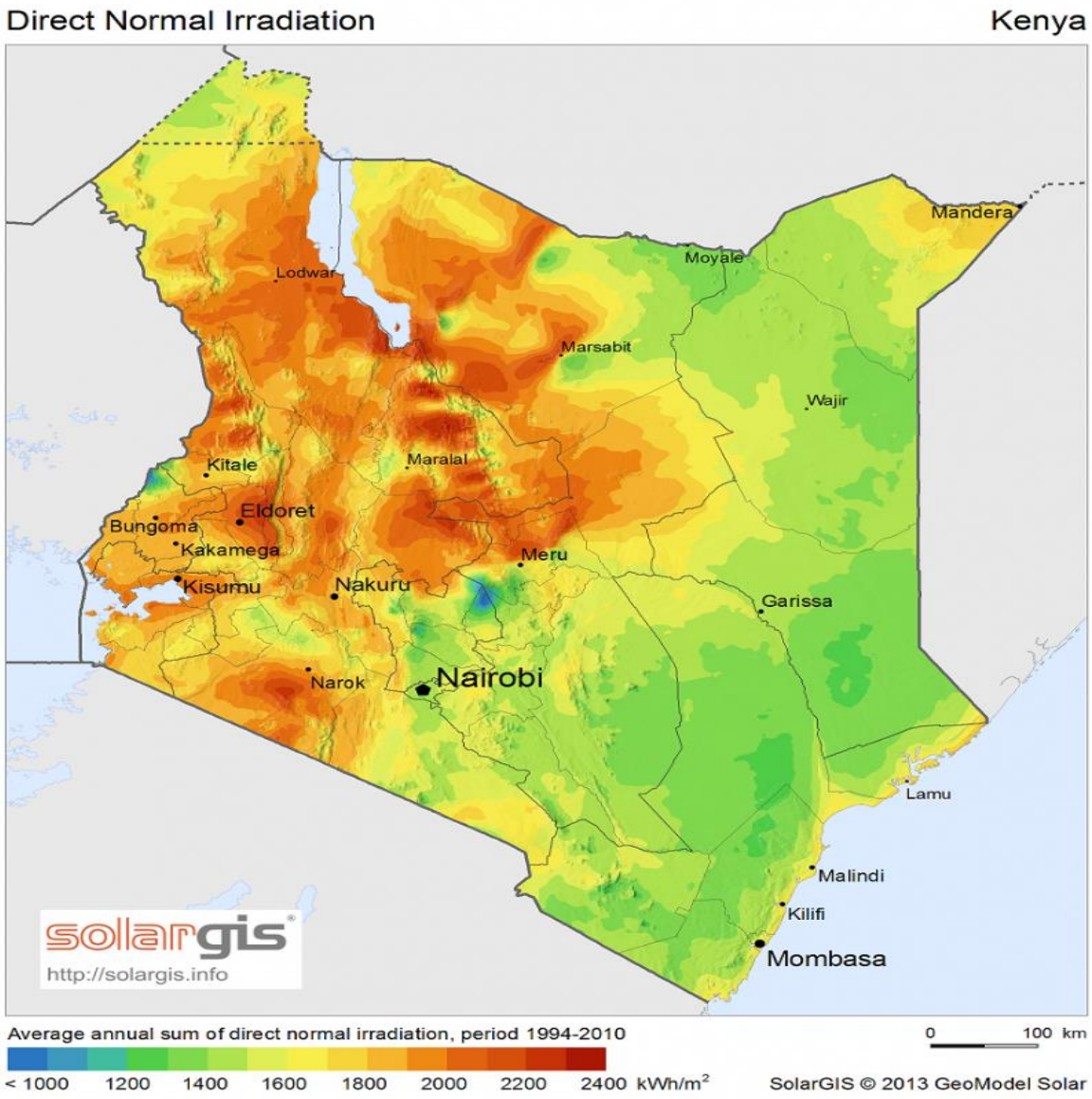

Figure 2. 2: Solar Irradiation in Kenya (Source: GeoModel Solar)

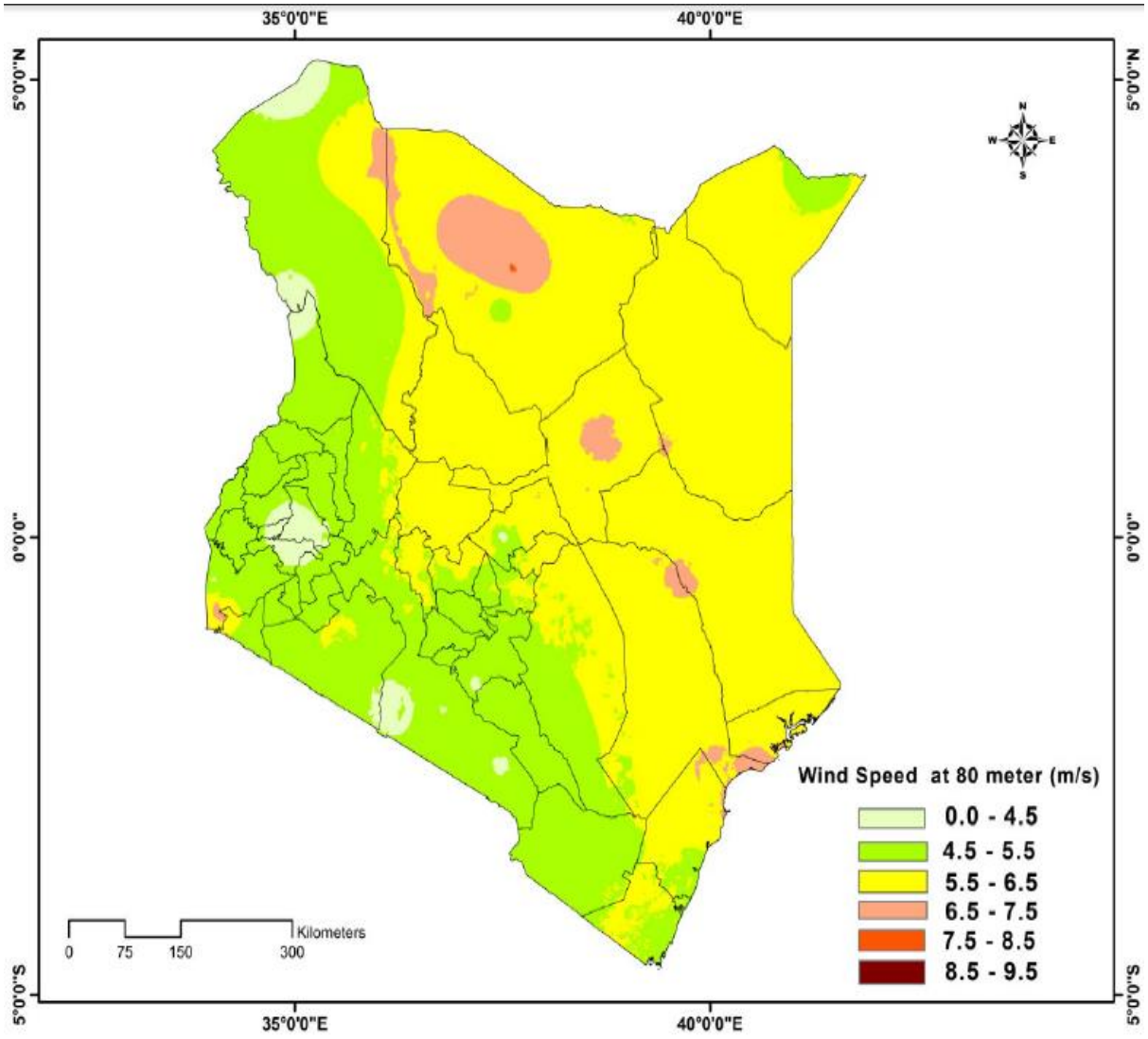

Figure 2. 3: Wind speed map of Kenya [14].

2.2.3 Biomass

The Energy from plants is what is known as biomass. It is the conventional type of energy used in most countries of the world although it poses great challenges since it releases a considerable amount of harmful gases to the atmosphere as a result of burning dry trees in the process of its utilization either for cooking or for heating (warmth). In modernized way, use biomass has been utilised in methane generation and alcohol production used in automobile fuel and in electrically driven power plants.

According to the Energy Regulatory Commission (ERC), Kenya, biomass influences its final demand for energy. About 70% of the energy demand in Kenya is biomass with it contributing above 90% of the energy demand in the rural communities. The source of this energy is mainly from agricultural wastes including charcoal, sawdust and wood fuel [15]. Biomass is widely used in industries in Kenya such as in tea factories as wood fuel to provide heat, and in brick burning. Charcoal industry in Kenya employs approximately 1 million people across the value chain on a part- and full-time basis contributing about USD 1.3 billion to the national economy. The regulation of the biomass sector is essential in ensuring sustainability. However, attempts to have high-level policy support have not been possible due political sensitivity of the matter. In addition, the government agencies required to spearhead the process lack coherence making it difficult to develop a comprehensive regulatory framework.

2.2.4 Hydropower

Water from a certain height falls on a turbine which initiates kinetic energy used to drive the turbine connected to a generator for power production. Kenya has been known for power production through hydro. Its history goes back to 1940s when the first dams were developed in Masinga along the Tana River Basin. It current percentage in the generation mix is 35.12% (table 2.1).

2.2.5 Geothermal Energy

Kenya has a great potential for geothermal energy. Currently, she is the leading country in Africa Kenya in terms of geothermal energy generation. This source of energy is found at the Great Rift Valley of the country. As at 2018, Kenya has total installed geothermal power generation capacity of about 627MW accounting for about 27% of its total power generation capacity (table 2.1). Currently, the total geothermal potential in Kenya stands at values ranging from a minimum of 7,000MW to maximum of 10,000MW with about

2,000MW existing in the Rift Valley. In 2030, Kenya aims to have about 5,530MW geothermal installed capacity which would make the country best in terms of clean energy generation in Africa.

2.2.6 Biogas

Biogas is another source of energy that is widely used in Kenya. The country has about 8000 biogas plants which utilises several materials including wastes from agriculture, animal wastes and other wastes such as the municipal wastes. Although this source of energy is widely used in Kenya, its production lacks documentation giving rise to the country not able to estimate the total capacity in use. In the country, this source of energy originates from tea production, sisal and municipal wastes. There have been power production (between 29 -131 MW) recorded from this energy source but at the moment, none has been inculcated into the national grid. However, the government is currently working on formulating standards to enable adequate harnessing of this energy. The potential of biogas in Kenya stands above 1000MW [12].

2.3 Review of Related Studies

Hybrid power generation has been done in many countries in the last few decades to provide electricity that can power discrete communities and institutions. Determination of optimum hybrid renewable energy systems for reliability and cost effective power solution has become an area of great interest due to the high increase in the use of off-grid and on-grid renewable and non-renewable energy systems. The purpose of this literature review is to provide evidence that validates the necessity for this study and to assist as sustenance for the methods utilised in this present study.

K.M. Iroma Udumbara [4] carried out study on the technical and economic sizing of hybrid energy systems for provision of power to rural areas of Sri Lanka. The aim of this study was to come up with the best system that can supply affordable and reliable power to this

location. The location has a total number of 150 households with mean daily power usage of 270kWh and peak demand of 25kW. The analysis of the data and the sizing of this system were done in HOMER energy software. A hybrid power system comprising of diesel generator, batteries, wind turbine ad solar PV was identified. His findings gave a considerable COE and also proved that on reduction of O&M costs which are viable for most renewable energy power systems, the energy cost would be $0.2/kwh which is affordable to the rural dwellers.

Munuswamy et al. [16] carried out comparison of the electricity cost of fuel cell based power generation with grid power cost. This research was carried out for a health centre located in the rural area of India using HOMER simulations. The aim of this research was to determine which one of this power supplies is cheaper. The results for the study illustrate that off-grid power generation and supply is cheaper at a distance greater than 44km.

Rohit Sen and Subhes C.B [17] using HOMER energy software, carried out studies on an off-grid power generation the use of renewable energy sources/technologies with the renewable energy technologies in India. The objective of the study was suggest optimal hybrid technological combination that can be used effectively in the combination of different renewable energy sources to generate power which is connected to the nation grid in order to meet the electricity demand of a village in India with a high degree of reliability and affordability. The result of this study showed that off-grid power generation for power supplies in rural areas is cost-effective than the extension of conventional grid to these areas. The study also showed that adopting this method will contribute towards reduction of greenhouse gas emissions and consequently tackle climate change.

Another interesting study related to this present study is the analysis carried out by Hafez and Bhattacharya [18]. The paper designed and analysed a hybrid power system for a rural community with a base load of 600kW load demand and peak load of 1183kW. The

maximum consumption of this community was 5000kWh/day. The study aimed to simulate several systems that can meet this peak load and consumption and select the best. The VRES where considered together with energy sources from diesel and hydro. The simulation of the data was done in HOMER energy software considering 24 hours power consumption which made the result unrealistic.

Also, Lau et al. [19] with the use of HOMER software carried out analysis for the case of a rural area located in Malaysia. The aim of the study was to evaluate the economic viability of an off-grid power system based on renewable energy. 40 households were assumed for this location with peak power demand of 80kW and base load of 30kW. The assumptions made on this study and the methods applied to estimate the load profile of this location is made the research unrealistic because the system design may have been oversized or undersized.

Izael D.S. et al published a report on the 600kW solar grid-tied system project carried out at the Strathmore University, Kenya. The project aimed to reduce the amount of greenhouse gas emission from Institutional Buildings located in the Sub-Sahara Africa. The 600kW project was successful and the Institution was able to sign a Power Purchasing Agreement (PPA) with the Kenyan Power and Lighting Company (KPLC). However, the method used to establish the load profile of the establishment and the renewable energy data remains unclear.

In the literatures reviewed, there has been a problem of establishing the load profile of the sites. This resulted in many of the results obtained becoming unrealistic. This present study will use Power and energy logger and real time monitoring such as the eGuage to establish the load profile. Another flaw of the previous studies is the sensitivity analysis. Many of them had not taken into account how change in say, the fuel price will affect the power production and the cost of the system. Also the as a result of climate change, the solar and wind data will vary in years to come therefore it is necessary to consider these changes during the design of these systems. The present study takes into account of the above scenarios by carrying out sensitivity analysis to come up with how the system and its parameters are affected when

there is any change in the future. In many part of the globe, cost of CO_2 emissions has been attached to both independent and dependent power producers in the form of tax, especially in the Europe. Many literatures had not considered the effects of this CO_2 emission taxation and how it affects the Net Present Cost of the System. In the present study, this will be considered. Also, many literatures have focused on either off-grid power generation combining different renewable energy sources. It is important to become aware that even if power is available in the cities, it is not cost effective. Therefore it is of great interest to examine how grid-tied systems will help reduce the cost of electricity in these urban regions.

This study will focus on the determination of the superlative combination or arrangement of hybrid systems based on renewable energy sources with a back-up diesel generator in the form of an off-grid and on-grid power generation to achieve the objective of this project. HOMER PRO and HOMER grid shall be used as tools for analysis. HOMER PRO is the modification of the original HOMER software which had been used in the analysis of other works. This modified software is capable of analyzing the data using several sources and variables. The software is also able to download accurately the renewable energy resource data of any site given the geographical coordinate of the area.

2.4 Renewable Energy Systems

2.4.1 Solar Photovoltaic Systems

There are three basic types of solar PV systems: grid-tied system, standalone system and hybrid PV system. Standalone systems are mostly applicable in small scale applications such as solar home systems, used for provision of energy to small and large businesses, schools, hotels, hospitals etc. especially in isolated places. The grid connected systems mainly used for large scale solar power generation, mini grid systems and in some solar home systems where the energy in excess is channelled back to the conventional grid and vice versa. The hybrid solar PV systems involve the using solar PV in combination with other sources of

renewable energy. Depending on the efficiency of the PV module, the cell can convert 10 – 14% of solar irradiation to electricity. They also have a lifetime of more than 25 years after which it can be recycled. It does not produce noise or pollute the environment [20].

Figure 2.4 shows the functioning of photovoltaic cell. As sunlight hits the cell, electric field is created across the films which give rise to the production of electrons (electricity) to flow. The higher the intensity of the sun, the higher the electricity production

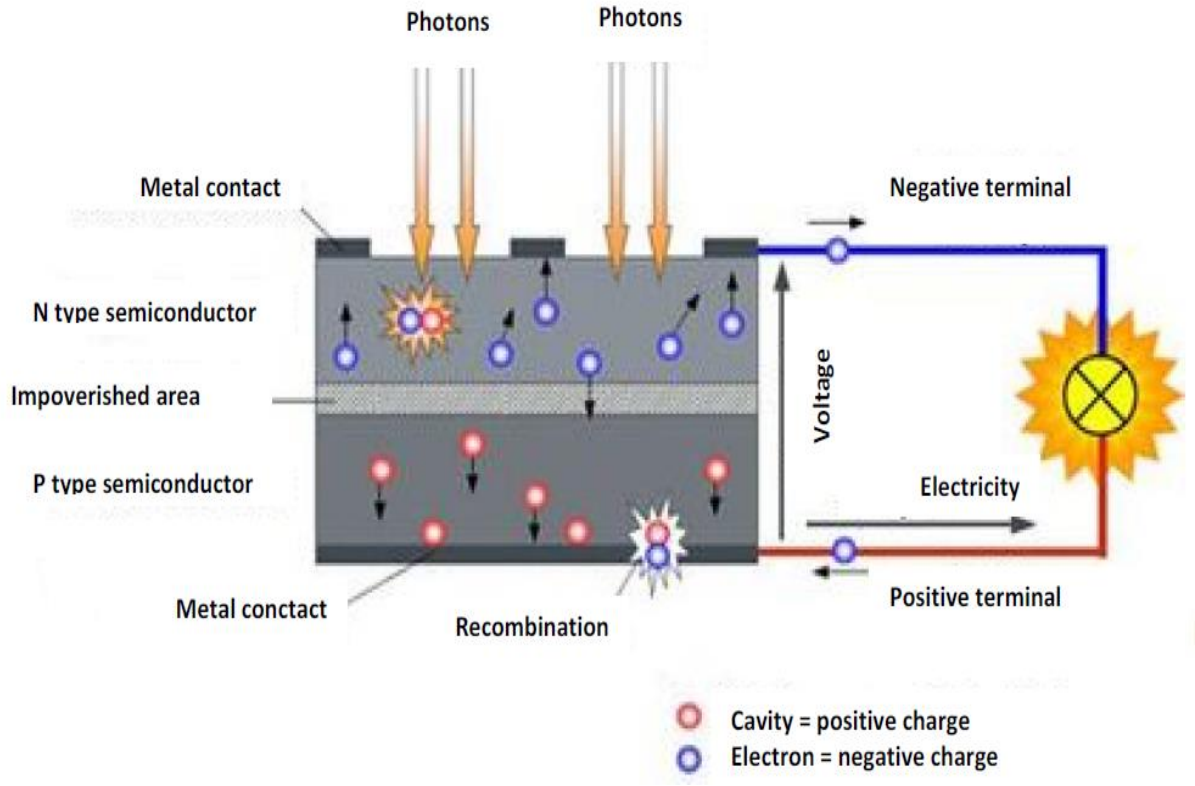

Figure 2. 4: Functioning of the Photovoltaic cell [20].

2.4.3 Electrical Characteristics of PV Cells

Given the electric circuit in figure 2.5 below, the following equation which describes the Current-Voltage characteristics of PV cells is derived [27].

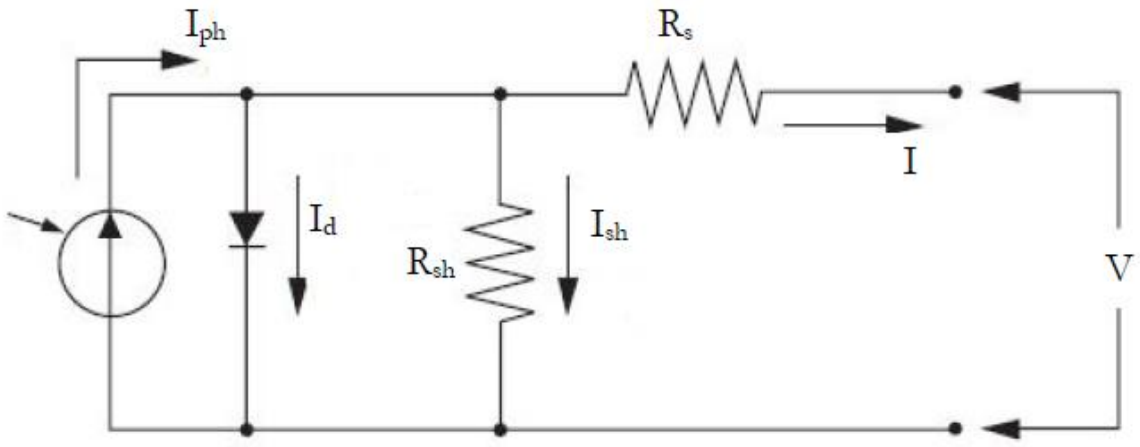

Figure 2. 5: Equivalent circuit of a PV module

$$I = I_{ph} - I_0 \left[\exp\left(\frac{V + IR_s}{K_B T / q} \right) - 1 \right] - \frac{V + IR_s}{R_{sh}} \qquad 2.1$$

Where:

I_0 is the diode saturation current (A)

K_B is the Boltzmann constant (1.38×10^{-23} m^2 kg s^{-2} K^{-1})

T is the absolute temperature (K)

I is the load current (A)

V is the voltage at the terminals of the cell (V)

q is the electronic charge (C)

The photo current I_{ph} has a relationship with the photon flux that is incident on the cell which also has a dependable relationship with the light's wavelength. Series resistance (R_s) stands for the internal resistance which opposes the flow of current and is dependent on the depth of the p-n junction together with the contact resistance and the impurities. The shunt resistance, R_{sh} is related inversely to the current leaking to the earth. On some occasions, current leakage to the ground and small diode can be neglected in the equivalent electrical circuit. This implies that the short circuit current *Isc* becomes equal to the photon generated current, therefore open circuit voltage becomes;

$$V_{oc} = \frac{K_B T}{q|} \ln\left(1 + \frac{I_{ph}}{I_0}\right) \quad 2.2$$

2.4.4 PV Cell Temperature

PV array has a temperature that exists at its surface which is regarded as the Photovoltaic cell temperature. This temperature remains the same as the ambient temperature during the night but during the day, when the sun is at its peak, it exceeds the ambient temperature with about 30^0C or greater. The formula below gives the relationship for calculating the cell temperature and the radiation incident on the PV array according to [28].

$$\tau\alpha\, G_T = \eta_c G_T + U_L (T_c - T_a) \quad 2.3$$

where:

τ = the solar transmittance of any cover over the PV array [%]

α = the solar absorptance of the PV array [%]

G_T = the solar radiation striking the PV array [kW/m2]

η_c = the electrical conversion efficiency of the PV array [%]

U_L = the coefficient of heat transfer to the surroundings [kW/m2°C]

T_c = the PV cell temperature [°C]

T_a = the ambient temperature [°C]

Equation 2.3 shows that there is a balance which exists between the absorbed solar energy by the PV cell and the electrical production in addition with the transfer of heat to the surrounding. Equation 2.3 can be solved to arrive at equation 2.4:

$$T_c = T_a + G_T\left(\frac{\tau\alpha}{U_L}\right)\left(1 - \frac{\eta_c}{\tau\alpha}\right) \quad 2.4$$

Measuring τ_α/U_L directly is difficult so the nominal operating temperature from manufacturer is used to arrive at equation 2.5.

$$\frac{\tau\alpha}{U_L} = \frac{T_{c,NOCT} - T_{a,NOCT}}{G_{T,NOCT}} \qquad 2.5$$

where:

$T_{c,NOCT}$ = the nominal operating cell temperature [°C]

$T_{a,NOCT}$ = the ambient temperature at which the NOCT is defined [20°C]

$G_{T,NOCT}$ = the solar radiation at which the NOCT is defined [0.8 kW/m2]

If we assume that τα/UL is constant, we can substitute this equation into the cell temperature equation to yield:

$$T_c = T_a + G_T\left(\frac{T_{c,NOCT} - T_{a,NOCT}}{G_{T,NOCT}}\right)\left(1 - \frac{\eta_c}{\tau\alpha}\right) \qquad 2.6$$

The value of τ_α is assumed to be 0.9 in HOMER. Another assumption made in HOMER is that the PV efficiency is always equal to the maximum point efficiency in the same way it operates in concentrated PV cells with Maximum Point Tracker. This implies that the maximum power point efficiency is at all times same as the cell efficiency hence:

$$\eta_c = \eta_{mp} \qquad 2.7$$

where:

η_{mp} = the efficiency of the PV array at its maximum power point [%]

So in the equation for cell temperature, we can replace ηc with ηmp to yield:

$$T_c = T_a + \left(T_{c,NOCT} - T_{a,NOCT}\right)\left(\frac{G_T}{G_{T,NOCT}}\right)\left(1 - \frac{\eta_{mp}}{\tau\alpha}\right) \qquad 2.8$$

There is linear variation between the efficiency (η_{mp}) and the temperature (T_c) according to equation 2.9.

$$\eta_{mp} = \eta_{mp,STC}\left[1 + \alpha_P\left(T_c - T_{c,STC}\right)\right] \quad 2.9$$

where:

$\eta_{mp,STC}$ = the maximum power point efficiency under standard test conditions [%]

α_P = the temperature coefficient of power [%/°C]

$T_{c,STC}$ = the cell temperature under standard test conditions [25°C]

Substituting the efficiency equation (equation 2.9) into the cell temperature equation and solving for T_c we obtain equation 2.10. The efficiency of PV cell drops with a rise in cell temperature. This is because the coefficient of power is always negative.

$$T_c = \frac{T_a + \left(T_{c,NOCT} - T_{a,NOCT}\right)\left(\frac{G_T}{G_{T,NOCT}}\right)\left[1 - \frac{\eta_{mp,STC}\left(1 - \alpha_P T_{c,STC}\right)}{\tau\alpha}\right]}{1 + \left(T_{c,NOCT} - T_{a,NOCT}\right)\left(\frac{G_T}{G_{T,NOCT}}\right)\left(\frac{\alpha_P \eta_{mp,STC}}{\tau\alpha}\right)} \quad 2.10$$

In this study, the cell temperature was calculated in each time step of 1 hour.

2.4.5 The PV power output

Equation 2.11 can be used to deduce the power output of the PV.

$$P_{pv} = Y_{pv} f_{pv}\left[\frac{\bar{G}_T}{\bar{G}_{T,STC}}\right]\left[1 + \propto_p \left(T_c - T_{c,STC}\right)\right] \quad 2.11$$

where:

Y_{PV} = the rated capacity of the PV array, meaning its power output under standard test conditions [kW]

f_{PV} = the PV derating factor [%]

$\overline{G}_T$ = the solar radiation incident on the PV array in the current time step [kW/m^2]

$\overline{G}_{T,STC}$ = the incident radiation at standard test conditions [1 kW/m^2]

α_P = the temperature coefficient of power [%/°C]

T_c = the PV cell temperature in the current time step [°C]

$T_{c,STC}$ = the PV cell temperature under standard test conditions [25°C]

Temperature coefficient of Power becomes zero if one chooses to neglect temperature effects during the modelling. In that case equation 2.11 becomes:

$$P_{pv} = Y_{pv} f_{pv} \left[\frac{\bar{G}_T}{\bar{G}_{T,STC}} \right] \qquad 2.12$$

2.5 Hybrid Energy System

By combination of Hybrid energy sources and their corresponding systems, power can be generated in form of DC/AC. This power is converted to AC or DC by the use of a two-way inverter and rectifier. Figure 2.6 shows a schematic of a typical energy system of hybrid. Hybrid energy systems can be linked in different ways to the electrical bus bars. Below are three different ways this can be linked.

- AC fixed hybrid system
- DC fixed Hybrid system
- AC/DC fixed hybrid system

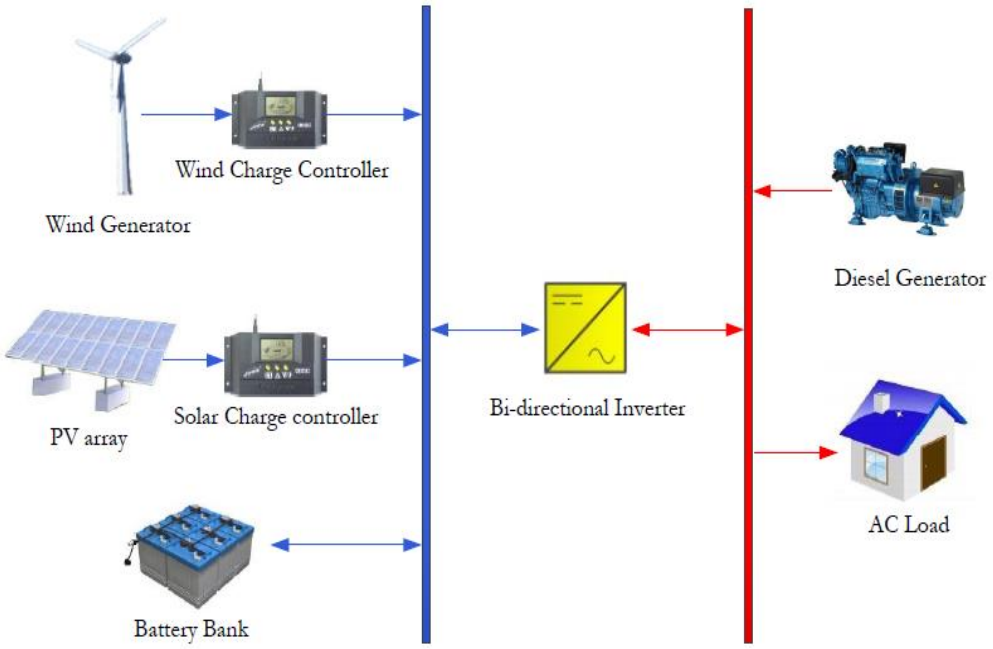

Figure 2. 6: Schematic representation of a hybrid energy system [4]

For the DC fixed system, all the electrical components are coupled to a single DC bus through the means of efficient circuits. The DC power has to be converted to AC by the use of inverters which can lead to the drop of the system efficiency. It also poses a great difficulty I sizing the inverter to supply to meet the peak power since it is almost impossible to operate the diesel generator in parallel with the inverter. The AC fixed system has all the components connected to the AC bus bar. This system also has losses due to the electrical energy conversion processes. AC/DC fixed system is the type of configuration where all the AC components are connected to the AC bus bar while all the DC electrical components are connected to the DC bus bar. The system is made up of both AC and DC bus bar with a two way inverter which enables the DC power to be converted to AC and AC power also converted back to DC in case energy stored in the battery storage bank drains. Figure 2.7 illustrates the types of hybrid systems in existence.

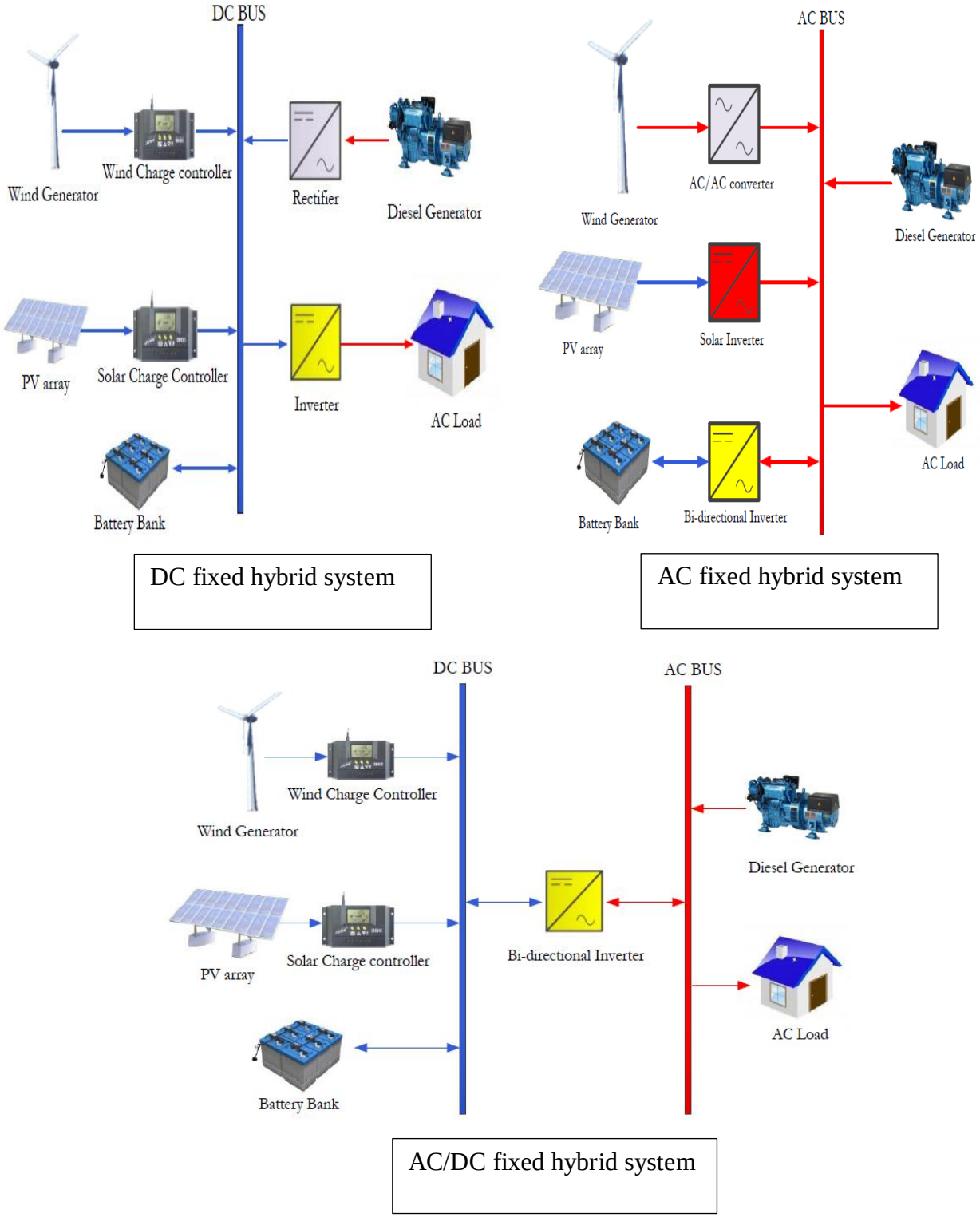

Figure 2. 7: Types of Hybrid System [4]

2.6 HOMER Energy

HOMER is an acronym standing for Hybrid Optimization of Multiple Energy Resources. It is a powerful computer software modelling tool for designing, simulating, and analysing off-grid and grid-connected electrical systems containing many combinations of renewable energy sources and conventional generators, run-off river hydropower, biomass power plant, micro-turbines, hydrogen storage, batteries, combined heat and power, fuel cells, boilers, electrolysers, AC/DC bi-directional converters and others, to serve both thermal and electric loads [22]. HOMER is used extensively for simulation and optimization power systems with a simple process. First, the software needs specification of the geographical coordinates of the site so as to download renewable energy data specifically for the location. The load profile of the site to be modelled is specified or imported from a time series file. Specification of the load profile can be done either manually for each month or assume a specific daily load profile (usually the peak day). System components (PV, wind turbine, grid, batteries, generators, charge controllers, inverters etc.) and their respective costs are also specified on the software interface. Economic constraints are also specified and sensitivity variables given. If the setting is done properly, simulation can be done. The time it takes to complete a simulation is dependent on the values of sensitivity variables specified. The result of the simulation is ranked in the software based on the economic criteria. Realistic of the result is dependent on how accurate the data specified in the software is.

2.7 HOMER Input Data

Analysis in Homer requires specification of data for example, energy resource data of the site, load data, components types and installations (including size, costs, lifetime, replacement costs, maintenance costs, operation costs etc.), expected lifetime of the entire

project, inflation rate, discount rate, fuel cost, efficiency rate, etc. Figure 2.10 illustrates the summary of the fundamental input data in HOMER software.

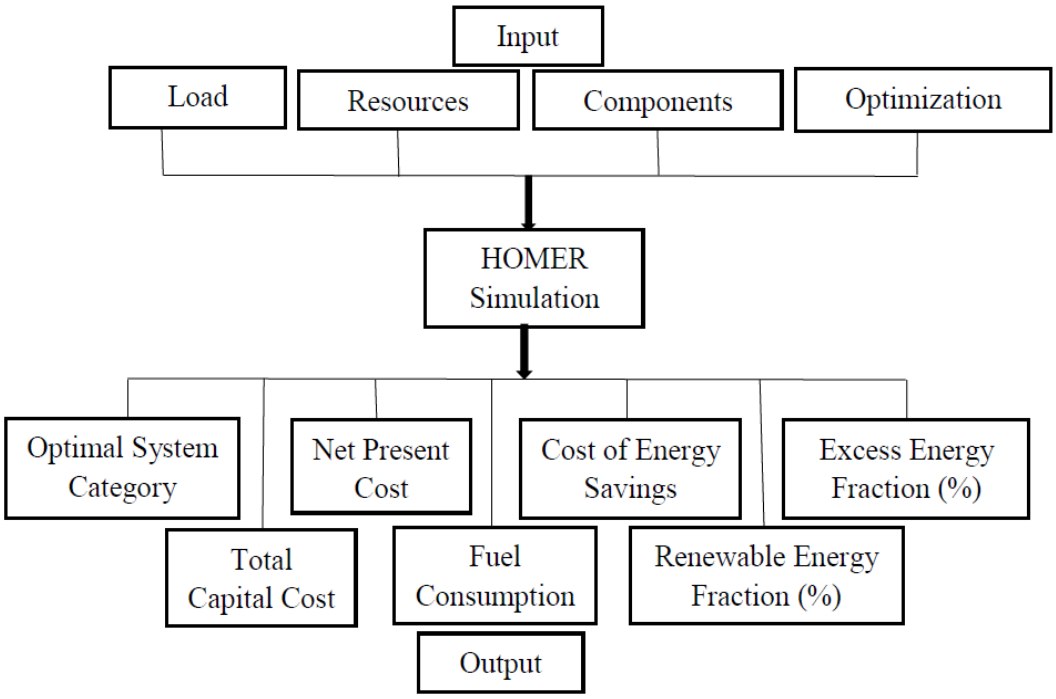

Figure 2. 8: HOMER input-output parameters.

CHAPTER THREE

RESEARCH METHODOLOGY AND PRILIMINARY FINDINGS

3.1 Description of the site

The School of Engineering University of Nairobi is located in Kenya on the Latitude of $1^{o}16.7'S$ and Longitude $36^{o}49.1'E$. The school has provided quality engineering teaching and research since it establishment in 1956 under the Royal Technical College. Students were admitted from all part of the world. The School consists of five departments which include department of Electrical and Information Engineering, department of Civil and Construction Engineering, department of Mechanical and Manufacturing Engineering, department of Environmental and Biosystems Engineering, department of Geospatial and Space Technology and the Institute of Nuclear Science and Technology. Power is supplied to school from KPLC transformer which has the mains located at the School power house. The power from this mains supply power to all laboratories and workshops together with other sections of the school including:

- Office of the dean, school of engineering
- Transport section
- Estate Management block
- Maintenance and construction section
- School Sacco section

Figure 3.1 shows the Google earth view of the school. Most of the power is consumed by the equipment in laboratories, workshops and offices. Lighting also consumes most of this power.

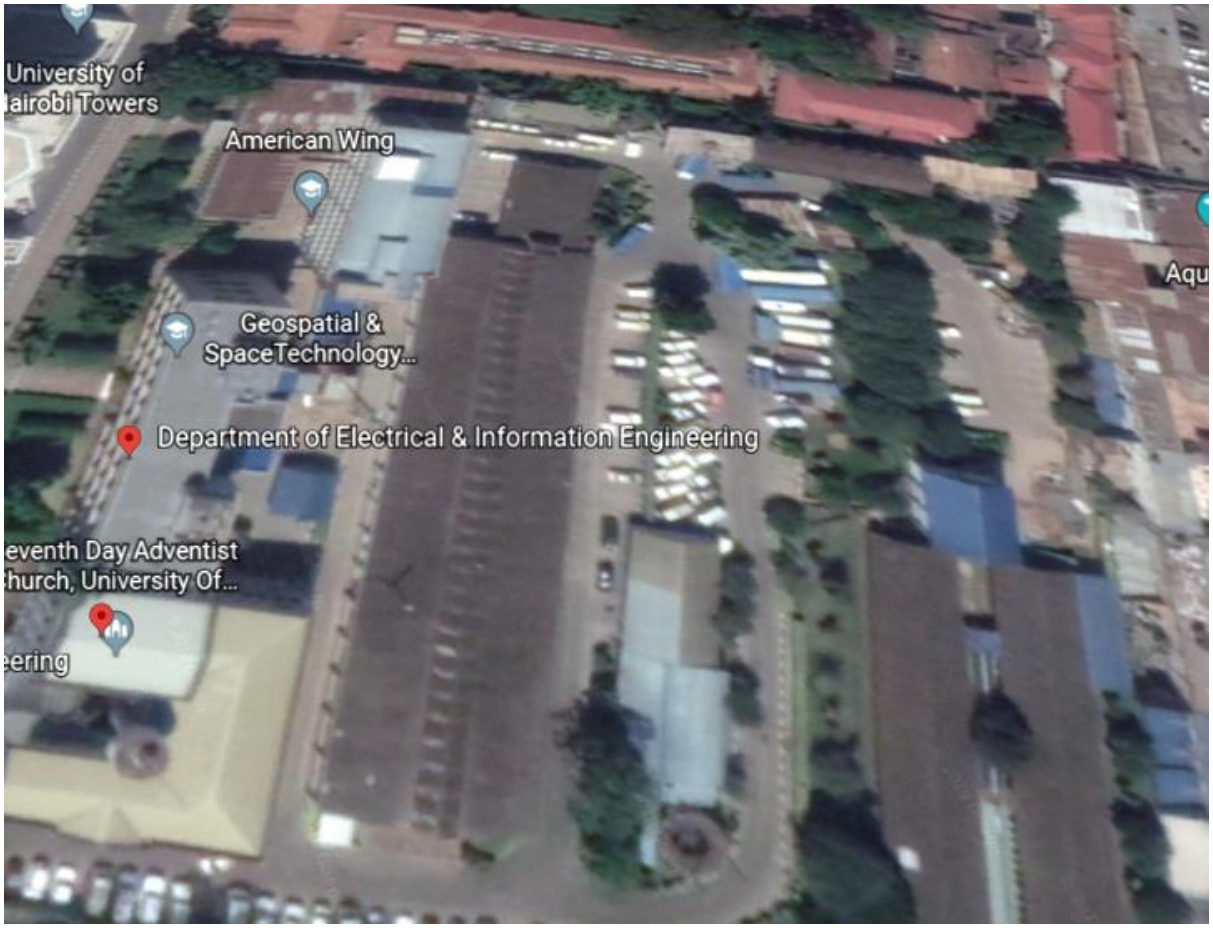

Figure 3. 1: School of Engineering (View from google earth)

3.2 Determination of the Load Profile of the School

The research method used to capture the energy demand and consumption data of the establishment primarily consists of the following three approaches:

- Obtaining the energy demand and consumption of the establishment from Kenya Power and Lighting Company (KPLC) for at least one year period in order to identify the suitable period (peak month) for monitoring.
- Studying the energy equipment used by the establishment to obtain their performance characteristics.
- Use of Power and Energy Logger to monitor the electrical power demand and consumption of the establishment from the mains during the peak month.

These approaches were used to establish the demand and consumption pattern of the school. Energy demand and consumption was monitored for a one month period (peak month), using

the PEL. The first two weeks was during the exam period when several activities such as printing, photocopying, night classes by students etc. are on in the school. The second two weeks was after the exam, during the fourth term of the school when activities are carried out daily in the laboratories and workshops. In addition, the renewable energy potential of the site was determined using HOMER software by inputting the geographical coordinates of the site.

3.2.1: Electricity Bill Analysis of the School

The electricity bill for the period of 13 months for the site was obtained and analysed. Table 3.1 shows the demand and consumption data of the school from July 2017 to July 2018 as obtained from the bills. The power factor is the ratio of demand in kW to the demand in kVA. From the analysis, the PF for this site is relatively above the minimum standard value of 0.9 set by Kenyan Government. The average monthly Electricity consumption at the School of Engineering, University of Nairobi stands at 27,851kWh which translates to average monthly bill of Ksh. 552,155.46. This demand and consumption from the bill is similar to the result from the monitoring. However the real time data logged with Power and Energy logger is used for analysis since it proves more realistic.

Table 3. 1 Demand and Consumption data of the school from July 2017 to July 2018 (energy bills)

	Demand		Consumption (kWh)						
Months	**kVA**	**kW**	**Low rate**	**High rate**	**Total**	**Bill days**	**kWh/day**	**Power factor**	**Total bill (kshs.)**
Jul-17	96	93	11,762	12,573	24,515	31	790.81	0.97	487,915.05
Aug. 2017	96	93	10,268	13,254	23,522	31	758.77	0.97	507,348.88
Sep. 2017	96	93	11,861	15,263	27,124	27	1004.59	0.97	533,041.00
Oct. 2017	96	93	11,582	14,983	26,565	29	916.03	0.97	535,313.00
Nov. 2017	96	93	10,246	12,872	23,118	19	1216.74	0.97	499,473.00
Dec. 2017	99	96	9,589	9,639	19,228	31	620.26	0.97	446,827.00
Jan. 2018	99	96	9,589	9,639	19,228	31	620.26	0.97	446,827.00
Feb. 2018	-	-	-	-	-	-	-	-	-
Mar-18	125	121	11,922	15,897	27,819	45	618.20	0.97	649,543.00
Apr-18	128	119	15,534	23,751	39,285	29	1354.66	0.93	868,222.00
May-18	128	120	16,984	24,892	41,876	31	1350.84	0.94	868,222.00
Jun-18	125	121	14,586	20,878	35,464	30	1182.13	0.97	758,091.00
Jul-18	90	66	12,980	13,488	26,468	31	853.81	0.73	577,198.00

552,155.46

Average Bill Per Month

3.3. Solar Resource

As discussed in chapter two, the mean peak sunshine hours in Kenya is 5-7 with mean daily solar isolation of 4-6 kWh/m^2. Electricity generation potential in Kenya from solar PV is far greater than what is consumed yearly from the national grid [23]. At the time of this research, the ground measured data was unavailable for the selected site therefore data from NASA surface meteorological database had been used.

3.3.1 Optimal Placement of Solar Arrays

Power produced from the PV array is dependent on the solar irradiation striking its surface which in overall is not horizontal. In every time step, the global solar irradiation striking the surface of the PV array is calculated. Description of this process has been demonstrated below based on the methodology used in [25]. Two important parameters are used to define the alignment of the PV array otherwise known as the PV orientation. First is the slope which is the angle between the PV panel and the horizontal and second is the azimuth which is the direction that the surface faces. In this study, due to the terrain of the site, the convention whereby azimuth of zero corresponds to due south and positive values corresponding to due west was adopted. Other important factors to be considered include the period of the year, period of the day and latitude. "The period of year affects the solar declination, which is the latitude at which the sun's rays are perpendicular to the earth's surface at solar noon". The solar declination angle is calculated using the following formula:

$$\delta = 23.45\sin\left(\frac{360(284+n)}{365}\right) 100 \quad 3.1$$

n is a value which represents the day of the year. The yearly change in solar declination angle from analysis is shown in Figure 3.2. The sign convention varies with the counter clockwise direction angles positive and clockwise direction angles negative.

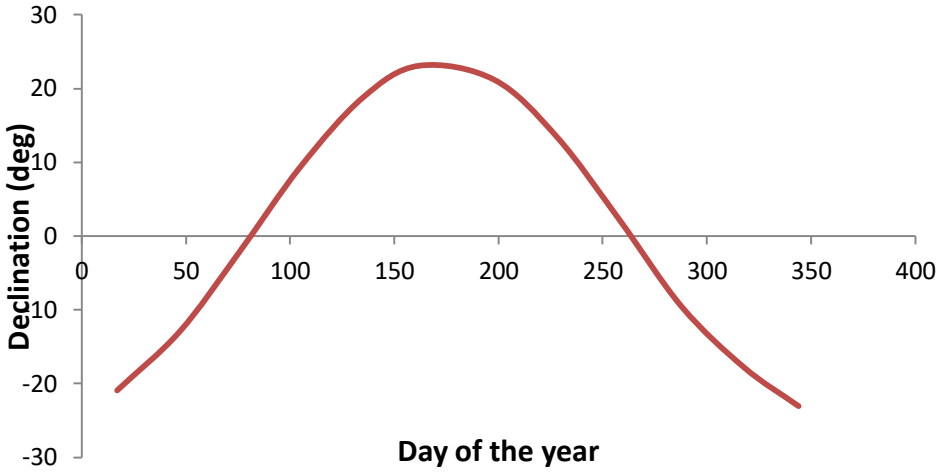

Figure 3. 2 Annual variation of the solar declination

The position of the sun in the sky is not constant because it is affected by the time of the day which is usually designated by a 60 minutes angle (1 hour). At noon, it is assumed that the sun is directly above our heads therefore HOMER assumes that this hour angle is zero at this time. Before solar noon it is zero it is negative while after solar noon it becomes positive. This hour angle is estimated using equation 3.2.

$$\omega = (t_s - 12hr).15^0/hr \qquad 3.2$$

t_s = solar time measured in hours. At solar noon, t_s is 12 hr and after 90 minutes, it becomes 13.5 hours. Recalling the fact that the sun moves 15 degree for every one hour, equation 3.2 is then validated.

3.3.2 Solar Radiation on a tilted PV Array

Estimation of the amount of solar radiation striking the PV array is important. To calculate this value, the global horizontal radiation data will be used as explained in [25].

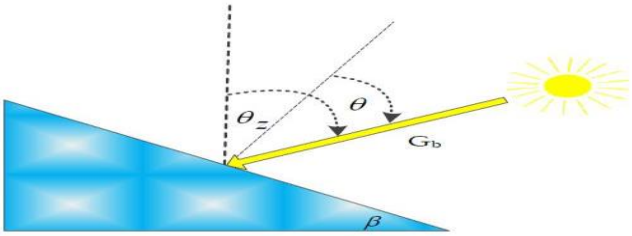

Figure 3. 3 Solar energy on inclined PV array analogy

It is assumed in HOMER that all data which depend on time (solar data and electrical load data) are given in civil time, which is referred to as local standard time and not in solar time. The Solar time from civil time is then calculated using equation 3.3

$$t_s = t_c + \frac{\lambda}{15°/\text{hr}} - Z_c + E \tag{3.3}$$

where:

t_c = the civil time in hours corresponding to the midpoint of the time step [hr]

λ = the longitude [°]

Z_c = the time zone in hours east of GMT [hr]

E = the equation of time [hr]

It is important to note that the longitude towards west is negative together with the time zones west of the Greenwich Mean Time (GMT). Since time is an important factor in this estimation, equation of time will be considered. It takes into account the effects of obliquity and how the peculiarity of the orbit of the earth. Equation of time is given in equation 3.4

$$E = 3.82\begin{pmatrix} 0.000075 + 0.001868 \cdot \cos B - 0.032077 \cdot \sin B \\ -0.014615 \cdot \cos 2B - 0.04089 \cdot \sin 2B \end{pmatrix} \tag{3.4}$$

The parameter B can be deduced as follows:

$$B = 360^o \frac{(n-1)}{365} \tag{3.5}$$

Where *n* represents the day of the year, beginning with day one of the month

Angle of incidence is the angle between the beam of the sun and the normal to the surface. Since many surfaces are oriented, the angle of incidence can be defined as follows in equation 3.6:

$$\cos\theta = \sin\delta \sin\varphi \cos\beta - \sin\delta \cos\varphi \sin\beta \cos\gamma + \cos\delta \cos\varphi \cos\beta \cos\omega + \cos\delta \sin\varphi \sin\beta \cos\omega + \cos\delta \sin\beta \sin\gamma \sin\omega \quad 3.6$$

θ = the angle of incidence [°]

β = the slope of the surface [°]

γ = the azimuth of the surface [°]

φ = the latitude [°]

δ = the solar declination [°]

ω = the hour angle [°]

Another important incidence angle is the zenith angle. This is the angle between the vertical line and the rays of the sun. At solar noon, the zenith angle (Q_z) is zero but 90° when the sun is at the horizon. The Zenith angle can then be derived by setting $\sin\beta$ = 0° in equation 3.6. This is because for a horizontal line or surface, there exist a zero slope. The zenith angle is therefore given as:

$$\cos\theta_z = \sin\delta \sin\varphi + \cos\delta \cos\varphi \cos\omega \quad 3.7$$

Although HOMER works under the assumption that the amount of energy from the sun remains the same at all times, there is variation in the amount of sun radiation hitting the surface of the atmosphere annually due to the variation in the distance of the sun and the earth and as a result of the eccentricity of the orbit of the earth. The extra-terrestrial radiation

normal to the surface which is the amount of sun rays hitting the surface perpendicular to the radiation of the sun at the top of the earth's atmosphere can be calculated using equation 3.8

$$G_{on} = G_{sc}\left(1 + 0.033 \cdot \cos\frac{360n}{365}\right) \quad 3.8$$

where:

G_{on} = the extra-terrestrial normal radiation [kW/m2]

G_{sc} = the solar constant [1.367 kW/m2]

n = the day of the year [a number between 1 and 365]

Equation 3.9 is used for calculating the horizontal extra-terrestrial radiation. Tis parameter is the amount of energy from the sun which strikes a horizontal surface on the atmosphere. The expression is given as:

$$G_o = G_{on}\cos\theta_Z \quad 3.9$$

where:

G_o = the extra-terrestrial horizontal radiation [kW/m2]

G_{on} = the extra-terrestrial normal radiation [kW/m2]

θ_z = the zenith angle [°]

The simulation in HOMER is done on a one hour time step therefore we integrate equation 3.9 over a time step to get equation 3.10

$$\overline{G_o} = \frac{12}{\pi}G_{on}\left[\cos\phi\cos\delta(\sin\omega_2 - \sin\omega_1) + \frac{\pi(\omega_2 - \omega_1)}{180^\circ}\sin\phi\sin\delta\right] \quad 3.10$$

where:

$\overline{G_o}$ = the extra-terrestrial horizontal radiation averaged over the time step [kW/m2]

G_{on} = the extra-terrestrial normal radiation [kW/m2]

ω_1 = the hour angle at the beginning of the time step [°]

ω_2 = the hour angle at the end of the time step [°]

The mean amount of solar radiation hitting a horizontal surface on the atmosphere is given in equation 3.10. The clearness index is also taken into consideration. This defines how clear the atmosphere is to allow the penetration of solar radiation into the PV arrays. It is given as the ratio of the surface radiation to the extra-terrestrial radiation and is given in equation 3.1.

$$k_T = \frac{\bar{G}}{\overline{G_o}} \qquad 3.11$$

where:

$\overline{G}$ = the global horizontal radiation on the earth's surface averaged over the time step [kW/m2]

$\overline{G_o}$ = the extra-terrestrial horizontal radiation averaged over the time step [kW/m2]

The extra-terrestrial horizontal radiation is related to the beam radiation and the diffuse radiation by the relationship expressed in equation 3.12.

$$\bar{G} = \overline{G_b} + \overline{G_d} \qquad 3.12$$

$\overline{G_b}$ = beam radiation in kW/m^2

$\overline{G_d}$ =diffuse radiation in kW/m^2

Although the diffuse and beam radiation are significant in the calculation of the extra-terrestrial horizontal radiation, they are different from each other when we want to calculate the quantity of radiation that are incident on a tilted surface. The beam radiation is affected more by the orientation of the surface than that of diffuse radiation. This is because the

diffuse radiation comes from different direction of the sky unlike the beam radiation which stems from only a part of the sky. Most times, global horizontal radiation (GHR) is measured leaving out both the beam and the diffusion components. In this study, the global horizontal radiation data of the sun was used for the solar resources data input in HOMER software. This GHR data is resolved into beam and diffuse components in order to find the incident radiation on the PV array. HOMER then uses the relationship in [36] to express the diffuse fraction as a function which is dependent on the clearness index as given in equation 3.13.

$$\frac{\overline{G}_d}{\overline{G}} = \begin{cases} 1.0 - 0.09 \cdot k_T & \text{for } k_T \le 0.22 \\ 0.9511 - 0.1604 \cdot k_T + 4.388 \cdot k_T^2 - 16.638 \cdot k_T^3 + 12.336 \cdot k_T^4 & \text{for } 0.22 < k_T \le 0.80 \\ 0.165 & \text{for } k_T > 0.80 \end{cases}$$

3.13

HOMER uses the mean GHR to estimate the clearness index and the diffuse radiation for every one hour time step. It estimates the beam radiation by subtraction of the diffuse radiation from the GHR. During the simulation, the HDKR model is used in HOMER. This model adopts the existence of three parameters to the diffuse solar irradiation which include the following as described in [36]: “an isotropic component that comes from all parts of the sky equally, a circumsolar component that emanates from the direction of the sun, and a horizon brightening component that emanates from the horizon”. The HDKR model includes parameters such as the anisotropic index, A_i which can be deduced by taking the ratio of beam radiation on an inclined surface to beam radiation on the horizontal surface. This ratio is given in equation 3.14:

$$R_b = \frac{\cos\theta}{\cos\theta_z}$$

3.14

The anisotropy index (A_i) can be expressed as given in equation 3.15

$$A_i = \frac{\overline{G}_b}{\overline{G}_o} \tag{3.15}$$

Another important factor to be considered is the factor used that accounts for the horizon brightening. This factor has a relationship with the degree of cloudiness and is given in equation 3.16:

$$f = \sqrt{\frac{\overline{G}_b}{\overline{G}}} \tag{3.16}$$

HDKR model is therefore given in equation 3.17 and is used to calculate the global radiations which are incident on the PV array:

$$\overline{G}_T = \left(\overline{G}_b + \overline{G}_d A_i\right) R_b + \overline{G}_d \left(1 - A_i\right) \left(\frac{1+\cos\beta}{2}\right) \left[1 + f \sin^3\left(\frac{\beta}{2}\right)\right] + \overline{G}\rho_g \left(\frac{1-\cos\beta}{2}\right) \tag{3.17}$$

where: β = the slope of the surface [°]

ρg = the ground reflectance, which is also called the albedo [%]

3.4 Wind Resource

3.4.1: Variation of Wind Speed with Height

Wind speed fluctuates with altitude above the ground mainly due to roughness of the surface of the earth. This deviation is defined by equation 3.18 [4].

$$u(h) = u(h_1)\frac{\ln\left(\frac{h}{z}\right)}{\ln\left(\frac{h_1}{z}\right)} \quad 3.18$$

Where h_1 = the height of anemometer
h = the height of the wind speed to be calculated
z = surface roughness
u(h) = the wind speed to be calculated
$u(h_1)$ = the wind speed at the anemometer height

The length of the surface roughness of nearby terrain is taken into account since it affects the speed of the wind. It is a factor that symbolises how rough the surrounding terrain is and has been found for different types of terrains as shown in table 3.2 [26].

Table 3. 2: Representative surface roughness lengths

Terrain Description	***z***
Very smooth, ice or mud	0.00001 m
Calm open sea	0.0002 m
Blown sea	0.0005 m
Snow surface	0.003 m
Lawn grass	0.008 m
Rough pasture	0.010 m
Fallow field	0.03 m
Crops	0.05 m
Few trees	0.10 m
Many trees, few buildings	0.25 m
Forest and woodlands	0.5 m
Suburbs	1.5 m
City center, tall buildings	3.0 m

The mean monthly wind speed data of the school of Engineering was downloaded from the NASA database [24]. The wind data was measured at an elevation of 50m above the earth surface for a terrain analogous to airports. The monthly mean values over 10 years period and zero altitude above sea level in meters was downloaded and used for analysis. The surface roughness is taken as 0.01m for terrain similar to airports (rough pasture).

3.4.2 Autocorrelation

Autocorrelation factor: Wind speed data measured over time is dependent on preceding values. The degree of dependency on the preceding values is defined by an autocorrelation. Autocorrelation factor is the measurement of how strong the current wind speed relies on the previous wind speed. The terrain of the area affects this factor. Places with complicated terrains have factors ranging between 0.7 to 0.8 while places with uniform terrain have factors ranging between 0.9 to 0.97. The autocorrelation factor of 0.9 had been specified in HOMER in this present study during the simulation since the terrain is uniform.

Diurnal Pattern Strength: Time of the day is another factor that affects the wind speed. Wind speed at night is usually not the same with the wind speed in during the day as a result of the availability of sunlight. The measure how strong or weak the time of the day affects the wind speed is known as the diurnal pattern strength. This factor as calculated is about 0.25.

Peak Wind Speed Hour: The time of the day during which the wind speed is high is known as the peak wind speed hour. The peak wind speed hour of 12 was used for this simulation after specifying the wind speed data downloaded from [24]. Figure 3.4 shows how the wind speed varies annually on the average with height at the site under consideration.

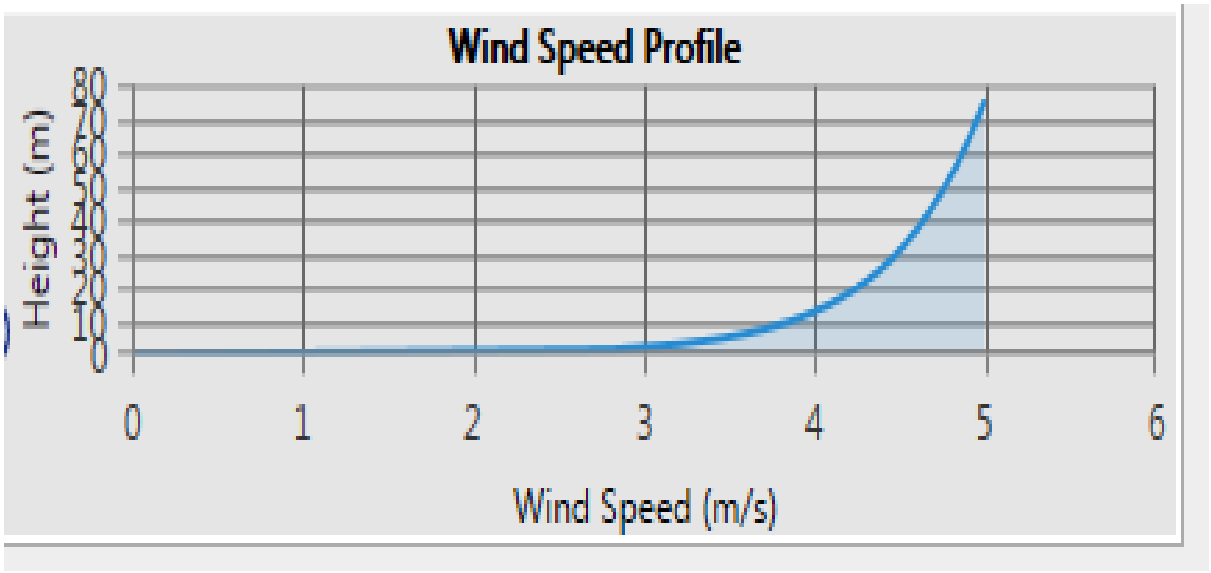

Figure 3. 4: The annual mean wind speed variation with height at the School of Engineering

Figure 3.4 shows that the wind speed at the sight varies non-linearly with height. At a height 10m, the average wind speed is still below 4m/s. The wind speed becomes fierce (about 5m/s) at a height above 50m.

At any given site, we can use Weibull distribution function to define the variation of wind speed. This function explains the chances of diverse mean wind speeds taking place at the site during a particular time. Equation 3.19 defines the probability density function as explained in [4].

$$f(u) = \frac{k}{\lambda}\left(\frac{u}{\lambda}\right)^{k-1} exp\left[-\left(\frac{u}{\lambda}\right)^{k}\right] \quad 3.19$$

Where u = wind speed in m/s,

k = Weibull shape factor (k value ranges between 1.5~2.5)

λ = the Weibull scale parameter in m/s.

The mean wind speed is related to two Weibull parameters as shown in equation 3.20.

$$\bar{u} = \lambda \Gamma\left[\frac{1}{k} + 1\right] \quad 3.20$$

The quantity **Γ** is known as gamma function.

Figure 3.5 illustrates the Weilbull distribution using four different k values with average wind speed of 6 ms^{-1} for each of them. The figure shows that k values ranging between 0 to 10 has higher distributions.

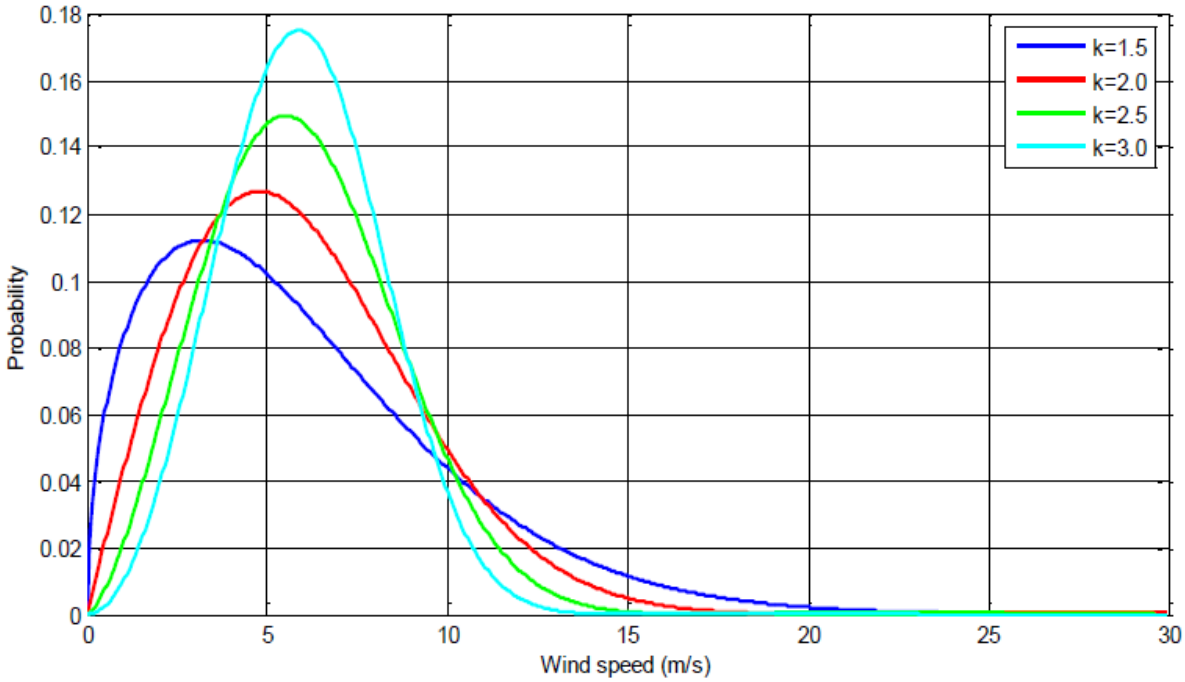

Figure 3. 5: Weibull probability distribution for different *k* values [4]

3.4.3 Wind Power Density at the Site

The wind energy potential of the case study site can be explained using the wind power density. The WPD expresses the mean wind power per square meter (W/m^2). WPD is given in equation 3.21

$$WPD = \frac{1}{2}\rho u^3 \qquad 3.21$$

Where: *WPD* = wind power density (W/m^2)

ρ = air density (kg/m^3)

u = undisturbed wind speed (m/s)

Equation 3.22 can be used to estimate the air density.

$$\rho = \frac{P}{RT} \qquad 3.22$$

Where: P = air pressure (N/m^2)

R = specific gas constant ($287 Jkg^{-1}K^{-1}$)

T = Temperature in Kelvin (K)

Since the wind speed is not constant, equation (3.22) will be modified to estimate accurately the wind density. This is done by adding up the wind speed data which were measured over time. The modification is shown in equation 3.23:

$$WPD = \frac{1}{2n}\sum_{j=1}^{n} \rho_j u_j^3 \quad 3.23$$

The parameter *n* is the number of wind speed values read while $\rho_j u_j$ is the jth term values read for the wind speed and air density.

CHAPTER FOUR

HYBRID SYSTEM COMPONENTS, CHARACTERISTICS AND COSTS

In this study, hybrid system considered include components such as: solar PV panels, wind turbine, diesel generator, batteries, converters, charge controllers, an inverter, and conventional grid system. The components of this system were selected based type of configuration and composition which are suitable and feasible for the selected site. The cost information of these components are obtained from local suppliers and where absent, the manufacturers and foreign retailers' prices were used. A detailed specifications and price estimations of these components are as shown below. All the systems considered in this study will have different lifespan based on manufacturer's specification and project lifetime as 25 years is specified.

4.1 Photovoltaic Panels

The physical examination of the site shows that the PV panels installation can be done on the roof tops of the buildings on a fixed axis, at an angle that is equivalent to the site's latitude for optimum solar radiation capturing. Factors including the size of panel, types, the brand manufacturer, the vendors and his location in particular affect the cost of PV modules. In this research, the CS3U-355P-40MM Canadian Solar with the characteristics given in table 4.1 had been selected.

Table 4. 1 Characteristics of PV Panel (Module) Selected [33]

CHARACTERISTICS OF PV PANEL SELECTED	
Item code	Canadian Solar, Inc.
Model Number (STC)	CS3U-355P-40MM
Nominal Max Power (P_{max})	355 watts
Optimum Operating Voltage (V_{mp})	39.4V
Optimum Operating Current (I_{mp})	9.02A
Open Circuit Voltage (V_{oc})	46.8V
Short Circuit Current (I_{sc})	9.59A
Module Efficiency	17.89%
Maximum System Voltage	1500V (IEC/UL)
Maximum Series Fuse Rating	30A
Cell Type	Poly-crystalline Split Cell
Cell Arrangement	144 [2x (12 x 6)]
Operating Temperature	-40°C ~ +85°C
Frame	Silver Aluminium w/Back Crossbar
Dimensions	78.7 x 39.1 x 1.57in (2000 x 992 x 40mm)
Weight	49.6 lbs (22.5 kg)
Connectors/Cables	T4/12 AWG Cables
Life time	25 years

4.1.1 The PV panel cost

The cost of this panel is $0.50 per Watt and $180.00 per panel from [29] as at 7th January 2019. The cost of shipping to Kenya is estimated by the seller to be $5.00 per panel while the cost of local transportation to the site and installation is estimated to be $20.00 per panel. The total capital cost is therefore $225.00 per panel and a replacement cost of $0.00 per panel since the lifetime of the project life is equal to the lifespan of the PV panels. To take care of the declination in efficiency of the PV cells due to the fluctuation in temperature, accumulation of dusts and losses due to wiring, the study included a derrating factor of 0.8. The PV derrating factor has been established ranging between 0.7 – 0.8. Ground reflectance is also accounted for in this study. Ground reflectance is the part of solar radiation incident on the gorund which reflects back to the atmosphere that is dependent on nature of the ground. The value of ground reflectance ranges between 20 – 70% [30]. Because at the site, there are

no such things as snow and the dust accumulation is negligible, 20% had been used as the ground reflectance in this present study. The mounting of the PV panels will be done on fixed axis and inclined at an angle which has the same orientation with the roofing surfaces of the buildings. For flat roofs, the mounting will be done at an angle of inclination between 20 to 30 degrees.

4.2. Wind Turbine

The wind turbine is expected to generate enough electricity to make a significant contribution to the renewable fraction although this depends largely on the wind speed potential. In selection of a wind turbine, factors such as the number of turbines, height of hub, service times, costs type of electricity produced (AC or DC) and the cut-in wind speed are all considered. In this study, 10kW Aeolos wind turbine had been selected putting the wind speed potential of the site into consideration.

Table 4. 2 Specifications of selected wind turbine [29]

Aeolos Wind Turbine 10kW Specification	
Turbine	
Rated Power	10 kW
Maximum Output Power	13 kW
Start-up wind speed	2.5m/s
Rated wind speed	10m/s
Survival wind speed	25 m/s
Design lifetime	20 years
Overall weight	520kg (1146.4 lbs)
Rotor	
Swept area	50.2 m^2 (26.2ft)
Rotor Blade Diameter	8 m (26.2 ft)
Rotor speed	180 rpm
Blade material	Glass fibre
Generator	
Drive type	Direct drive (Without gearbox)
Generator type	Three phase PMG
Generator Voltage	300 VDC (Grid-off) 450 VDC (Grid-on)

4.2.1 Wind Turbine Power Curve

The power curve of the wind turbine illustrates the trend of power produced at different wind speeds at deferent hub heights. At every point in the hub height, HOMER interpolates linearly to estimate the wind turbine power output. The wind turbine selected has a Start-up wind speed of 2m/s, rated wind speed of 10m/s and maximum surviving wind speed of 25m/s. These parameters were specified in the simulation. At wind speed greater than the maximum or lower than the minimum, the wind turbine shuts down and power production reads a zero value. Figure 4.1 and 4.2 show the power curve of the selected wind turbine and the curve generated by the manufacturer.

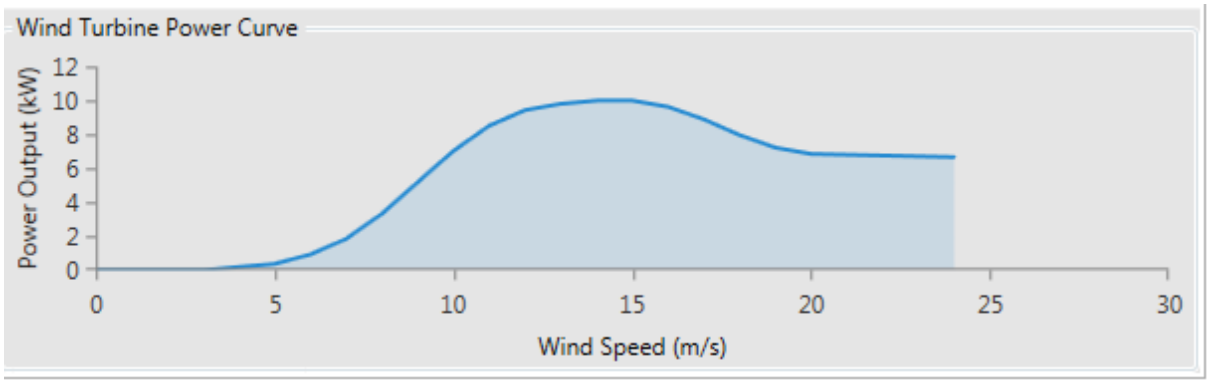

Figure 4. 1: Wind turbine power curve for Aeolos 10kW wind turbine generated in HOMER

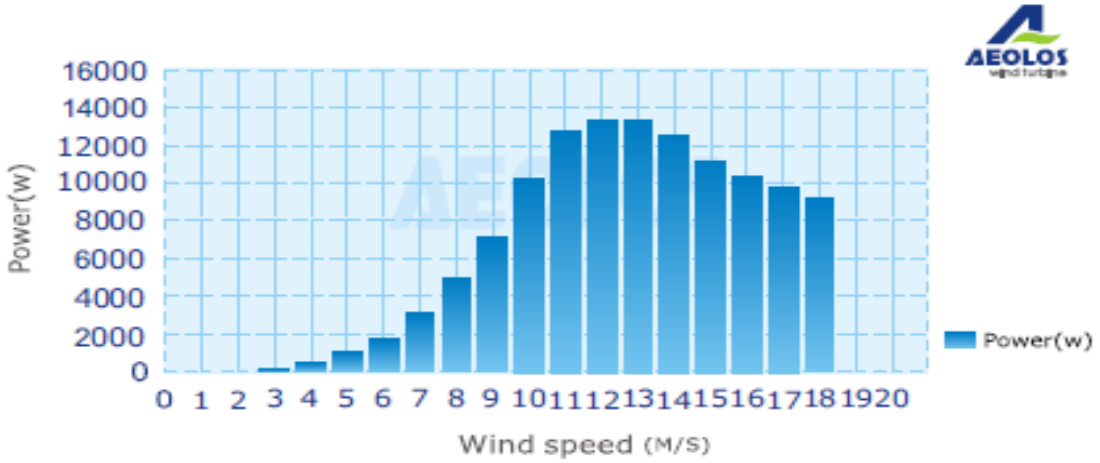

Figure 4. 2: Power curve for Aeolos 10kW wind turbine (manufacturer's curve)

The power production increases with the speed until it reaches the maximum surviving speed of the device. As can be observed from the figures above, the power production of the wind

turbine selected is very small. At 5m/s which is the maximum speed at the site, the turbine generates power less than 2000W. We shall see if this would be the case in the result of the analysis and result.

4.2.3: Effects of Altitude on Wind Turbine

The height above the average sea level is known as the altitude. As the altitude increase, the air density decreases and consequently the temperature decrease and this affects the efficiency of the wind turbine. At higher altitude, the wind speed becomes steadier which implies that the wind turbine efficiency will increase. The analysis below shows how HOMER considers the altitude as it affects wind turbine power output. As derived in [31] air density is given by:

$$\rho = \frac{P}{RT} \tag{4.2}$$

where:

ρ = air density [kg/m^3]
P = pressure [Pa]
R = gas constant [287 J/kgK]
T = temperature [K]

The ratio of actual air density to the air density under standard condition is termed the air density ratio. This ratio is what HOMER uses and is given in equation 4.3.

$$\frac{\rho}{\rho_0} = \frac{\rho}{\rho_0}\left(\frac{T_0}{T}\right) \tag{4.3}$$

where:

P_0 = standard pressure [101,325 Pa]
T_0 = standard temperature [288.16 K]

Since on temperature and pressure, there is an effect of elevation, the US standard atmosphere assumes that temperature drops as altitude increases to a height of 11,000m. This assumption is shown in equation 4.4.

$$T = T_0 - Bz \tag{4.4}$$

Where B is the laps rate with approximated value of 0.00650 K/m and z is the altitude in meters (m). Using this assumption, it can be shown that the air pressure is dependent on elevation as in equation 4.5:

$$P = P_0 \left[1 - \frac{Bz}{T_0}\right]^{g/RB} \quad 4.5$$

Where $g$is the acceleration due to gravity (9.81 m/s^2).

Combining equation 4.3 and 4.5, we obtain equation 4.6 for the proportion of the air density:

$$\frac{\rho}{\rho_0} = \left[1 - \frac{Bz}{T_0}\right]^{g/RB} \left(\frac{T_0}{T_0 - Bz}\right) \quad 4.6$$

We equation 4.6 has shown that altitude is a function of the air density ratio which HOMER uses to estimate the power production of the wind turbine with different hub heights.

4.2.4. Wind Turbine Cost

The cost of Aeolos 10kW wind turbine as at January 2019 is approximately $20,000 per assemble. Cost of shipping from United Kingdom to Kenya is estimated to be $1,200 with local transportation estimated to be $300. Installation cost is estimated to be $5,000 while O &M cost is taken to be $500/year. The total capital cost of this wind turbine is therefore rounded up to $27,000 to accommodate miscellaneous costs. The replacement cost is taken as $22,000. For quantity (number) consideration of this wind turbine, quantities 0, 2, 4, and 6 had been specified for reliable optimization. Depending on how fierce the wind speed is, HOMER will select the appropriate quantity to give a maximum result.

4.3. Diesel Generator

Diesel Generators performs a crucial role in hybrid renewable energy system by improving the quality and availability of power supply. They usually serve as backup systems, especially when there is low power output from other energy generators in the hybrid

system so as to ensure reliability and effectiveness of the system towards satisfyingthe entire load demand. The use of generators can take the place of battery storage banks since it can produce the supplement power needed when the renewable energy systems are not generating enough. To model a diesel generator for the optimum power generation of the hybrid system, the diesel price is taken into consideration. At present, the diesel price in Kenya is Kshs 112.56 ($ 1.13). Since the site is located in urban centre, transportation cost is not included. Sensitivity cases had been used in this study since the cost of fuel is not constant. The size and capacity of a commercially available diesel generator is proportional to its cost. Although a diesel generator already exists in the site, for the study, a Kohler 360kW standby diesel generator had been selected during sizing of the system. The replacement cost for this generator is $30,000. However, zero initial capital cost was specified since the existing generator serves the purpose at present.

4.3.1. Fuel Curve

Fuel consumption is very crucial in hybrid system consisting diesel generators. HOMER uses equations 4.7 to estimate the fuel curve in congruent with the generator's power output in units/hr:

$$F = F_0 \cdot Y_{gen} + F_1 \cdot P_{gen} \qquad 4.7$$

where:

F_0 = the fuel curve intercept coefficient [units/hr/kW]

F_1 = the fuel curve slope [units/hr/kW]

Y_{gen} = rated capacity of the generator [kW]

P_{gen} = the electrical output of the generator [kW]

4.3.2. Efficiency Curve

It is also important to define the efficiency curve of the generator. This efficiency is the ratio of the power output (electrical energy) of the generator to the chemical energy of the injected fuel. Equation 8.8 describes the relationship HOMER uses to estimate the efficiency curve with the fuel units measured in kilograms.

$$\eta_{gen} = \frac{3.6 \cdot p_{gen}}{\left(F_0 + F_1 \cdot p_{gen}\right) \cdot \mathrm{LHV}_{fuel}} \qquad 4.8$$

The analysis in HOMER gives Figure 4.4 which shows the shape of fuel curve and efficiency curve of the selected generator

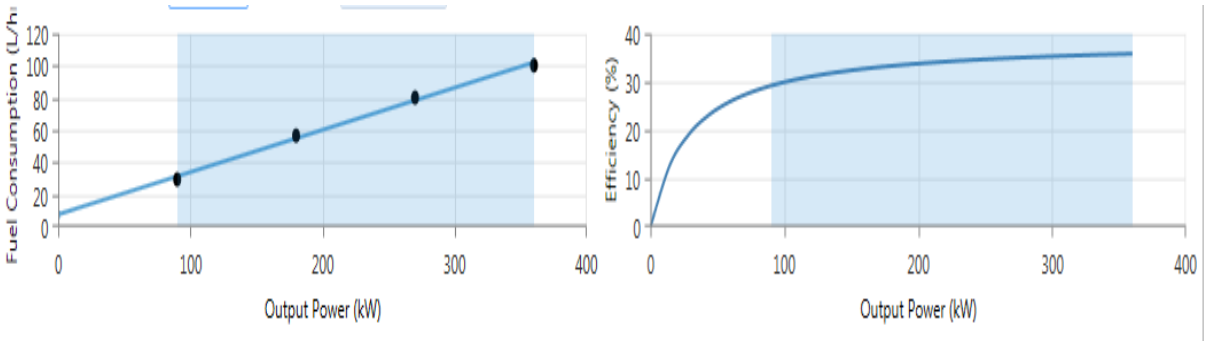

Figure 4. 3 fuel and efficiency curves of the selected generator [HOMER analysis]

4.4. Storage Battery

Storage batteries are needed to store the excess energy generated by the renewable energy systems. Power banks are usually needed especially in off-grid systems to conserve the energy that can be used when power generation becomes low. However, for on grid system, batteries can be discarded since the grid can serve this purpose. The most commonly used battery types for this purpose is usually the lead acid batteries because of they have high voltage generation per cell. They are relatively cheap and cheap and have good lifetime quality, although different types of batteries are available including “Nickel Cadmium, Lithium, Zinc Bormide, Zinc Chloride, Sodium Sulphur, Nickel hydrogen and Vanadium

batteries" [8]. Equation 4.9 and 4.10 are used to describe both battery charging and battery discharging respectively according to [4].

$$SoC_{(t)} = SoC_{(t)}(t-1)(1-\sigma) + \eta_B\left(E_{(t)} - \frac{E_{L(t)}}{\eta_{inv}}\right) \quad 4.9$$

$$SoC_{(t)} = SoC_{(t)}(t-1)(1-\sigma) + \left(\frac{E_{L(t)}}{\eta_{inv}} - E_{(t)}\right) \quad 4.10$$

Where :

$SoC_{(t)}$ is the state of charge of the battery bank at the time t

$SoC_{(t)}(t-1)$is the state of charge of the battery bank at the time t

σ is the hourly discharge rate

$E_{(t)}$ is the total energy generated by the renewable systems

$E_{L(t)}$ is the load demand at time t

η_{inv} is the inverter efficiency

η_B is the battery bank efficiency

4.4.1. Battery Calculations in HOMER

The Maximum Battery Charge Power

HOMER uses the Kinetic Battery Model (KBM) which combines three limitations to estimate the amount of power absorbed by the battery. One of the limitation it uses is the maximum power which two-tank system can absorb. This expression is given in equation 4.11:

$$P_{batt,cmax,kbm} = \frac{kQ_1 e^{-k\Delta t} + Qkc\left(1 - e^{-k\Delta t}\right)}{1 - e^{-k\Delta t} + c\left(k\Delta t - 1 + e^{-k\Delta t}\right)} \quad 4.11$$

where:

Q1 = the available energy [kWh] in the storage at the beginning of the time step

Q = the total amount of energy [kWh] in the storage at the beginning of the time step

c = the storage capacity ratio [unitless]

k = the storage rate constant [h-1]

Δt = the length of the time step [h]

Anther constraints in the KBM is the storage charge power which is in correspondence with the maximum charge rate of the battery is given in equation 4.12 as:

$$P_{batt,cmax,mcr} = \frac{\left(1 - e^{-\alpha_c \Delta t}\right)\left(Q_{max} - Q\right)}{\Delta t} \qquad 4.12$$

Where α_c = the maximum storage charge rate measured in A/Ah and Q_{max} = the overall storage bank capacity. Finally we look at the third constraint which appear on the power bank page and expresses the maximum power bank corresponding to the maximum charge current. The expression is given in equation 4.13

$$P_{batt,cmax,mcc} = \frac{N_{batt} I_{max} V_{nom}}{1000} \qquad 4.13$$

where:

N_{batt} = the number of batteries in the storage bank

I_{max} = the storage's maximum charge current [A]

V_{nom} = the storage's nominal voltage [V]

HOMER then combines these three limitations by setting the maximum storage charge power is equivalent to the minimum of these three limitations, with an assumption that they apply after charging losses have occurred therefore:

$$P_{batt,cmax} = \frac{\mathrm{MIN}\left(P_{batt,cmax,kbm}, P_{batt,cmax,mcr}, P_{batt,cmax,mcc}\right)}{\eta_{batt,c}} \qquad 4.24$$

Where $\eta_{batt,c}$ is efficiency of the storage charge

4.4.2. Battery Selection and cost

In this study, Surrette 6CS-25PS battery which cost around $1,100 per one had been selected. The total capital cost including the shipment and installation cost is $1,200 per one. Its properties are given in *table 4.3* while the lifetime curve and capacity curve is shown in *figure 4.5* below [33]. In terms of quantity required to meet the maximum load, 0, 150, 200, and 300 has been specified in HOMER search space. HOMER will pick the appropriate number for simulation and optimization.

Table 4. 3 Properties of Surrette 6CS-25PS battery

Capacity	840Ah
Nominal Voltage	6V
Noinal capacity	6.91kWh
Maximum Capacity	1156Ah
Minimum State of charge	40%
Maximum discharge current	41A
Round trip efficiency	80%
Capacity Ratio	0.237

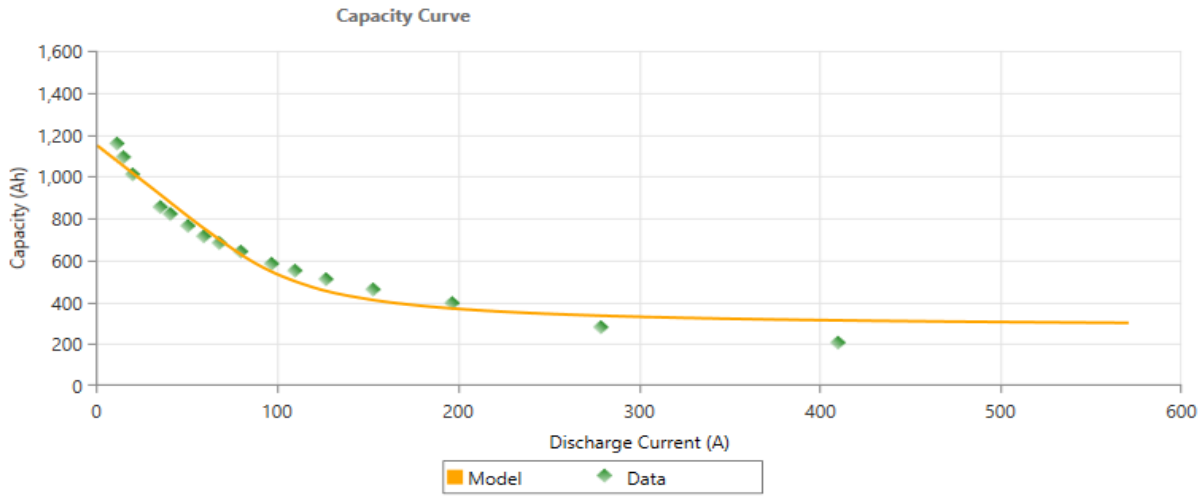

Figure 4. 4 capacity curve of Surrette 6CS-25PS battery

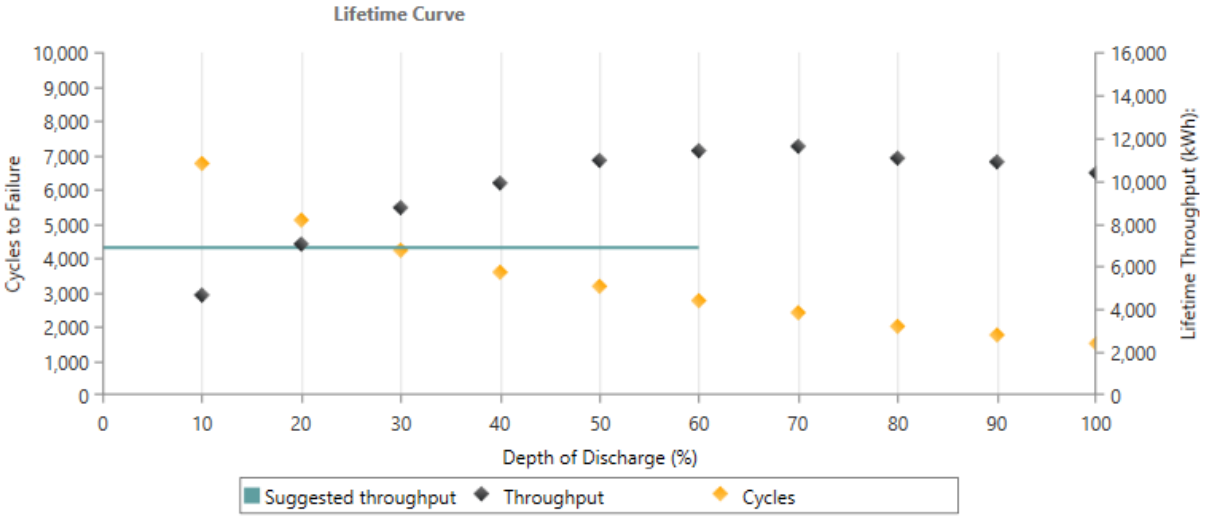

Figure 4. 5 Lifetime curve of Surrette 6CS-25PS battery

4.5 Inverter/converter

Hybrid system consists of both the AC and DC components therefore inverters or converter are needed to convert the to an appropriate and usable form of power. When power generated from the renewable energy power systems is small, the generator and/or the grid will do the work of charging the batteries. Grid-tied inverters are usually separated from off-grid inverters but due to advancement in technology, these two are now incorporated in one in the case where both are required. These two-way converters are called bidirectional converters (able to work as both inverters and rectifiers simultaneously). The inverter to be used should be rated to the same capacity as the peak load or larger but because in this design, the power shall be supplied by both renewable and renewable power sources, the inverter with the same capacity as the peak demand is selected. O&M costs for this equipment are were neglected since they have little or no maintenance when installed. In this study, OutBack 8kw 48V pure waveform hybrid inverter has been selected. The important specifications of this inverter are given below:

Nominal DC input voltage	48VDC
DC input voltage range	40 to 64VDC
Maximum AC input current	50AAC @ 240ADC
Typical Efficiency	93%
Output voltage regulation	±2%
Grid-interaction voltage range	(L1-N or L2-N) 106 to 132VAC
Continuous output power at 250C	8000VA
Capacity	8kW

Converter sizes considered are: 0, 50, 100, 200 and 250kW; Capital cost of converter is taken as $4,500 per 8kW and the replacement cost is about $4,000. The typical efficiency of the converter is at 93% with a lifetime of 15 years.

4.6. Controller

Charge controllers are also considered as the power being absorbed by the batteries should be controlled. Numerous controllers can be specified in HOMER together with their costs and it will simulate as well as optimise systems with charge controllers giving their performance characteristics

4.7 Dispatch strategy

There are some standards and through which the generator and the batteries must adhere to whenever they have to supply power. This standard is referred to as dispatch strategy. In this study, the only dispatchable energy sources used are the diesel generators. Power from the renewable energy sources is used to supply the power demand but when in excess, they are used to charge the batteries. When the power generated from renewable energy power sources is low, the generator does the work of charging the batteries. At times it is more economic viable to operate the generator at its full capacity when needed and use excess power to charge the batteries. In HOMER energy software, two dispatch strategies are used:

Cycle Charging (CC): When power from generator is needed, it is operated at its full capacity with the excess power being used to charge the batteries. This strategy is suitable for a system with small or no renewable energy power sources. It is represented with the acronym CC in the result sheet.

Load Following (LF): When power from the generator is needed, it operated in less than its full capacity to meet the load demand at the moment. The strategy is suitable where power from renewable energy sources is considerably high. It is denoted with the acronym LF in the result sheet. In this study, Load Following was adopted.

4.8. Grid

Since the conventional grid exists at this site, it might not be economical to go entirely off-grid. However, for the sake of research, both off-grid and grid-tied hybrid system is accounted for in this study. The Grid page in HOMER allows specification of grid in many different ways which includes:

- *Simple rates mode* allows specification of site's constant but average electricity cost per kWh, the sell back cost, and the capacity that can be sold back. This rate had been adopted in this study. The analysis of the 13 months electricity bills of the site showed that the peak energy tariff is approximately Kshs 20.00 ($0.20). This price has been specified in HOMER for optimization. Connecting the system to grid means that at sometimes, excess power would be generated by the renewable energy sources and when this happens, the extra power is sold back to the grid. Since Feed in Tariff (FiT) policy in Kenya enables power producer to sell back to the grid at a maximum price of Ksh 12.00 ($0.12) per kWh, this value had been specified during the simulation.
- *Real time rates* mode which describes costs on 1 hour basis through introducing accurately configured text file which has time-series data. This is usually suitable for advanced grid modelling and therefore was not adopted for this study

- *Scheduled rate***s** mode which permits different costs of power at every time of day as well as every month of the year to be specified. Also this is suitable for advanced grid modelling and therefore was not adopted in this research.
- *Grid extension mode* which allows the comparison of the price of grid extention and the price of every standalone power system in the system arrangement. Again, this is suitable for advanced grid modelling and therefore was not adopted in this research.

.

The concept planned behind this project is that the institution would sign the PPA with the KPLC, which would allow them to sell power back to the grid at the maximum rate of $0.12/kWh as given by the policy and have been done [37]:

4.9. Economic Criteria

4.9.1 The total Net Present Cost (NPC): This is the difference between the present value of the total costs which the system incurs throughout its lifetime and the present value of the revenue from the system throughout its lifetime.

The present value of the costs that the system will incur in *n*-years later can be estimated using equation 4.15.

$$C_{NPC} = C\left[\frac{1+i'}{1+d}\right]^{n} \qquad 4.15$$

Where ;

d is the nominal interest rate (%)

$i'$is the annual inflation rate (%)

To determine the Levelized Cost of Energy (LCOE), the overall NPC of the system has to be definitely converted to sequence of same yearly cash flows which is referred to as overall annualized cost. Equation 4.16 can be used to deduce the overall annualized cost of the system:

Total annualized cost ($/year) = Total NPC x CPF 4.16

Where, CPF equal to capital recovery factor which is defines the ratio utilised in estimating the present value of sequence of yearly cash flows. The CPF can be calculated using equation 4.17:

$$Capital\ Recovery\ Factor = \frac{i(1+i)^N}{(1+i)^N-1} \quad 4.17$$

Where N = the number of years (equivalent to the lifetime of the entire project)

i = real interest rate

HOMER computes the yearly real discount rate the "Nominal discount rate" and "Expected inflation rate" inputs. It makes use of real interest rate to compute discount factors together with the annualized costs from the project's net present costs. Equation 4.18 gives the real discount rate:

$$i = \frac{d-i'}{1+i'} \quad 4.18$$

Discount factor, f_d is estimated in HOMER using the expression given in equation 4.19:

$$f_d = \frac{1}{(1+i)^N} \quad 4.19$$

Kenya inflation rate fluctuates. As at November 2018, it is 5.58% with annual rate of 4.59% however, it has been projected to 6.5% therefore; the inflation rate of 7% had been used in this simulation. The discount rate is kept constant at 9% by the CBK. It means that Kenya can borrow at 13% [35]. In this regard, the discount rate of 13% had been chosen in this simulation.

4.9.2. Annualised system cost (ASC)

ACS is the addition of the annualised cost (capital, replacement and maintenance) of all the system components.

$$ASC = Annualised\ (capital + replacement + maintenance)costs \quad 4.20$$

4.9.3 Levelized cost of Energy

LCOE evaluates the system taking into account the overall recurring and non-recurring costs throughout the lifespan of the project. It is the ratio of the overall ASC to the annual electrical energy production (E_{Total}) in kWh. Mathematically,

$$LCOE = \frac{Total\ Annualised\ cost\ (USD/yr)}{Annual\ Load\ Served\ (kWh/yr)} = \frac{ASC}{E_{Total}} \quad 4.21$$

4.9.4 Internal rate of return

The IRR is sometimes referred to as the return on investment (ROI) or time adjusted rate of return. It is the interests earned by the system throughout its lifespan. This is evaluated by setting the project NPV value to zero and then compute the discount rate.

4.9.5 Payback period (PBP)

This is the period in time during which the original investment made on the system is recovered from the cash inflow generated from the project. It is given as:

$$PBP = \frac{Initial\ Investment}{Cash\ Flow\ per\ period} \quad 4.22$$

4.10. Search Space

To find the optimum system architecture, search space in HOMER is utilized. This space in HOMER is where component capacities and/or quantities are specified to enable the software select and optimise the best capacity and/or quantity.. The table below shows the search space for this system.

Table 4. 4 HOMER Search Space

Converter Capacity (kW)	Generator Capacity (kW)	Grid Purchase Capacity (kW)	PV size (kW)	Surr6CS25P Strings (Number)	10kw Wind Turbine (quantity)
0	0	999999	0	0	0
50	360		50	150	2
100			100	200	4
200			200	300	6
250			250		
300			300		

4.11 Sensitivity Variable

Sensitivity variables are variables specified in HOMER to account for what happens when different parameters such as wind speed, solar irradiation, temperature, diesel price etc changes in the future. HOMER carries out simulations and optimisation separately for each of the sensitivity variable specified. The table below gives the sensitivity cases performed in this study.

Table 4. 5 Sensitivity Cases

Diesel fuel price (USD/L)	Solar scaled average (kW/m2/day)	Temperature Scaled average (0C)	Wind scaled average (m/s)
0.9	5.93083333	19.8975	4.764166667
1.0	4.931	18.5	3.764
1.2			

4.12. Constraints

The Constraints page permits one to specify conditions that the system must satisfy. A system which does not satisfy these conditions is discarded by HOMER during the optimization and the sensitivity analysis. Some of the constraints are explained below.

Maximum annual capacity shortage: This is the maximum permissible value of power that the system can allow as a shortage per annum. It is the ratio of the total capacity shortage to the yearly electric load measured in percentage. In this study, the yearly capacity shortage was given as 10%.

Minimum renewable energy fraction: This is the fraction of power that goes to the demand which come from the renewable energy electrical systems. Renewable energy fraction is given in equation 4.23.

$$f_{ren} = 1 - \frac{E_{nonren} + H_{nonren}}{E_{served} + H_{served}} \quad 4.23$$

where:

E_{nonren} = nonrenewable electrical production [kWh/yr]
$E_{grid,sales}$ = energy sold to the grid [kWh/yr] (included in E_{served})
H_{nonren} = nonrenewable thermal production [kWh/yr]
E_{served} = total electrical load served [kWh/yr]
H_{served} = total thermal load served [kWh/yr]

Minimum annual capacity shortage is the minimum permissible value of yearly renewable fraction, in %. In this study this value had been taken as 50%.

Operating Reserve: This is a factor which allows adequate and reliable power supply when the demand rises or when the generation from the renewable energy sources falls. Four inputs are used to define the operating reserve needed for a hybrid system in HOMER. Table 4.5 shows the four inputs used to define the operating reserve in this study.

Figure 4. 6: Operating reserve inputs [32].

Variable	Description
As a percentage of load: Load in current time step (%):	HOMER adds this percentage of the primary load in the current time step (AC and DC separately) to the required operating reserve in each time step. A value of 10% means that the system must keep enough spare capacity operating to serve a sudden 10% increase in the load. 10% had been specified here.
As a percentage of load: Annual peak load (%):	HOMER adds this percentage of the peak primary load (AC and DC separately) to the required operating reserve in each time step. It, therefore, defines a constant amount of operating reserve. This specified as default.
As a percentage renewable output: Solar power output (%):	HOMER adds this percentage of the PV array power output to the required operating reserve in each time step. A value of 80% means that the system must keep enough spare capacity operating to serve the load even if the PV array output suddenly decreases 80%. In most cases, the output of the PV array is less variable than the output of a wind turbine, so this input is usually set at a lower value than for the Wind power output.
As a percentage renewable output: Wind power output (%):	HOMER adds this percentage of the wind turbine power output to the required operating reserve in each time step. A value of 50% means that the system must keep enough spare capacity operating to serve the load even if the wind turbine output suddenly decreases 50%. The more variable you expect the output of the wind turbine to be, the higher you set this input.

CHAPTER FIVE

RESULTS AND DISCUSSION

5.1 Load Profile of the Site

Figure 5.1 and 5.2 show the energy demand pattern of the school during the first two week and the second two weeks of energy monitoring. The peak demand has been identified to be 84.59kW during the first two weeks and 82.56kW during the second week.

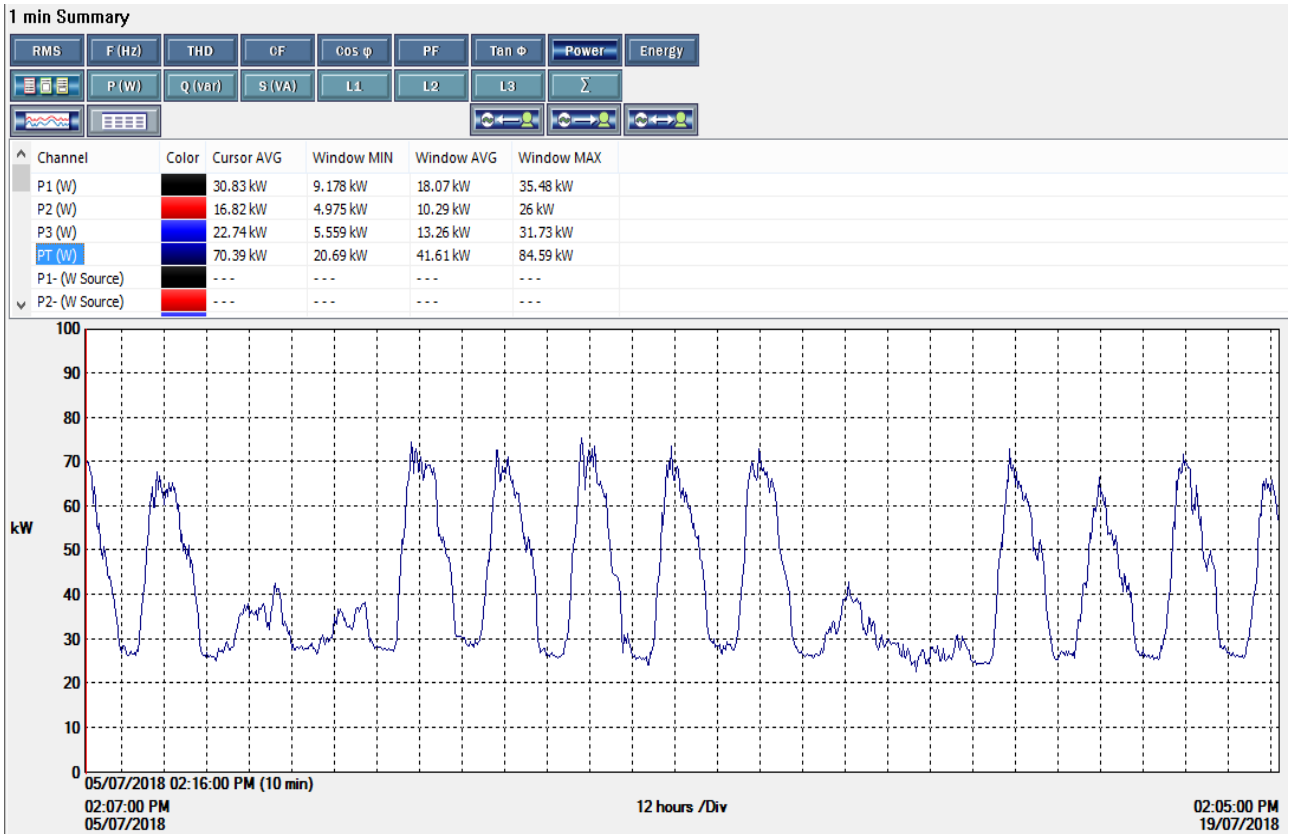

Figure 5. 1: Energy demand pattern of the school for the first two weeks

Table 5.1 shows the daily peak demand and consumption while table 5.2 shows the hourly power demand for the baseline period. The day with the highest peak demand in kW was selected to obtain the hourly load profile of the establishment. Figure 5.3 and 5.4 shows the demand per minute and the demand per hour respectively during the peak day over the

baseline period. From table 5.1, the peak demand and the consumption for the baseline period is 84.59kW and 1172kWh respectively.

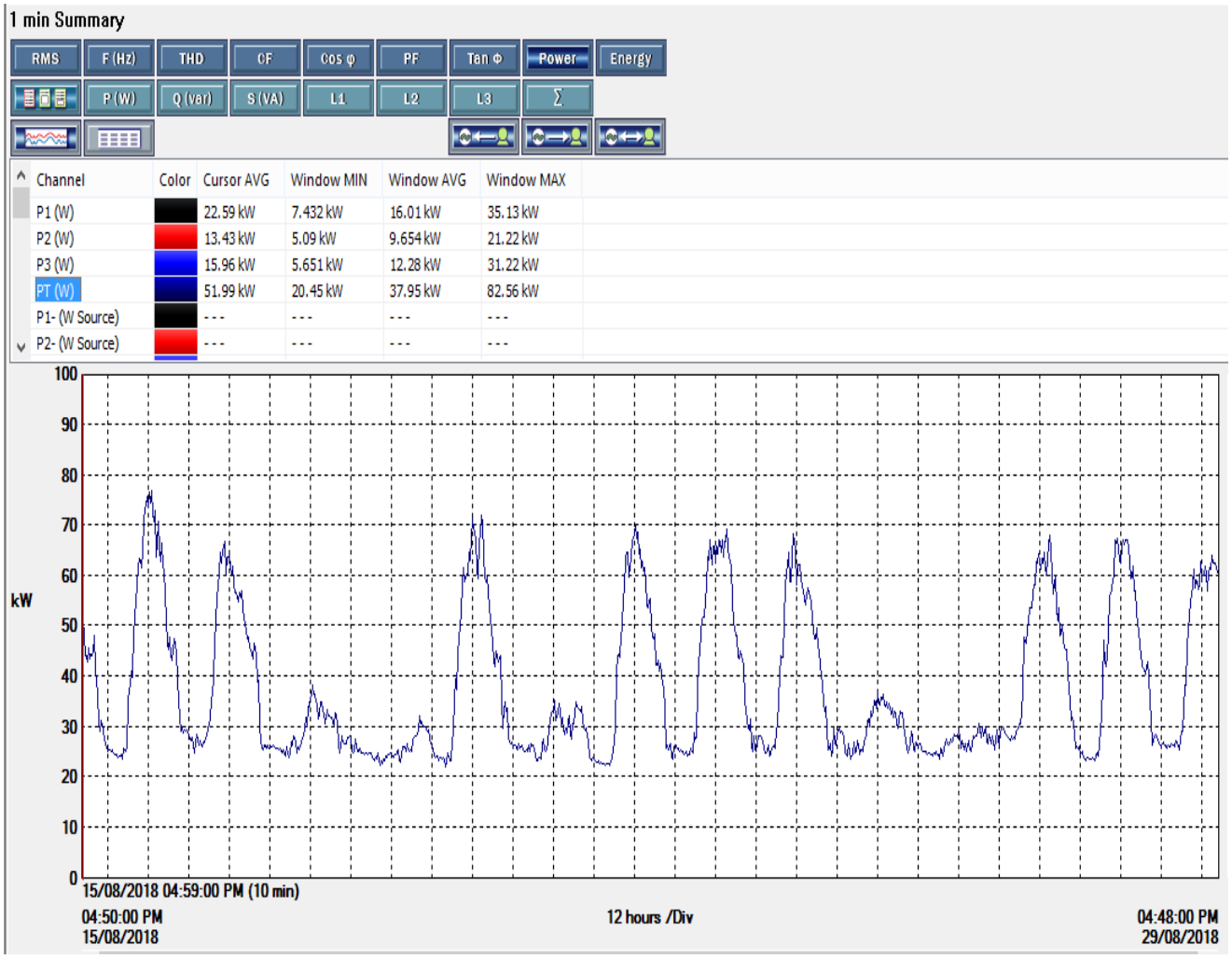

Figure 5. 2: Energy demand pattern of the school for the second two weeks

Table 5. 1: Daily peak demand and consumption of the school for the baseline period

Date	Peak Demand (kW)	Consumption (kWh)
06/07/2018	82.56	1098.0
07/07/2018	72.43	1049.0
08/07/2018	54.55	755.6
09/07/2018	36.22	626.1
10/07/2018	78.87	970.1
11/07/2018	59.2	748.0
12/07/2018	74.98	971.1
13/07/2018	74.12	1049.0
14/07/2018	72.19	1032.0
15/07/2018	53.86	761.7
16/07/2018	35.98	647.0
17/07/2018	72.4	975.0
18/07/2018	74.89	1051.0
19/07/2018	69.07	1019.0
16/08/2018	74.22	1147.0
17/08/2018	70.98	891.8
18/08/2018	45.45	777.0
19/08/2018	79.09	1020.0
20/08/2018	78.08	**1172.0**
21/08/2018	81.1	1135.0
22/08/2018	80.59	1087.0
23/08/2018	79.45	1130.0
24/08/2018	70.7	892.0
25/08/2018	41.53	706.3
26/08/2018	76.18	895.4
27/08/2018	72.59	1045.0
28/08/2018	**84.59**	1035.0
29/08/2018	73.15	1045.0

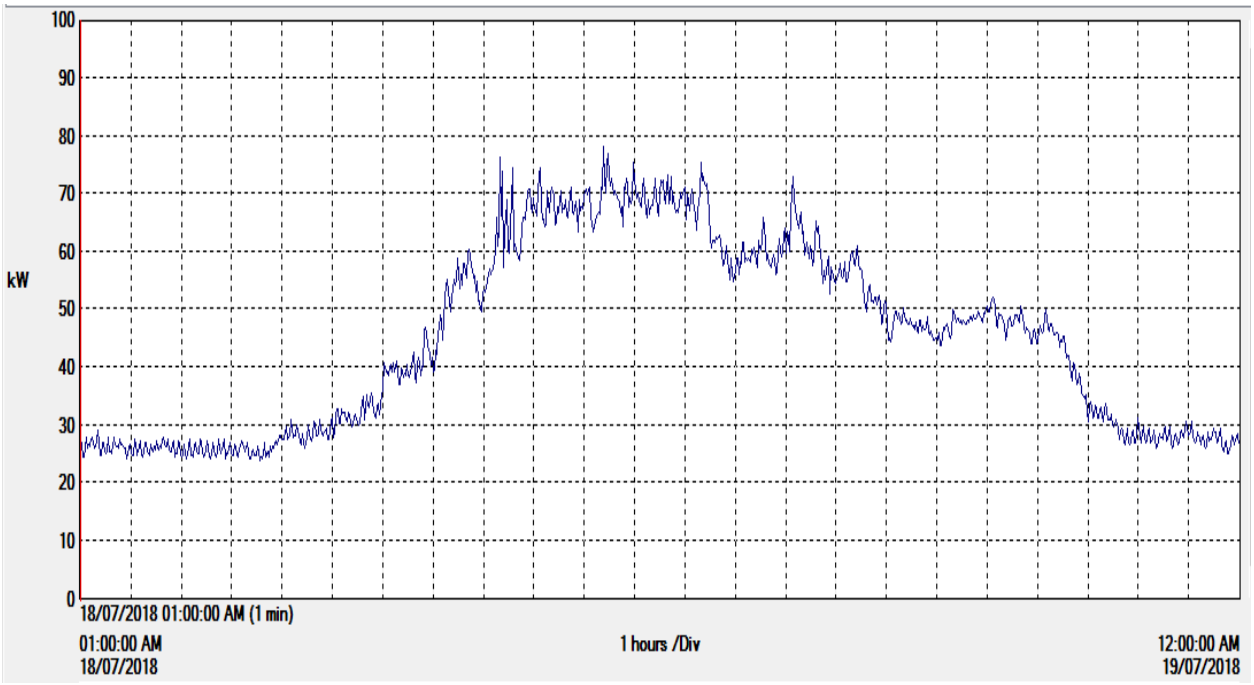

Figure 5. 3: One minute summary of energy demand of the site during the peak day

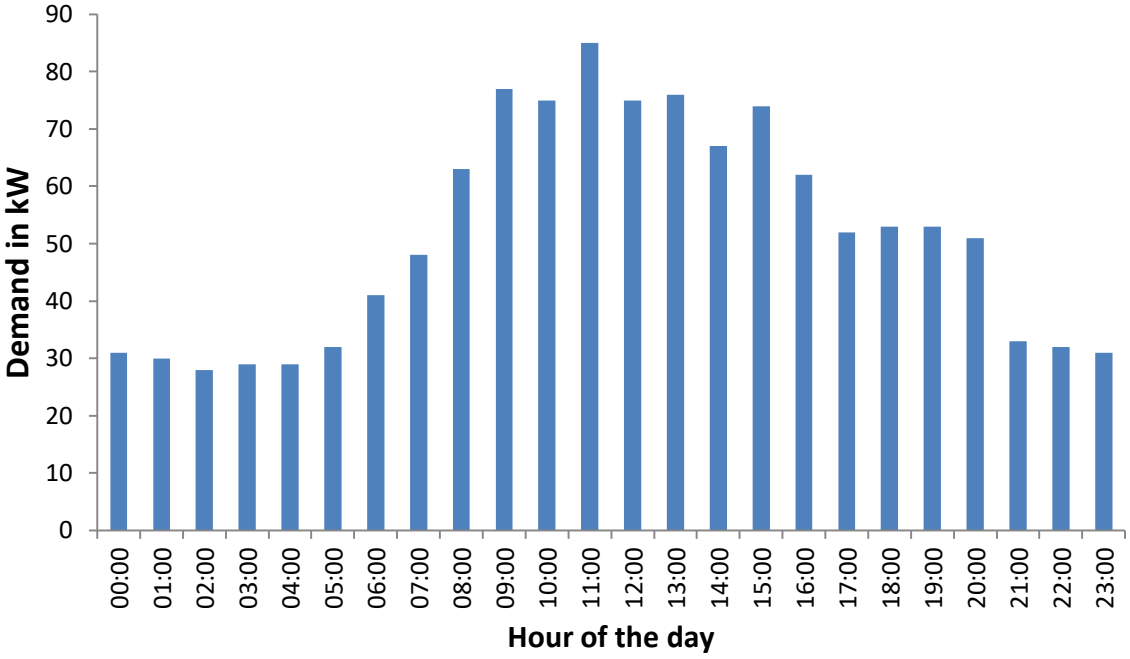

Figure 5. 4: Hourly energy demand of the site during the peak day

5.2 The identified suitable renewable energy resources for the proposed hybrid system

As a result of the unavailability of other renewable energy resources in the site, the study focused on the Variable Renewable Energy Sources (VRES) – wind and solar resources. The potential of these resources was examined in chapter two. The mean speed of wind at the site and the solar irradiation for the site were obtained from NASA meteorological database. Figure 5.5 gives the daily mean solar irradiation incidents on a horizontal surface and their corresponding clearness index throughout a year. This value is highest during the month of February the daily solar irradiation and clearness index of 6.68kWh/m2/day and 0.655 respectively. This is a period when the weather tends to be hottest with the sun radiation at its peak. The mean of these values was found giving that the annual average solar irradiation is 5.93kWh/m^2/day. The standard deviation was found to be 0.55 meaning that the variation of solar irradiation between the months can be negligible.

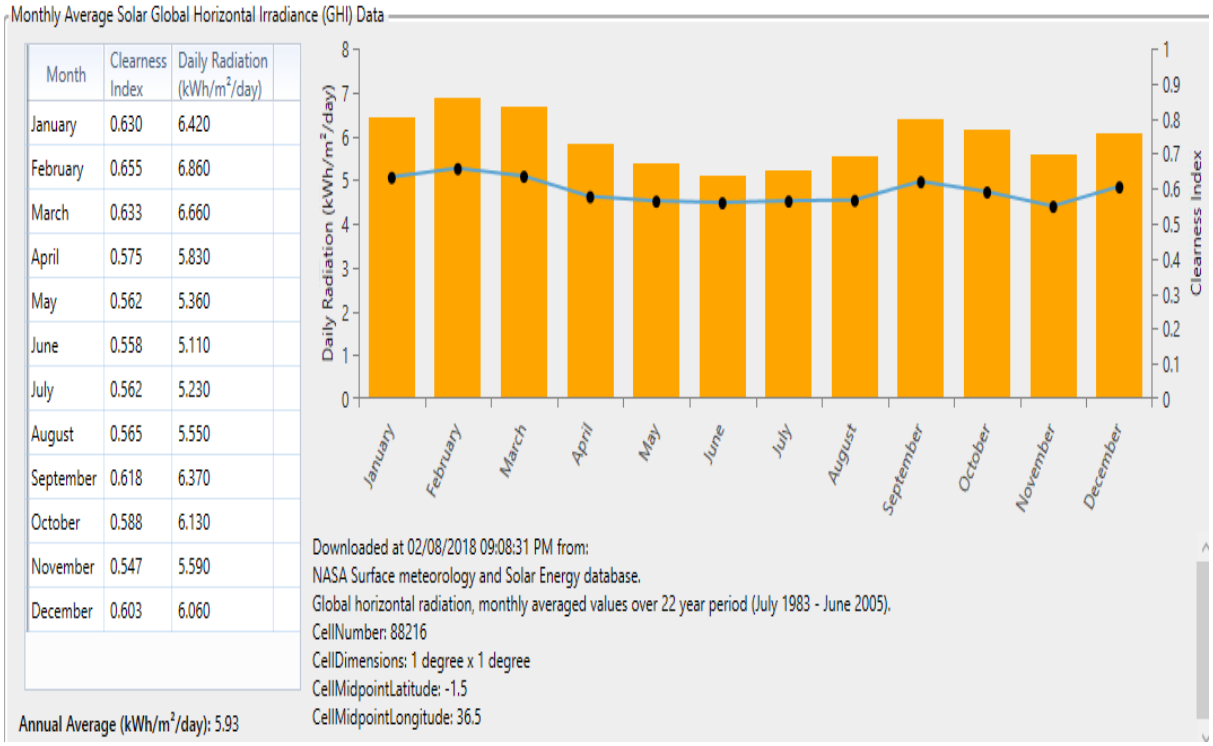

Figure 5. 5: Daily mean annual solar insolation incidents on a horizontal surface at the site[24]

Figure 5.6 shows the average (mean) monthly wind speed for the site. The annual average wind speed was determined to be 4.76m/s. The wind speed is highest in the month of September with an average value of 5.15m/s and lowest in December with an average speed of 4.32m/s. The standard deviation for these values was determined as 0.76 showing that the values are spread apart from the mean and suggests that the power generation by the wind turbine may be minimal.

Figure 5. 6 Average monthly wind speed at the School of Engineering[24]

The monthly average temperature at the School of Engineering, University of Nairobi ranges from 18.58^{0}C to 21.04^{0}C throughout the year as can be observed from figure 5.5. The temperature experienced during the day and during the night varies by values between 3^{0}C to 5^{0}C. The site is not affected much by annual weather variations. Also, as a result of the topography of the site, the number of hours in a day does not deviate much from themselves all year round. This means that load curve does not have significant deviation for the whole

year which is the reason why the load profile of the peak day observed from data analysis has been used and assumed to be the same throughout the reaming months of the year.

Since the energy produced by PV panels is proportional to roof-top area available, the school roof-top areas had been measured. The school has abundant roof space for PV installation and ground space for wind turbine installation. The total roof space available for PV installation is 1970m^2 as measured (roof-tops with asbestoses not considered since it poses a great challenge in removal). It has been estimated that using PV panels of 15.5% efficiency, 1m^2 of roof space can produce approximately 150Wp of power putting spaces for walkaways into consideration. This shows that the available roof space has PV capacity of about 295.5kW.

The temperature of the site is an important parameter for power generation although at the present site, it varies between one month and another. At the school of Engineering, February has the highest temperature with approximately 21.04^{0}C while July has the lowest temperature of approximately 18.6^{0}C [28]. Figure 3.8 and table 3.5 show the average monthly temperature variation of the site. The annual average temperature of the site is calculated in HOMER as 19.90^{0}C.

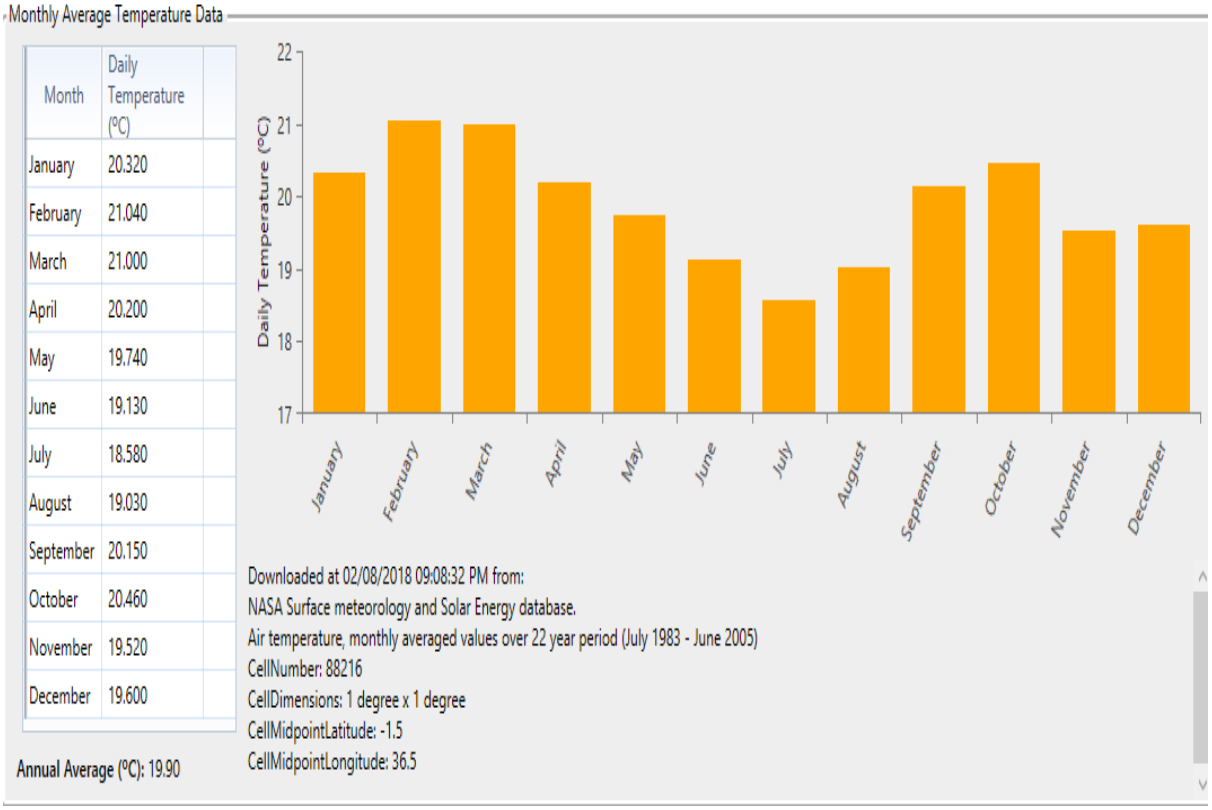

Figure 5. 7: Monthly temperature variation of School of Engineering [24]

5.3 Simulation and Optimization

In this section, detail of the simulation and optimization results for the systems under consideration which were required to meet the load demand of 145kW peak and 1200kWh/day consumption were given. The design and optimization were carried out in HOMER Pro Micro-grid Analysis Tool (version x64.3.12.3). Based on the economic criteria, the optimum hybrid renewable energy system was selected. This is the system which can be able to meet the load demand at affordable price and minimized CO_2 emission. The simulation is run severally to make sure a result that is feasible is obtained, after inputting the entire input variable in the modelling tool and the results of the optimization are shown as total but categorized with the most feasible system that can supply the peak load demand and the constraints specified ranked on top of the result table. The ranking is done based on the economic criteria and satisfaction of the specified constraints. This entails that the first system on the result table is the best system followed by the next and the next. The economic criteria that HOMER considers for ranking include but not limited to NPC, LCOE, Initial

Capital Costs, Fuel Costs, O&M costs etc. Other criteria include the renewable energy penetration, excess electricity generated, capacity shortage etc. Figure 5.8, shows a schematic of the hybrid system design with all the components (technologies) under consideration.

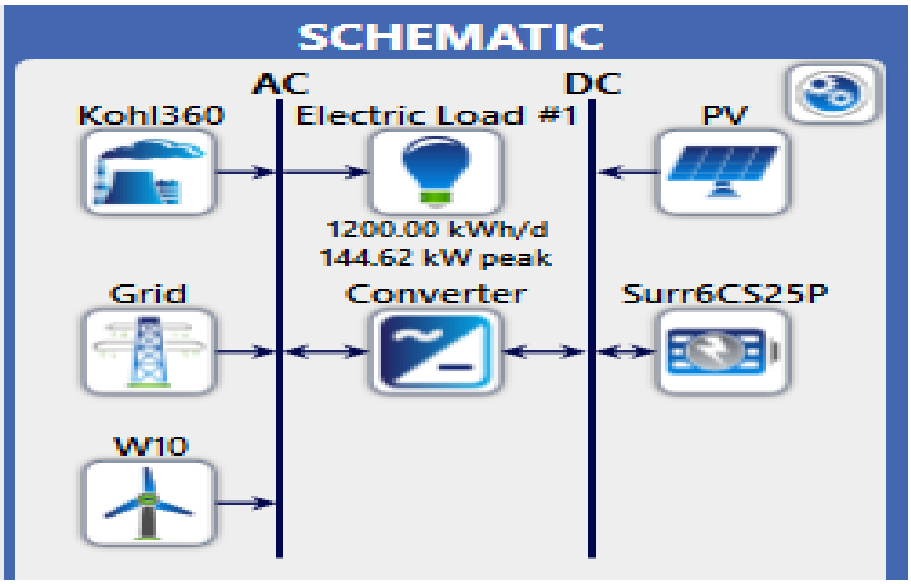

Figure 5. 8: System schematic

5.3 Systems optimization scenarios

The following simulation and optimization scenarios in table 5.2 are proposed for detailed analysis that will result in determining the best hybrid system. The system which gives the least NPC and LCOE, least capacity shortage and excess power production, higher renewable energy fraction and lowest fuel consumption at each study site would be chosen as optimum. All the scenarios were optimized using the same data set.

Table 5. 2: Proposed study and optimization scenarios

Proposed System	Scenarios
Grid/PV/Diesel generator system (grid-tied)	A
Grid/PV system (grid-tied)	B
Grid/PV/Wind/Diesel generator system (grid-tied)	C
Grid/PV/Wind System (grid-tied)	D
Grid/PV/Diesel generator/Battery system (grid-tied)	E
Grid/PV/Battery System (grid-tied)	F
Grid/PV/Wind/Diesel generator/Battery system (grid-tied)	G
Grid/PV/Wind/Battery system (grid-tied)	H
PV/Diesel Generator/Battery system (off-grid)	I
PV/Wind/ Diesel generator/Battery system (off-grid)	J

Table 5.3 shows the selected component capacity and their quantity. As shown in the table the optimization capacity of the PV is selected as 300kW. This viable since the roof top space is enough for this installation. If power is generated in excess, it can be sold back to the grid or used to supply power to other part of the intuition. Two 10kW wind turbine was selected during optimization, totalling the installed capacity of the wind turbine to 20kW. Since up to 6 of this 10kW wind turbine was specified, and HOMER picked two only, it implies that the viability of wind power generation is low due to the low wind speed that exists at the site. 300 pieces of 355W battery was chosen in other to store surplus power from the solar PV system. Also, 200kW two-way converter was utilized to convert DC to AC and vice versa when needed. The charging style chosen was load following which implies that power can be used as the batteries are being charged. Table 5.4 shows the resource input data as was found. The system was modelled based on the worst scenario. The diesel price was taken to be $1.2/L. The renewable energy resource data were used as found in HOMER for this specific site.

Table 5. 3: The system optimization components

PV (kW)	Wind Turbine	Diesel Generator	Battery	Coverter	Dispatch Strategy	Grid Maximum Purchase
300kW	2 X 10kW	360kW	300 pieces of 355W	200kW	Load Following	999,999kW

Table 5. 4: Resources input data

Diesel Fuel price	Solar scaled Average	Temp. scaled average	Wind scaled average
$1.2/L	5.93kWh/m^2/day	19.9^{0}C	4.76m/s

Table 5. 5: Categorised Optimization Result

Architecture													Cost				Syste
						PV (kW)	W10	Kohl360 (kW)	Surr6CS25P	Grid (kW)	Converter (kW)	Dispatch	NPC (US$)	COE (US$)	Operating cost (US$/yr)	Initial capital (US$)	Ren Frac (%)
						300		360		999,999	200	LF	US$695,121	US$0.0789	US$29,567	US$302,641	71.6
						300				999,999	200	LF	US$702,599	US$0.0797	US$30,130	US$302,641	71.6
						300	2	360		999,999	200	LF	US$739,297	US$0.0830	US$28,375	US$362,641	73.0
						300	2			999,999	200	LF	US$746,775	US$0.0838	US$28,938	US$362,641	73.0
						300		360	300	999,999	200	LF	US$1.22M	US$0.139	US$42,220	US$662,641	71.6
						300			300	999,999	200	LF	US$1.23M	US$0.140	US$42,783	US$662,641	71.6
						300	2	360	300	999,999	200	LF	US$1.27M	US$0.142	US$41,027	US$722,641	73.0
						300	2		300	999,999	200	LF	US$1.27M	US$0.143	US$41,591	US$722,641	73.0
						300		360	300		200	LF	US$1.48M	US$0.255	US$61,736	US$662,641	90.0
						300	2	360	300		200	LF	US$1.51M	US$0.259	US$59,063	US$722,641	91.5

Table 5.5 shows the categorised optimization results. From the table, it can be observed that the ranking was done based on economic viability as have mentioned earlier. The first system on that table is the best system, followed by the next but these systems will be analysed for proper understanding.

5.4 Comparison of Scenarios for Economic Power Systems

5.4.1 Based on Net Present Cost

Referring to table 5.2 and 5.5, system scenario A has the least NPC than all other scenarios with approximate value of ksh. 69,512,100.00. The next system with least NPC is system scenario with NPC of Ksh. 70,259,900. Following this order, scenarios (C, D, E, F, G, H, I and J) are ranked based on the value of the net present cost next to scenario A, respectively. Figure 5.9 shows the Comparison of Scenarios Based on Net Present Cost

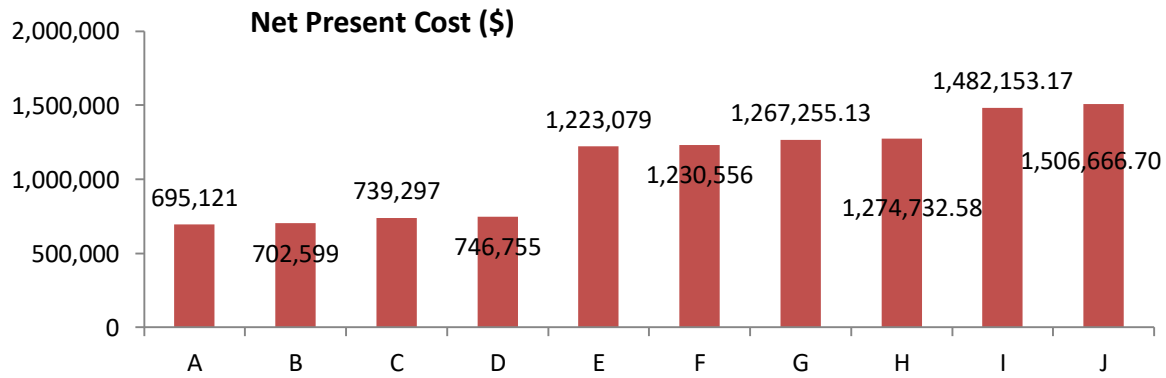

Figure 5. 9: Comparison of Scenarios Based on Net Present Cost

5.4.2. Based on Levelized Cost of Energy

The figure below shows the Levelized cost of energy for the different simulation results. Detail of this can be observed from table 5.5. The first four scenarios (A, B, C, and D) have almost the same cost of energy with values 0.0789, 0.0797, 0.0830 and 0.0838 respectively all in $/kWh. Scenarios E, F G and H also have very close cost of energy in $/kWh of 0.139, 0.140, 0.142 and 0.143 and 0.259 respectively. Finally Scenario I and J have the highest cost of energy in $/kWh of 0.255 and 0.259 respectively. Careful consideration indicates that Scenario A has the best configuration in consideration of LCOE. This is shown in figure 5.10.

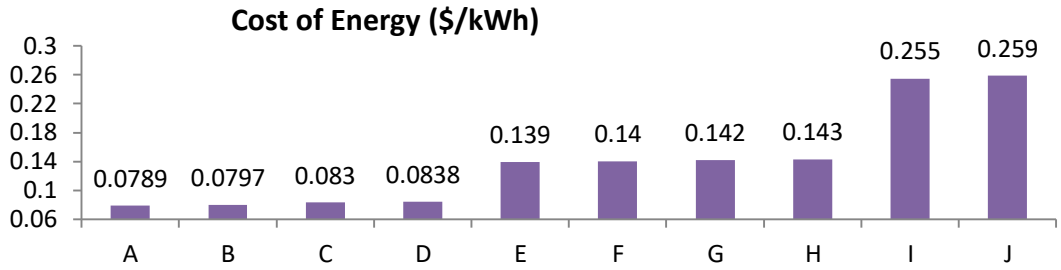

Figure 5. 10: Comparison of Scenarios Based on Net Present Cost

5.4.3. Based on Initial Capital Cost

Based on the initial capital costs, Scenarios A, B, C and D are relatively less with A and B having the same Initial capital cost of about $302,641. Others on the other hand, are relatively high with Scenarios G, H and J having the highest and same initial capital cost of $722,641.

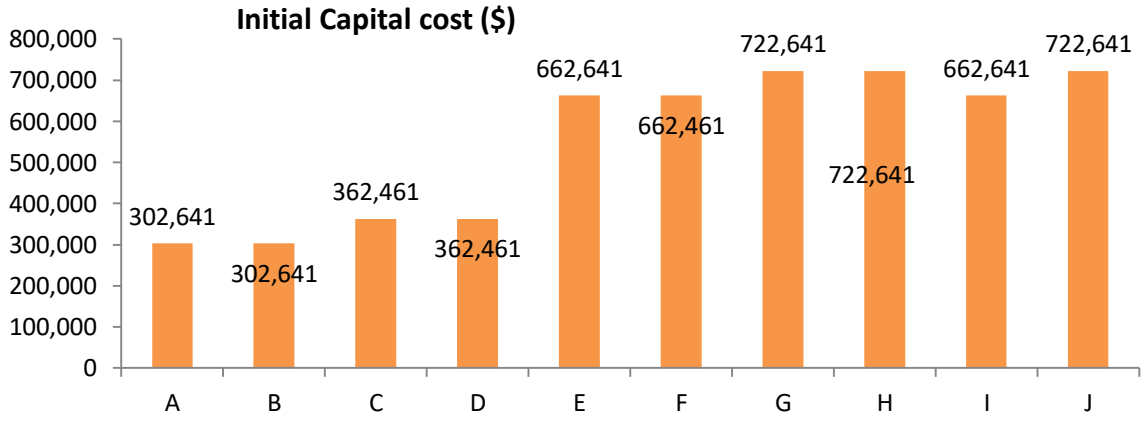

Figure 5. 11: Comparison of Scenarios Based on Initial Capital Cost

5.4.4. Based on fuel cost ($/yr) and total fuel (L/yr)

The fuel cost contributes immensely to the NPC and COE and other various costs for these systems. Although scenarios A, C, E, and G has diesel generator incorporated in them, the cost of fuel and the total fuel used remains $0.00/yr and 0.00 L/yr respectively for each of them. This is because they are grid-tied systems and the power purchased from the grid together with the power production by the renewable energy sources are sufficiently enough for the required load; hence the generator is not operated. However, scenarios I and J have significant amount of fuel consumed ($18,329/yr and $15,587/yr for I and J respectively)

thereby incurring a substantial amount of money (15,227L/yr and 12,990L/yr). These two systems are off-grid hybrid system and they require operation of the generator to supplement power from the renewable energy sources (solar and wind).

5.4.5. Based on the Excess Electricity Generated

The system has shown that there exists excess power which if not sold back to grid would be dumped or wasted elsewhere. This excess power generation is an important parameter when deciding which system to be selected. A system with high excess power is not regarded as a cost effective system although in this case it can be allowed since the PPA policy would allow the institution to sell power back to the grid. Without putting the PPA policy into consideration, scenarios C, D, G and H can be pronounced the winner of this contest because they have same lowest excess power of 2.45%. Following these four scenarios, scenarios A, B, E and F produce same excess electricity of 2.48% bringing them to the second position. Excess electricity production enables load demand accommodation but demands additional capital which makes them discouraging. Clearly, the best system cannot be decided with this parameter since other scenarios are yet to be considered. Figure 5.12 shows the excess power generation in % as we have discussed.

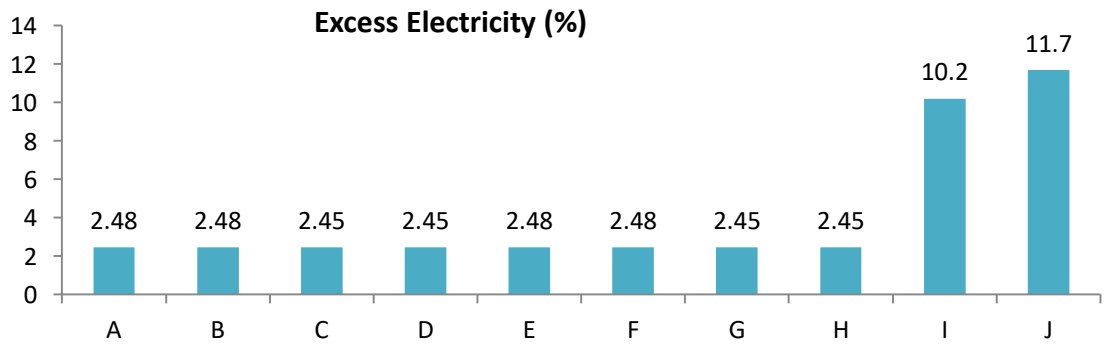

Figure 5. 12: Comparison of Scenarios Based on Excess Electricity

5.4.6. Based on Renewable Fraction (RF) and Capacity shortage

Looking at these two cases (RF and capacity shortage), the capacity shortage is 0.00% for all scenarios. This implies that no shortfall happens between the needed operating capacity and

the real amount of operating capacity which all the systems can provide. However, scenarios I and J have the highest RF with values 90% and 91.5% respectively. Scenarios A, B, E and F have the lowest RF with same value of 71.6%. C, D, G and H have same value of RF which is 73%.

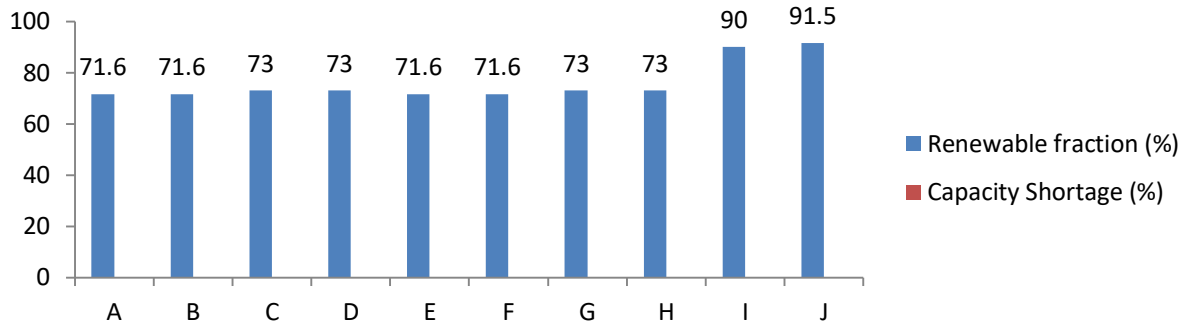

Figure 5. 13: Comparisons Based on Capacity Shortage and RF

5.4.7. Based on Present worth (PW) and Annual worth (AW)

These factors are much feasible to scenarios A, B, C and D and therefore this study considered the PW and AW only for these top four scenarios. The PW and AW are both highest in Scenario A followed by B and down to D. This implies that scenario A is the best configuration also in this regard.

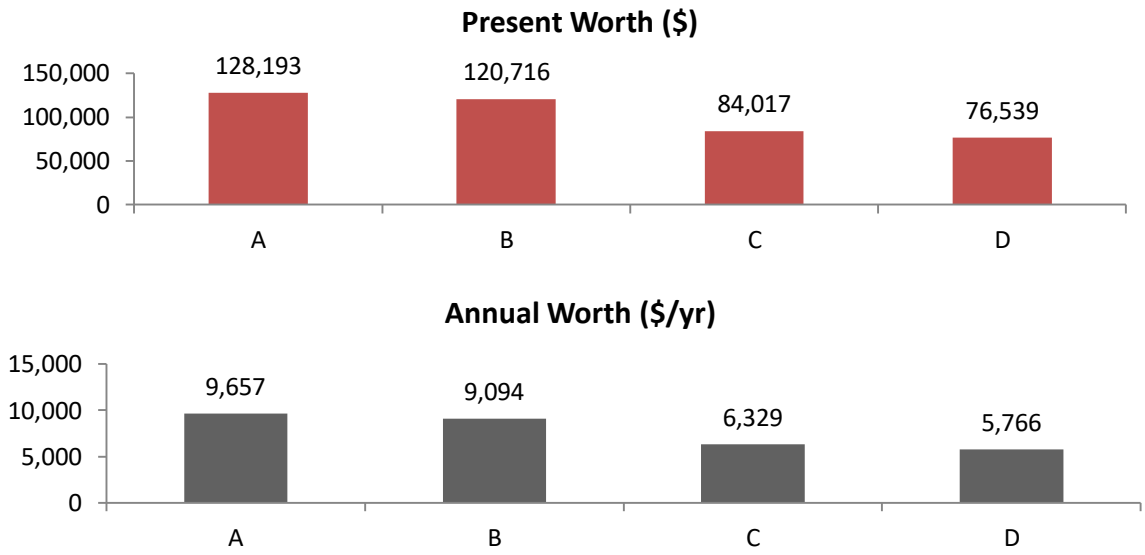

Figure 5. 14: Comparison of top four scinarios (A, B, C, and D) based on their PW and AW

5.4.8. Based on ROI, IRR, Simple and Discounted Payback

Again, I will consider the top four scenarios (A, B, C and D). The ROI and IRR is highest in scenario A with values of 12.1% and 15.2% respectively followed by scenario B down to scenario D. For simple payback and discounted payback, both A and B have the same number of years of 6.15 and 7.76 respectively. C and D have the same simple payback period but a slight difference in the discounted payback period. Upon all these considerations, scenario A remains the optimum configuration.

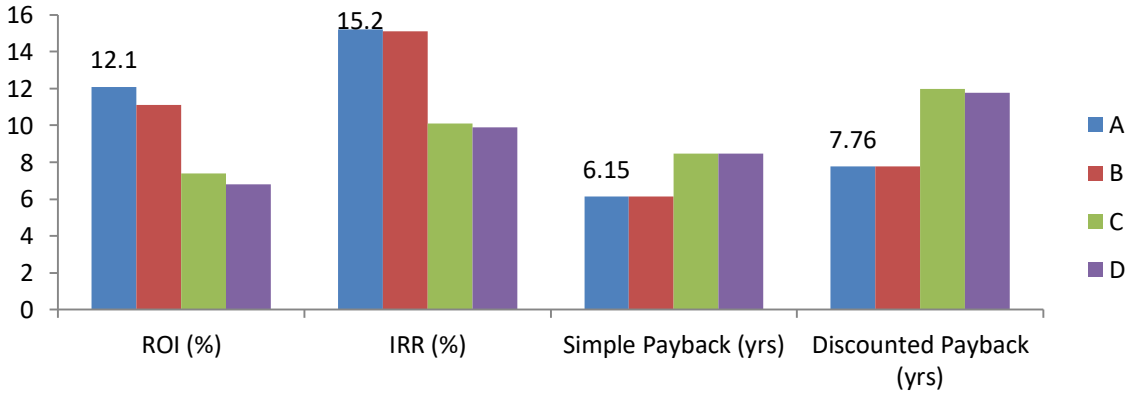

Figure 5. 15: Comparison based on ROI, IRR, Simple and Discounted Payback

From the careful consideration of the above comparisons, scenario A is the system architecture with the lowest NPC and COE. It has the highest PW and AW with lowest simple and discounted payback time. It also has the lowest capital cost and a considerable O&M costs. Based on these factors, I have concluded that among all the scenarios considered in this analysis, scenario A is the optimum hybrid renewable energy system the can supply adequate, reliable and affordable power to the school of engineering, University of Nairobi. This system is grid-tied with the configuration which Includes conventional grid, solar PV and diesel generator. This configuration has NPC of Ksh.69,512,100.00 with cost of energy of Ksh 7.89/kWh (approximately kshs 8.0/kWh). In the next section we shall analyse this system configuration.

5.5 Optimization Analysis of the Selected Optimum Hybrid System

To analyse this system, the components are taken part by part. In general, the pattern of monthly electricity production in kW achieved after simulation is shown in *figure 5.16*. The solar potential of the site is relatively high having maximum in February and minimum in July. The system produces the total electricity of 706,346kWh/yr with 663,791kWh/yr being utilised leaving an excess of 17,524kWh/yr (2.48%). The analysis showed that the system has no unmet load demand and capacity shortage. 73.4% of the overall energy generated is from the solar PV while the grid contributes only 26.6% of the total energy. Due to the high renewable fraction (71.6%) and maximum renewable penetration of 146%, the diesel generator is never utilised thereby it produces 0.00kWh/yr although its presence is required as standby. From the table below we can observe that out of about 85kW, the grid contribute only about 20kW.

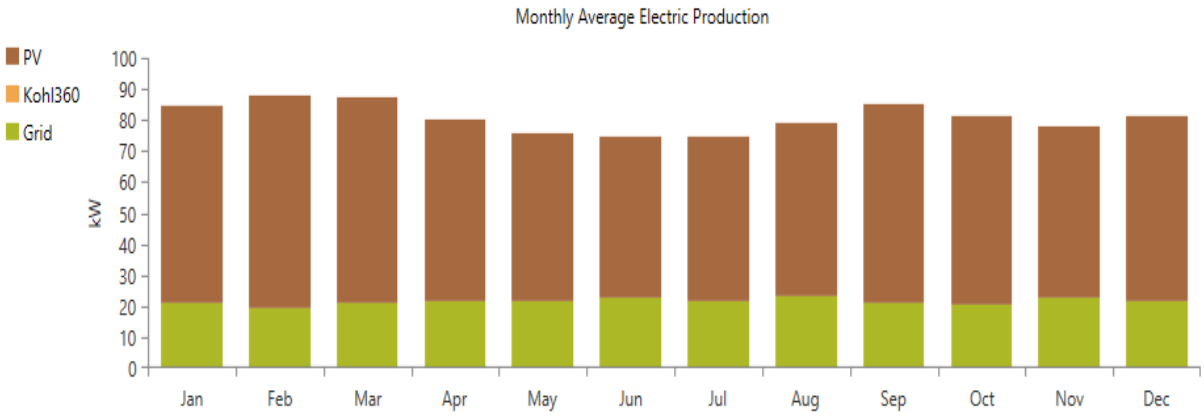

Figure 5. 16: Monthly average electric power production of the optimal system

5.5.1. PV Electrical Power Production and Distribution Analysis

The production capacity and distribution of power by the solar PV is depicted in table 5.6a and b and figure 5.14. As a result of high solar horizontal irradiance in this location, the PV is able to produce a maximum power output 291kW with cost of its energy as $0.0603/kWh. The mean output of this PV is 1,420kWh/day which means that power generated from it can supply adequately the maximum consumption of the establishment.

Table 5. 6a: Generic flat plate PV Electrical Summary

Quantity	Value	Units
Minimum Output	0	kW
Maximum Output	291	kW
PV Penetration	118	%
Hours of Operation	4,336	hrs/yr
Levelized Cost	0.0603	US$/kWh

Table 5. 6b: Generic flat plate PV Statistics

Quantity	Value	Units
Rated Capacity	300	kW
Mean Output	59.1	kW
Mean Output	1,420	kWh/d
Capacity Factor	19.7	%
Total Production	518,134	kWh/yr

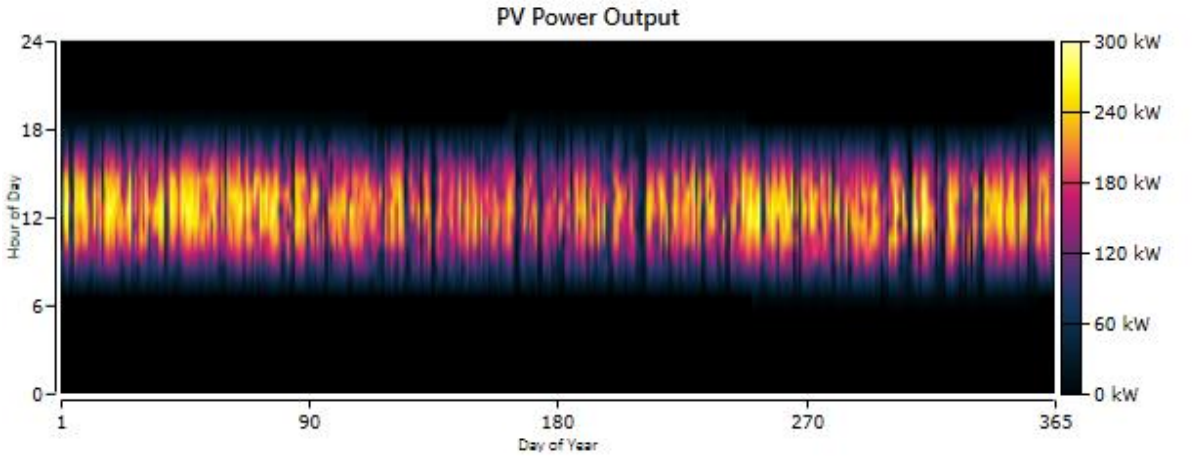

Figure 5. 17: PV power output of optimal system (kW)

From figure 5.17, we can observe that the power produced by the PV is sufficiently enough to power the establishment between 6am and 6pm each day of the year. The electrical energy from the grid is only utilised during the night (between 7pm to 7am).

5.5.2. Standby Diesel Generator Power production and distribution Analysis

The electrical summary, fuel summary and statistics of the diesel generator is presented in table 5.8 and the power production distribution is shown in figure 5.18, hence there is no power production at all as a result of the power produced by the PV and supplemented by the grid is sufficient to power the site.

Table 5. 7 Electrical summary, Fuel summary and the statistics of diesel generator of the optimal system

Kohler 360kW Standby Electrical Summary

Quantity	Value	Units
Electrical Production	0	kWh/yr
Mean Electrical Output	0	kW
Minimum Electrical Output	0	kW
Maximum Electrical Output	0	kW

Kohler 360kW Standby Fuel Summary

Quantity	Value	Units
Fuel Consumption	0	L
Specific Fuel Consumption	0	L/kWh
Fuel Energy Input	0	kWh/yr
Mean Electrical Efficiency	0	%

Kohler 360kW Standby Statistics

Quantity	Value	Units
Hours of Operation	0	hrs/yr
Number of Starts	0	starts/yr
Operational Life	1,000	yr
Capacity Factor	0	%
Fixed Generation Cost	11.7	US$/hr
Marginal Generation Cost	0.315	US$/kWh

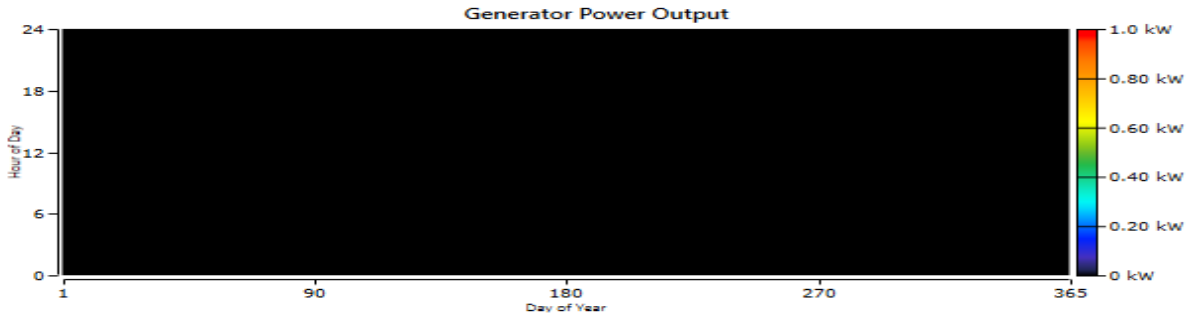

Figure 5. 18: Power production and distribution of diesel generator

5.5.3. System Converter Output analysis

The system converter operates for 4,336hrs/yr and produces energy output of 475,580kWh/yr with energy input of 500,610kWh/yr giving in to total losses of 25,031kWh/yr. Table 5.6a shows the electrical summary while table 5.6b shows the statistics. The capacity of the the converter is 200kW with minimum and maximum output of 0kW and 200kW respectively. The mean output is 54.3kW while the capacity factor is 27.1%

Table 5. 8: Converter Electrical summary and statistics of the optimal system

a. *System Converter Electrical Summary*

Quantity	Value	Units
Hours of Operation	4,336	hrs/yr
Energy Out	475,580	kWh/yr
Energy In	500,610	kWh/yr
Losses	25,031	kWh/yr

b. System Converter Statistics

Quantity	Value	Units
Capacity	200	kW
Mean Output	54.3	kW
Minimum Output	0	kW
Maximum Output	200	kW
Capacity Factor	27.1	%

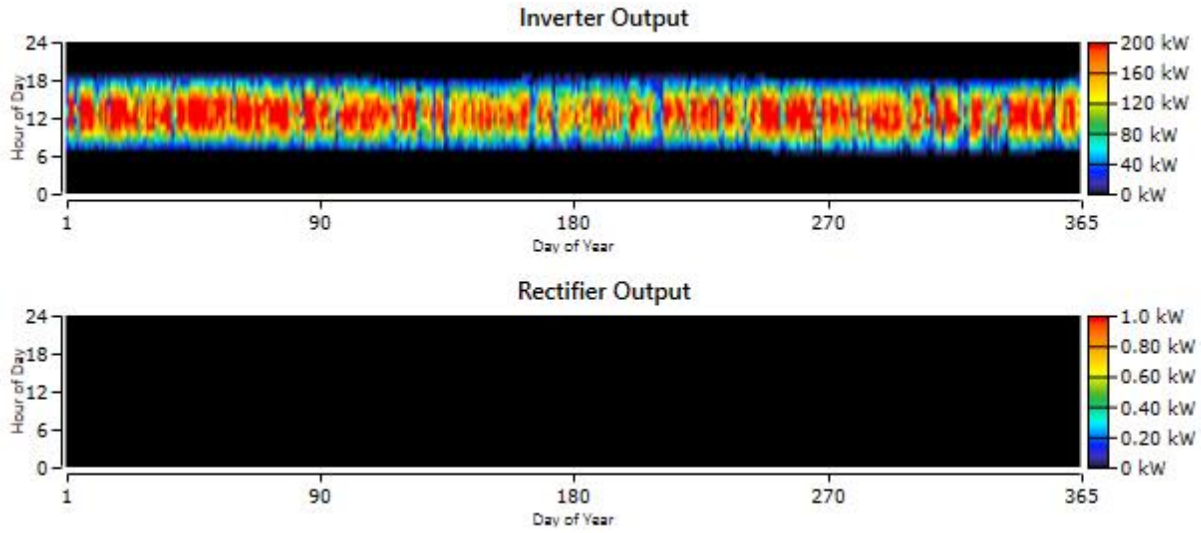

Figure 5. 19: Power production and distribution of the Converter for the optimal system

The converter does its work during the day when the power generation from the PV is active. During the nights, when the grid takes over, the converter output goes to 0kW. This can be seen from figure 5.16a. The rectifier remains inactive since no storage equipment such as battery in this system. Suppose the system has storage batteries, the grid would be used to charge them at night.

5.5.4. Grid Power Analysis

For this system, the power from the grid is only used when the power generation from the PV is minimal. Since there is no storage system, the PV only takes care of the power demand during the day while at night, the grid takes over. Table 5.10 below shows the monthly power demand bought from the grid and the amount sold back while Figure 5.20 gives more insight about the power market that exists for this system.

Table 5. 9: Grid Power Analysis of the optimal system

Month	Energy Purchased (kWh)	Energy Sold (kWh)	Net Energy Purchased (kWh)	Peak Demand (kW)	Energy Charge	Demand Charge
January	15,616	21,386	-5,770	93.7	US$556.88	US$0.00
February	13,053	21,569	-8,516	71.3	US$22.38	US$0.00
March	15,588	22,029	-6,441	81.5	US$474.18	US$0.00
April	15,528	18,642	-3,114	85.2	US$868.60	US$0.00
May	16,149	17,133	-984	83.3	US$1,174	US$0.00
June	16,500	14,953	1,546	89.3	US$1,506	US$0.00
July	16,082	16,022	60.2	90.2	US$1,294	US$0.00
August	17,107	16,886	221	76.8	US$1,395	US$0.00
September	15,297	20,132	-4,835	78.6	US$643.50	US$0.00
October	15,090	20,238	-5,148	75.1	US$589.45	US$0.00
November	16,248	17,219	-970	98.2	US$1,183	US$0.00
December	15,953	19,582	-3,629	82.0	US$840.70	US$0.00
Annual	188,211	225,791	-37,580	98.2	US$10,547	US$0.00

From figure 5.20, we observe that energy is purchased from the grid at night between 7pm and 7am each day when the little or no power is generated by the renewable energy power generation system. During the day, between 6am and 6pm, excess energy generated from the renewable energy source is sold back to the grid. This process puts the net energy purchased to negative thereby nullifying the demand charges; hence the establishment is not charged for the energy purchased from the grid.

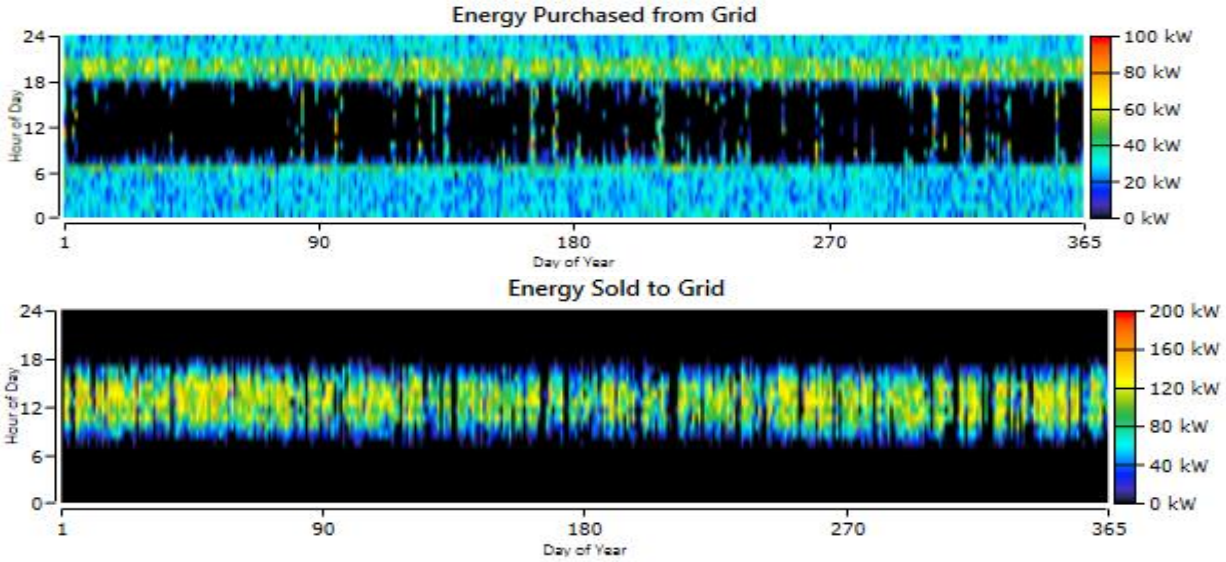

Figure 5. 20: Energy Purchased from the grid and Energy sold to the grid for the optimal system

5.6. Cost Summary of the Project

Figure 5.21 shows a summary of the NPC of various costs associated with the project for its lifetime of 25 years. It can be observed that the capital costs of the PV and the system converter gives a NPC of approximately $300,000.00 while operating the PV and grid gives the highest NPC of about $450,000.00. The replacement cost of the converter incurs a cost of about $30,000.00 for the overall lifetime of the project. It is also important to observe that the diesel generator does not incur any cost because it is already in existence at the site. Also, since it is not in operation throughout the lifetime of the project, its replacement never occurs. These costs are additionally demonstrated in figure 5.22 in form of discounted cash flow graph throughout the lifespan of the project with the detailed cost summary illustrated in figure 5.20. Here we can see, after 15 years converter replacement is made.

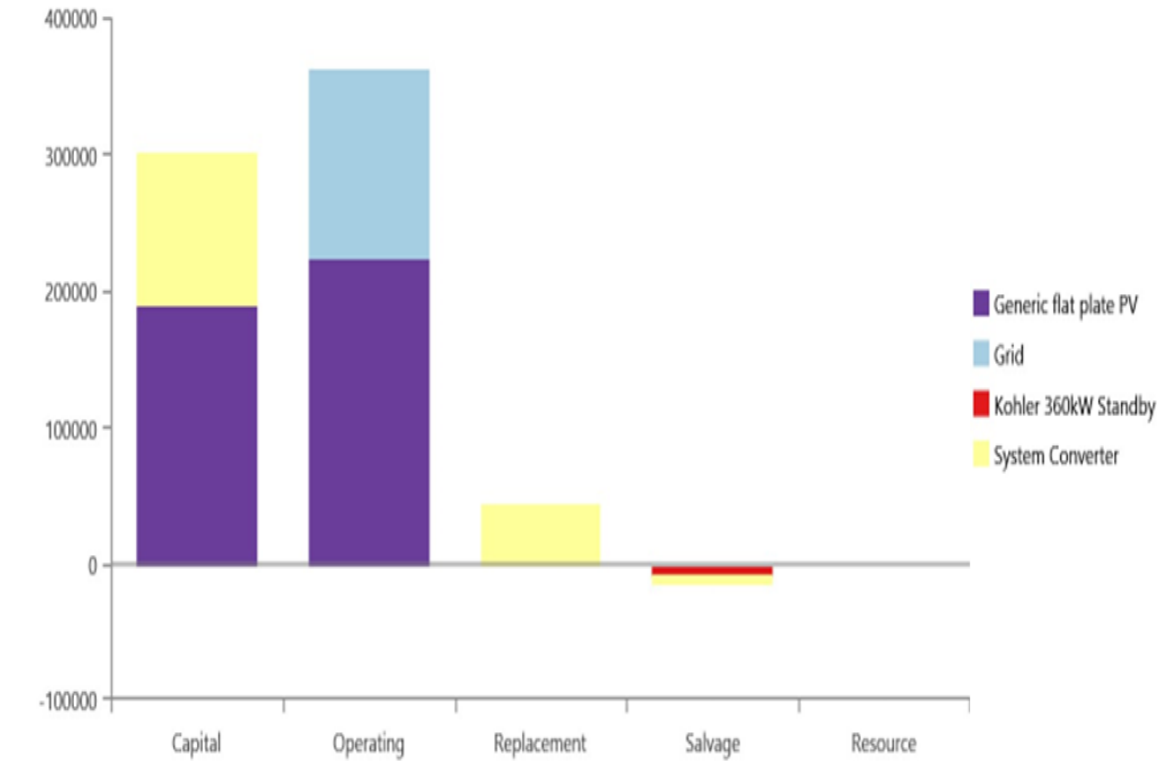

Figure 5. 21: summary of the net present values of different costs of each component for the optimal system

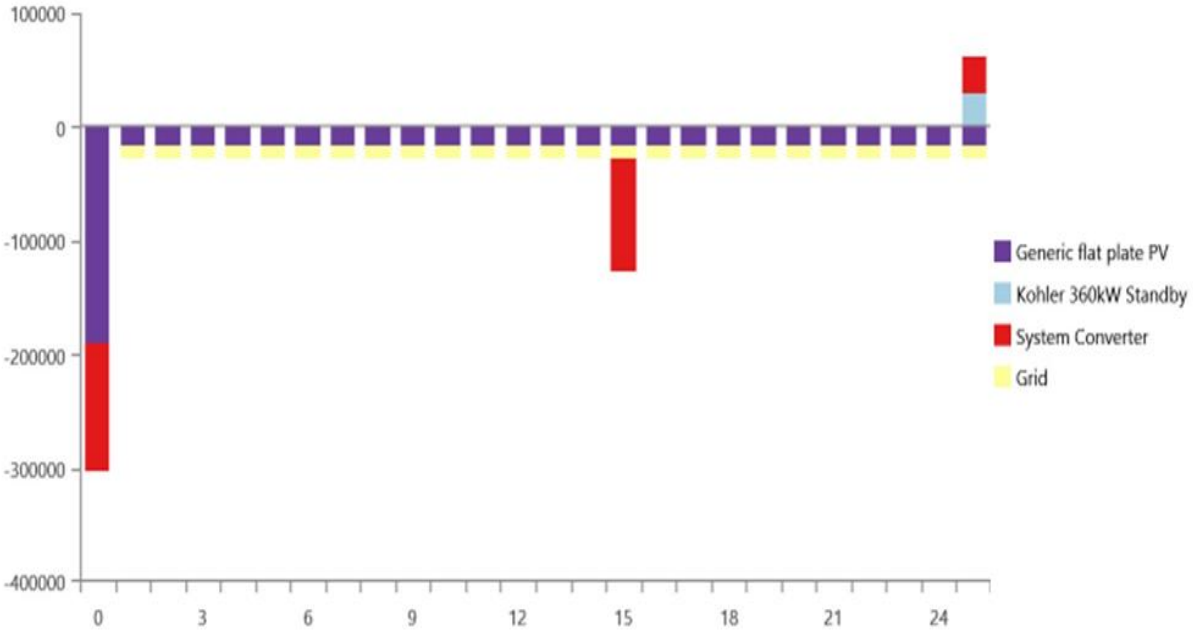

Figure 5. 22: Discounted cash flow of the project for the entire project life for the optimal system

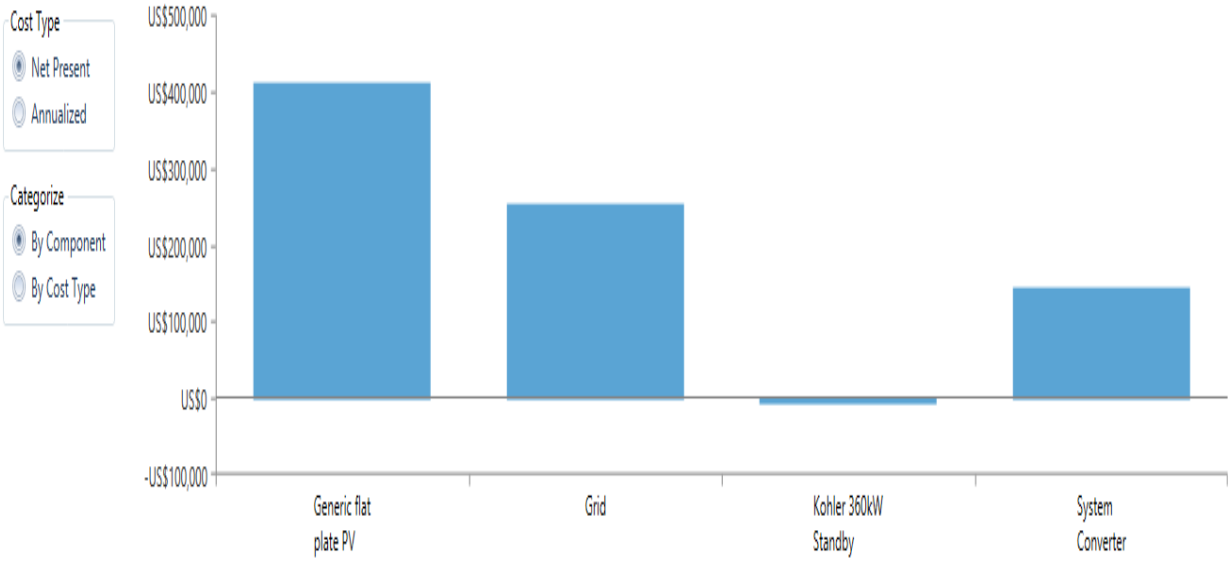

Component	Capital (US$)	Replacement (US$)	O&M (US$)	Fuel (US$)	Salvage (US$)	Total (US$)
Generic flat plate PV	US$190,140.85	US$0.00	US$224,355.59	US$0.00	US$0.00	US$414,496.43
Grid	US$0.00	US$0.00	US$256,886.55	US$0.00	US$0.00	US$256,886.55
Kohler 360kW Standby	US$0.100	US$0.00	US$0.00	US$0.00	-US$7,477.55	-US$7,477.45
System Converter	US$112,500.00	US$44,114.36	US$0.00	US$0.00	-US$8,521.42	US$148,092.94
System	US$302,640.95	US$44,114.36	US$481,242.14	US$0.00	-US$15,998.97	US$811,998.48

Figure 5. 23: Detailed cost summary of the project for the optimal system

The cost of PV is relatively high with the grid cost only coming from operating and maintenance. In general, the system has a salvage value of -$15,998.97 with -$7,477.55 arising from the diesel generator and -$8,521.42 arising from the system converter.

5.7. Economic Comparison

HOMER picks a base system to compare the economics of the current system. Although this base system selected by the analysis tool can be changed, it is set to default in this study. The base system for this comparison is a system with 200kW PV capacity, Grid, 100kW converter output, $823,314 NPC and $183,011 initial capital cost. The result of the comparison is given in table 5.11 below:

Table 5. 10 Economic comparison of the optimal system

IRR (%): 15.2
Discounted payback (yr): 7.76
Simple payback (yr): 6.15

	Base Case	Current System
Net Present Cost	US$823,314	US$695,121
CAPEX	US$183,011	US$302,641
OPEX	US$48,236	US$29,567
LCOE (per kWh)	US$0.126	US0.789
CO_2 Emitted (kg/yr)	133,135	118,950
Fuel Consumption (L/yr)	0	0

5.8. Comparison of the COE of the System with grid electricity cost in Kenya

Grid electricity rates in Kenya are dependent on the various consumer classes grouped into domestic consumers, commercial consumers and industrial and large-scale users. Also, the nature of connections: low, medium and high voltage connection lines are also considered. However from the 13 months energy bill analysis, the establishment pays approximately kshs 20.00/kWh on the average and the total average bill of kshs 590,616.95 per month approximately. This is relatively high compared to the proposed system which has the COE of Ksh 7.89/kwh (approx. Kshs 8.00). This is mainly as a result of the high capacity factor and efficiency of hydropower generation (main power source of Kenya).

5.9. Sensitivity Results

The aim of sensitivity analysis is to evaluate the effects of indecisions in the input variables. It answers the question "what if?" Parameters such as the solar scaled average in kWh/m^2/day, wind speed scaled average in m/s, the temperature scaled average in degree Celsius and the fuel price in USD per litre can change any time therefore it is required to examine the effects these changes may bring on the system specifications and efficiency. This helps to determine the viability and reliability of the project.

5.9.1. The effects of Diesel Price Changes and the solar scaled average on the COE

Figure 5.21 shows the effects of changes in the solar scaled average and the price of fuel on the COE for the wind speed of 4.76m/s and temperature scaled average of 19.9^{0}C. We can see that at the daily average solar radiation of 4.93kWh/m^2/day and the fuel price of $0.9/L, the cost of energy is $0.101/kWh. As the solar radiation increases, the power generated from solar increase and subsequently the cost of energy. We can notice that as the fuel cost increase, there is no significant change in the COE. This is because HOMER had assumed that the power bought from the grid is enough to supply the energy needed when the PV system generates less energy. The diesel generator is only used if and only if the grid power is off at night. Also, changing the temperature scaled average has no substantial effect on the COE. Wind energy is not included in the selected system and therefore will have no effect.

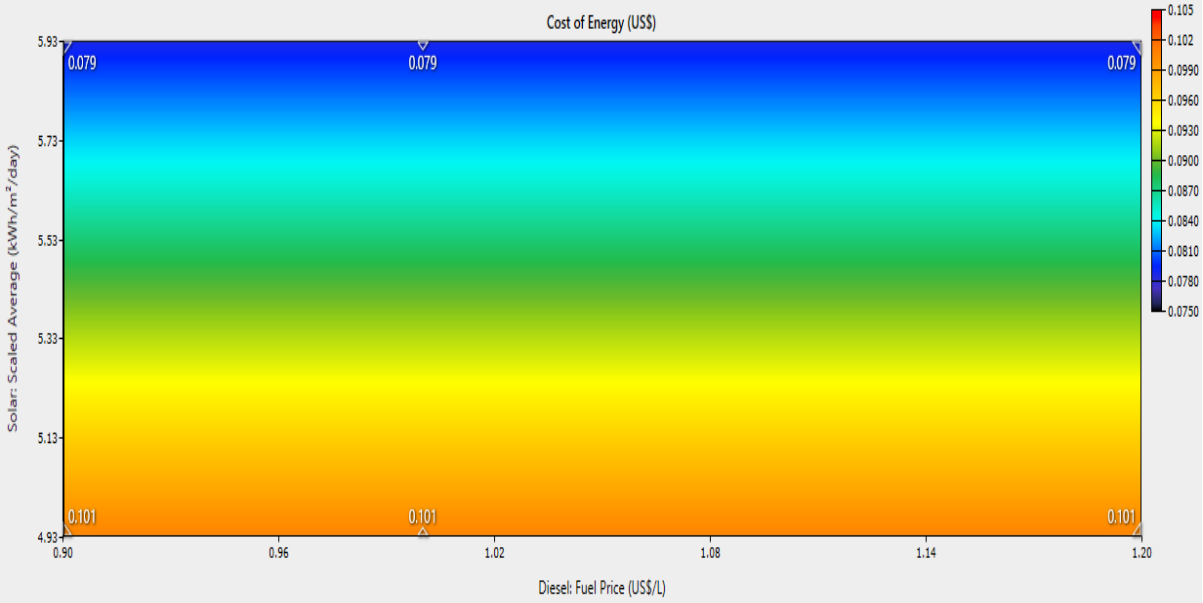

Figure 5. 24 The effects of Diesel Price Changes and the solar scaled average on the COE

5.9.2. The effects of Diesel Price Changes and the solar scaled average on the NPC

Figure 5.22 shows the effect on NPC. Similarly to the effect on the COE, there no much effect on the NPC. At the lowest solar irradiance (4.93kWh/m^2/day), the total NPC is $811,988.50 while at the nominal solar irradiance (5.93kWh/m^2/day), the total NPC is ksh.69,512,100.00. The price of fuel does not have significant effect with the same reason given for the effect on the COE (figure 5.20).

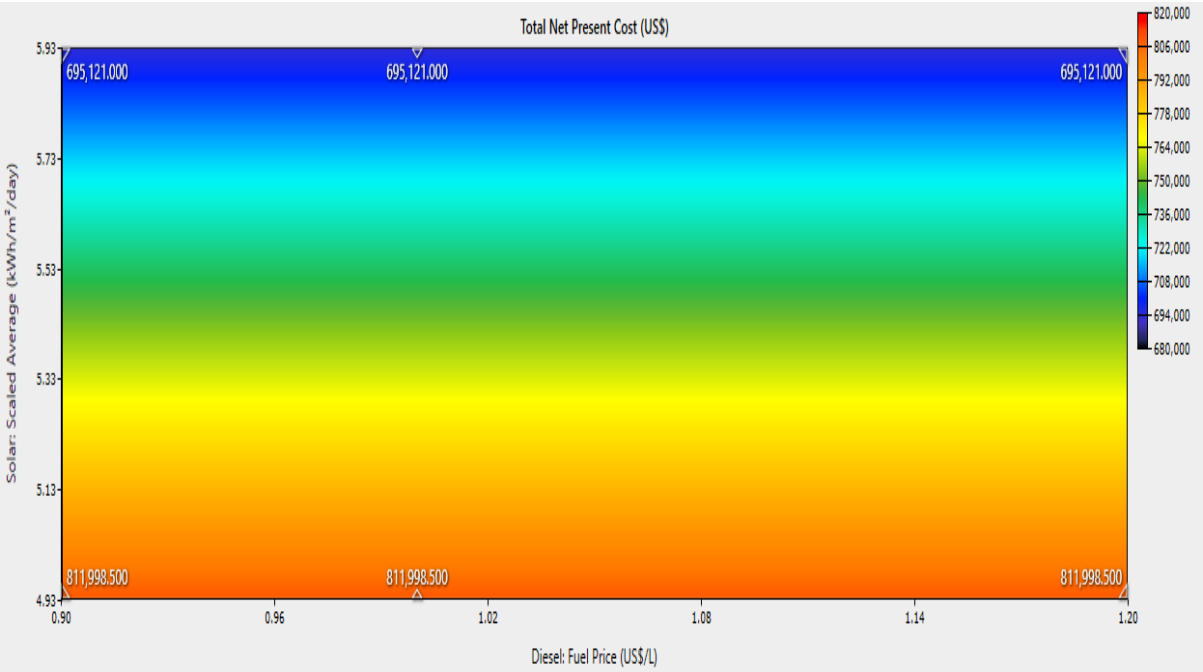

Figure 5. 25 The effects of Diesel Price Changes and the solar scaled average on the NPC

5.9.3. The effects of Diesel Price Changes and the solar scaled average on the PV Production

The energy generated by the PV is proportional to the solar irradiance of the site. Figure 5.23 shows how the system is affected based on the energy production by the PV. As can observe, there are no much changes on the deviation of the solar irradiance. At the lowest solar irradiance (4.93kWh/m^2/day), the total energy produced by the PV is 430,744kWh/yr while at the nominal solar irradiance (5.93kWh/m^2/day), the total energy produced is 518,134.3kWh/yr. The price of fuel does not have significant effect with the same reason given for the effect on the COE (figure 5.21).

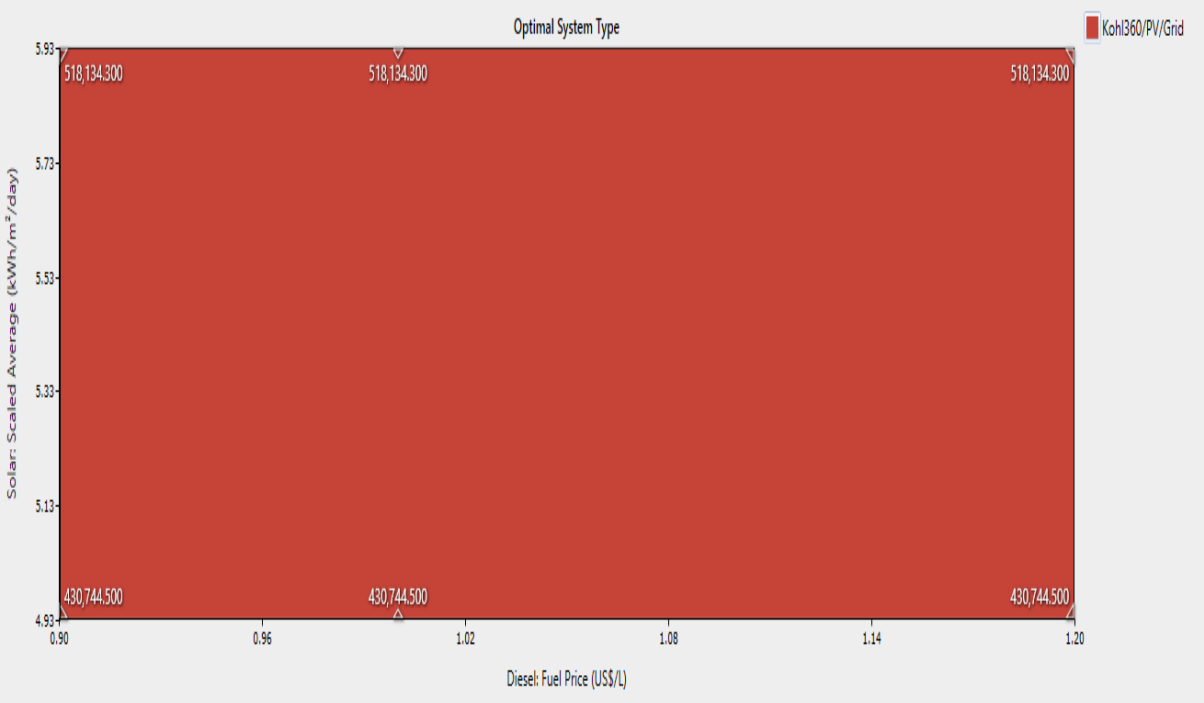

Figure 5. 26 The effects of Diesel Price Changes and the solar scaled average on the PV energy production

5.9.4. The effects of Diesel Price Changes and the solar scaled average on the energy bought from the Grid

The lower the solar irradiance of the site, the lower the power produced from the PV. At night, when the PV power generation is low, power is purchased from the grid to supplement the load demand. Figure 5.23 shows the deviation in the energy bought from the grid when the solar scaled average value changes. At the lowest solar irradiance (4.93kWh/m^2/day), the

overall energy bought from the grid is 196,718.3kWh/yr while at the nominal solar irradiance (5.93kWh/m^2/day), the total energy purchased is 118,211.3kWh/yr. The price of fuel does not have significant effect with the same reason given for the effect on the COE (figure 5.21).

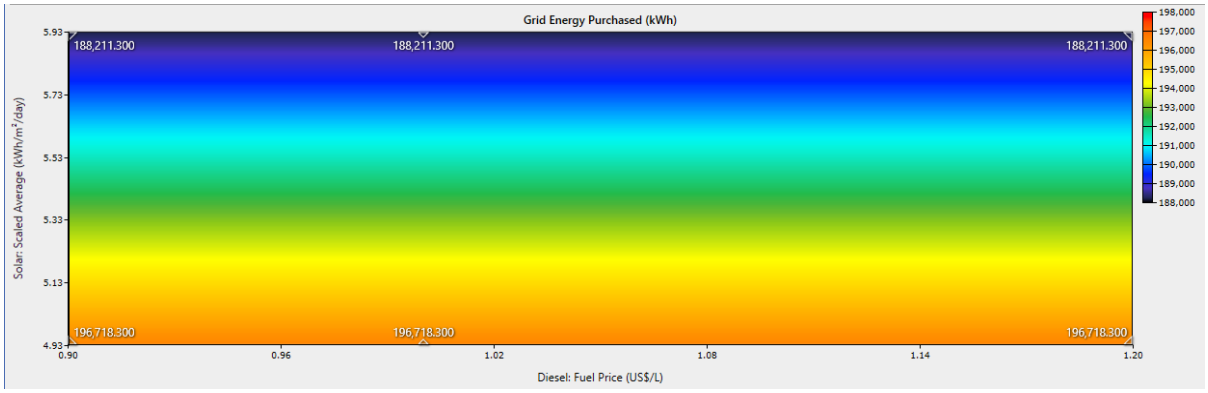

Figure 5. 27 The effects of Diesel Price Changes and the solar scaled average on the energy purchased from the Grid

In conclusion of this sensitivity analysis results, the effects of solar scaled average, diesel fuel price, temperature scaled average and the wind scaled average are not on the system implying that the system is reliable. Due to unavailability of wind turbine for wind energy in this system, the change in wind energy does not have any effect on the system. Also, while the temperature scaled average and the diesel fuel price have negligible effects on the system, solar scaled average has significant effects recorded.

CHAPTER SIX

CONCLUSION AND RECOMMENDATION

The objective of this research project was to determine and propose an optimal off-grid and/or grid-tied hybrid renewable energy system which can supply stable, inexpensive and dependable electricity to the school of Engineering, University of Nairobi. To comparatively asses the feasibilities of hybrid renewable energy systems (PV/Wind/Diesel generator) for reliable energy supply to this establishment. This goal was realized by achieving objectives which include: determining the daily load profile of the site and the examination of the renewable energy potential in this area; identifying the appropriate renewable energy resources for the suggested hybrid system and its constituents selection and cost analysis; modelling and simulation of the system using a computer software package and finally optimization and sensitivity analysis of the hybrid system and performance assessment of the best hybrid system.

The geographical coordinates of the establishment were obtained using a magnetic compass. These location coordinates were used in the online renewable energy catalogues, the NASA Surface Meteorology and Solar Energy data base (http://eosweb.larc.nasa.gov/) to obtain the wind and solar irradiation data of the site. The wind speed scaled average measured at 50m height, the mean global horizontal solar scaled average radiation and the temperature scaled average was 4.76m/s and 5.93kWh/m^2/day and 19.9^{0}C respectively. The data collection of the electricity consumption pattern of the establishment for determination of the average daily electricity demand and peak demand was carried out in three approaches consisting of: obtaining the energy demand and consumption of the establishment from KPLC with the use of the mains meter number; studying the energy equipment used by the establishment to obtain their performance characteristics and use of Power and Energy Logger (PEL 103) to monitor the power demand and consumption of the site from the mains for one month (the

peak month). The peak load demand and energy consumption was established as 84.59kW and 1172kWh/day respectively. The approximate average cost of energy and the approximate average monthly bill for the establishment was determined as $0.20/kWh (kshs 20.00) and $5,906/month (Kshs 590,616.95). The renewable energy data, together with the load characteristics and performance data of various energy equipment (solar PV systems, battery banks, wind turbines, inverters, diesel generator etc.), were used to model and simulate different possible configurations of the systems using optimization software. Economic feasibility, externalities and sustainability were used to compare and rank the systems at the sites. Ten system designs were used to scrutinise each of the above approach in order to select the best system which satisfactorily meet all the expectations of the parameters. The results obtained demonstrate that the best hybrid renewable energy systems is the grid tied system with component grid, PV and diesel generator. This system gives COE of Ksh 7.89, NPC of ksh 69,512,100.00, Initial capital cost of ksh 30,264,100.00, renewable fraction of 71.6%, simple payback period of 6.15years, discounted payback period of 7.76years, present worth of ksh 12,819,300.00, annual worth of ksh 965,700.00 excess electricity generation of 2.48% etc. The system proves to have reduced the power being purchased from the grid from 100% to 23% approximately (90kW to 20kW).

Sensitivity analysis was also carried out for the system, 9 sensitivity circumstances were used such as; 3 values for the cost of diesel fuel cost, 2 cases of solar scaled average irradiation, 2 cases of wind speed scaled average and two cases of temperature scaled average. The sensitivity analysis presented that the same arrangement was gotten except in a case where the size and prices of some components are changed.

5.2 Recommendation

- Off-grid hybrid system is not cost-effective at the school of engineering, University of Nairobi. This is because of the grid extension which is already in existence at this site. However, grid-tied system will reduce the energy demand from grid to almost zero and thereby is recommended.
- This study uses satellite datasets from meteorological stations at the various study sites. Future studies should consider using measured ground data for more precision.
- The diesel gen-set should be design to operate at full capacity in order to reduce the system cost.
- The wind resource of School of Engineering, University of Nairobi is very low. As such, systems with wind components are not advisable for economic reasons.
- HOMER optimization involves complex simulation, optimizations and sensitivity analyses. Thus, in complex system designs (systems with many components), it is recommended to use high capacity and processors computers.
- Future work should consider the feasibility of biofuels by addressing the likelihood of substituting diesel generator in the system with biofuels which are obtainable from the site.

References

1. J.K. Kiplagat, R.Z. Wang and T.X. Li (2011). Renewable Energy in Kenya: Resource Potential and Status Exploitation. Renewable and Sustainable Energy Review Journal.
2. UNDESA (2014). A survey of International activities in rural energy access and electrification. Retrieved on August 28, 2018 from https://sustainabledevelopment.un.org/content/documents/1272A%20Survey%20of%20International%20Activities%20in%20Energy%20Access%20and%20Electrification.pdf
3. International Energy Agency (2018). WEO - 2017 special report: Energy Acess outlook. Retrieved on 16/08/2018 from https://www.iea.org/publications/freepublications/publications/WEO2017SpecialReport_EnergyAccessOutlok.pdf
4. K.M. Iroma (2013); 'Techno-Economic Optimum of Hybrid Renewable Energy System', *Rural electrification in Sri Lanka. Thesis Report*
5. Worldometers (2018). United Nation Kenya Live Population Estimate
6. KPLC Report (2016/2017). Annual Report and Financial Statements for the year ended 30 June, 2017. Retrieved from www.kplc.co.ke/content/item/2255/2016--2017-full-annual-report-for-the-year-ended-30th-june-2017
7. Austin Wasonga, Michael Saulo and Victor Odiambo (2014). Solar-Wind Hybrid Energy System for New Engineering Complex- Technical University of Mombasa. International Journal of Energy and Power Engineering. Page 74.
8. Solomon Teklemichael Bahta (2013). Design and Analysing of an Off-grid hybrid Renewable Energy System for Rural Electrification in Ethiopia. Page 2. *Thesis Report*
9. Kenyan Ministry of Energy (2018). Energy Sources and Statistics. Retrieved on 17/08/2018 from http://energy.go.ke/?p=516
10. Kenyan Ministry of Energy (2018). Energy Sources and Statistics. Retrieved on 17/08/2018 from http://energy.go.ke/?p=516
11. Otuki, Neville (3rd July, 2018). Electricity demand crosses 1800MW mark. Business Daily Africa. Nairobi. Retrieved on July 3rd, 2018.
12. RECP (2018). Renewable Energy Potential, Kenya. Retrieved on Sept. 08, 2018 from https://www.africa-eu-renewables.org/market-information/kenya/renewable-energy-potential/

13. Henry Gichungi (2016). Solar Potential in Kenya. Conference paper presentation. Retrieved on 02/05/2019 from https://www.sv.uio.no/iss/english/research/projects/solar-transitions/announcements/Kenya-Henry_Gichungi.pdf

14. Rahul Kumar Kandoi, et al (2015). Scaling up Wind Energy Development Plans in Kenya. *Paper presented to winDForce Management Limited, Kenya*

15. Energy Regulatory Commission (2018). Renewable Energy Portal. Biomass. Retrieved on 08/09/2018 from https://renewableenergy.go.ke/index.php/content/29

16. Munuswamy, S., Nakamura, K., Katta, A. (2011) 'Comparing the cost of electricity sourced from a fuel cell-based renewable energy system and the national grid to electrify a rural health centre in India: A case study', *Renewable Energy 36, pp. 2978 – 2983.*

17. Rohit Sen, and Subhes C. Bhattacharyya (2013); 'Off-grid Electrification Generation with Renewable Energy Technology in India', *Pre-publication version*

18. Hafez, O. and K Bhattacharya, 2012, Optimal planning and design of a renewable energy based supply system for microgrids, Renewable Energy, 45:7-15.

19. Lau, K. Y., MFM Yousof, SNM Arshad, M. Anwari and AHM Yatim, 2010, Performance analysis of hybrid photovoltaic/ diesel energy system under Malaysian conditions, Energy, 35(8), pp. 3245-55.

20. Andrej Cotar, et al. photovoltaic systems, commissioning party: IRENA- Istrian regional energy agency; January 2012.

21. National Energy Foundation (2018). Types of Photovoltaic (PV) Cells. Retrieved on 10th Sept. 2018 from http://www.nef.org.uk/knowledge-hub/solar-energy/types-of-photovoltaic-pv-cells

22. Asrari, A., Ghasemi, A., and Javidi, M. H. (2012). Economic evaluation of hybrid renewable energy systems for rural electrification in Iran - A case study. *Renewable and Sustainable Energy Reviews*, *16*(5), 3123–3130. https://doi.org/10.1016/j.rser.2012.02.052

23. Rose, A., Stoner, R., & Pérez-arriaga, I. (2017). Prospects for grid-connected solar PV in Kenya : A systems approach. *Applied Energy*, *161*(2016), 583–590. https://doi.org/10.1016/j.apenergy.2015.07.052

24. HOMER Energy Resource Explanatory Note. Surface meteorology and Solar Energy, A renewable energy resource web site (release 6.0)," Prediction of Worldwide Energy Resource Project, [Online]. Available: http://eosweb.larc.nasa.gov/cgi-bin/sse/sse.cgi?rets@nrcan.gc.ca.

25. Duffie JA, Beckman WA (1991), Solar Engineering of Thermal Processes 2nd edition, Wiley, New York, NY
26. Manwell JF, McGowan JG, Rogers AL (2002), Wind Energy Explained, Wiley, New York, NY
27. A. Mcevoy, T. Markvart and L. Castaner, Solar Cells - Materials, Manufacture and Operation, Elsevier, 2013.
28. Duffie JA, Beckman WA (1991), Solar Engineering of Thermal Processes 2nd edition, Wiley, New York, NY
29. Alternative Energy Store Website; Solar Panels and Solar Gears. Retrieved on 07/01/2019 from https://www.altestore.com/store/solar-panels/canadian-solar-solar-panels-p41162/#CSI355-CS3U355P
30. Adaramola, M. S., Agelin-Chaab, M., and Paul, S. S. (2014a). Analysis of hybrid energy systems for application in southern Ghana. *Energy Conversion and Management*, *88*(2014), 284–295. https://doi.org/10.1016/j.enconman.2014.08.029
31. RENUGEN (2019). Aeolos –10kW Wind Turbine. Retrieved on 15/01/2029 from http://www.renugen.co.uk/aeolos-aeolos-v-10kw-10kw-wind-turbine/
32. Homer Energy Help tool version x64.3.12.3 (pro edition)
33. Rolls Battery Engineering (2019). Retrieved on 8th January 2019 from https://www.rollsbattery.com/battery/6-cs-25p/
34. Barley CD, Winn CB (1996), Optimal dispatch strategy in remote hybrid power systems, Solar Energy, **58**, 165-179
35. Central Bank of Kenya (2019). Inflation Rates. Retrieved on January 10th, 2019 from https://www.centralbank.go.ke/inflation-rates/
36. Erbs DG, Klein SA, Duffie JA (1982), Estimation of the diffuse radiation fraction for hourly, daily, and monthly-average global radiation, Solar Energy, **28**, 293
37. Izael Da Silva, et al (2017). Reducing Carbon Emission in Third Level Educational Institution in Sub-Sahara Africa; page 6

APPENDIX

Figure 6. 1: The HOMER modelling interface